

LEVEL II
A12
A

Report No. FAA-EE-78-29

MDA 022221

ANALYSIS OF OZONE AND WATER VAPOR FIELD MEASUREMENT DATA

By
R. Penndorf



Final Report
November 1978

D D C
P R O P R I E T A R Y
R E S E R V E D
AUG 13 1979
R E S E R V E D
A

Document is available to the public through
The National Technical Information Service,
Springfield, Virginia 22161

Prepared for
HIGH ALTITUDE POLLUTION PROGRAM

U.S. DEPARTMENT OF TRANSPORTATION
FEDERAL AVIATION ADMINISTRATION
Office of Environment and Energy
Washington, D.C. 20591

DDC FILE COPY

ANALYSIS OF OZONE AND WATER VAPOR FIELD MEASUREMENT DATA FAA-EE-78-29

79 08 13 070

This document is disseminated under the sponsorship of the Department of Transportation in the interest of information exchange. The United States Government assumes no liability for its content or use thereof.

Technical Report Documentation Page

1. Report No. FAA-EE-78-29	2. Government Accession No.	3. Recipient's Catalog No.
4. Title and Subtitle 6. Analysis of ozone and water vapor field measurement data		5. Report Date November 1978
7. Author(s) R. Penndorf		6. Performing Organization Code
9. Performing Organization Name and Address Dr. R. Penndorf 148 Oakland St. Wellesley Hills, MA 02181		8. Performing Organization Report No. R-149
12. Sponsoring Agency Name and Address U.S. Department of Transportation Federal Aviation Administration Office of Environmental Quality High Altitude Pollution Program		10. Work Unit No. (TRACIS) W1-78-3740-1 new
11. Contract or Grant No. W1-78-3740-1		
13. Type of Report and Period Covered Final Report April-November 1978		
14. Sponsoring Agency Code		
15. Supplementary Notes		
16. Abstract <p>Field measurements of ozone and water vapor are critically analyzed. For the total amount of ozone we derive quantitative estimates for natural aperiodic fluctuations, temporal and latitudinal variations, and global inventory. Ozone experiences the largest natural fluctuations (in local concentration) of ± 50 to 100% in the tropopause layer with ± 10 to 20% in the lower troposphere and above 20 km. The seasonal variation is the largest ($\pm 25\%$) periodic variation in the stratosphere. Reviewed are tropospheric concentrations and the magnitude of the various exchange processes transporting ozone through the tropopause.</p> <p>For stratospheric water vapor, the techniques, systematic errors, and results of all reliable field measurements are discussed in detail. We derive, for midlatitudes and the period 1969-70, an average mixing ratio of 4.15 ppmv, constant from the tropopause to at least 35 km. The magnitudes of natural aperiodic fluctuations and temporal variations are determined, resulting in deducing a $\pm 30\%$ (of stratospheric mass) long-term cyclic variation as being the largest temporal variation. Latitudinal variations are definitely very small. The global inventory, fluxes, residence time, sources and sinks are described quantitatively. Our estimate for the stratospheric mass is 2 to 2.5×10^{12} kg. Problem areas needing further work are indicated.</p>		
17. Key Words Trace gas measurements, atmospheric ozone, water vapor, stratosphere		18. Distribution Statement Document is available to the public through the National Technical Information Service, Springfield, Virginia 22151
19. Security Classif. (of this report) Unclassified	20. Security Classif. (of this page) Unclassified	21. No. of Pages 198
		22. Price

111235

ABSTRACT

Field measurements of ozone and water vapor are critically analyzed. For the total amount of ozone we derive quantitative estimates for natural aperiodic fluctuations, temporal and latitudinal variations, and global inventory. Ozone experiences the largest natural fluctuations (in local concentration) of 50 to 100% in the tropopause layer with ± 10 to 20% in the lower troposphere and above 20 km. The seasonal variation is the largest ($\pm 25\%$) periodic variation in the stratosphere. Reviewed are tropospheric concentrations and the magnitude of various exchange processes transporting ozone through the tropopause.

For stratospheric water vapor, the techniques, systematic errors, and results of all reliable field measurements are discussed in detail. We derive, for midlatitudes and the period 1969-70, an average mixing ratio of 4.15 ppmv, constant from the tropopause to at least 35 km. The magnitudes of natural aperiodic fluctuations and temporal variations are determined, resulting in a $\pm 30\%$ of stratospheric mass long-term cyclic variation as being the largest temporal variation. Latitudinal variations are definitely very small. The global inventory, fluxes, residence time, sources and sinks are described quantitatively. Our estimate for the stratospheric mass is 2 to 2.5×10^{12} kg. Problem areas needing further work are indicated.

Accession For	
NTIS GRA&I	<input checked="" type="checkbox"/>
DDC TAB	<input type="checkbox"/>
Unpublished	<input type="checkbox"/>
Journal	<input type="checkbox"/>
Classification	
Availability Codes	
Dist	Avail and/or special
<i>A</i>	

TABLE OF CONTENTS

<u>Section</u>		<u>Page</u>
SUMMARY	S.1 Purpose and Scope S.2 Total Amount of Ozone S.3 The Vertical Distribution of Ozone S.4 Water Vapor	S-1 S-2 S-7 S-11
A.	ATMOSPHERIC OZONE: THE TOTAL AMOUNT AND ITS FLUCTUATIONS	1
	Abstract	1
	A.1 Introduction	2
	1.1 The Role of Ozone in the HAPP Program	2
	1.2 A Brief Survey of Atmospheric Ozone	3
	A.2 Variations in Total Ozone	5
	2.1 Diurnal Variation	5
	2.2 Interdiurnal Variability	8
	2.3 Daily Variability	8
	2.4 Monthly Averages, Their Variability and Trends	13
	2.5 Annual Averages and Their Long-Term Trends	19
	2.6 Ozone and Weather	27
	2.7 Perturbations	29
	2.8 Density of Network	30
	2.9 Amplitude Comparison	30
	A.3 Global Distribution of Ozone	33
	3.1 Latitudinal Distribution	33
	3.2 Maps	33
	3.3 Inventory	39
	A.4 References	45
B.	ATMOSPHERIC OZONE: THE VERTICAL DISTRIBUTION AND ITS FLUCTUATIONS	48
	Abstract	48
	B.1 Vertical Profiles and Meridional Cross-sections	49
	1.1 Techniques	49
	1.2 Meridional Cross-sections	51
	1.3 Temporal Variations	57
	1.4 Natural Fluctuations	62
	1.5 Magnitude of Temporal Variations and Fluctuations	67

TABLE OF CONTENTS (Concluded)

<u>Section</u>	<u>Page</u>
B.2 Tropospheric Ozone	70
2.1 Tropospheric Content	70
2.2 Tropospheric Concentration	71
2.3 Exchange Through the Tropopause	72
B.3 Field Measurements Between 8 and 12 km Altitude	78
3.1 Overburden	78
3.2 In-situ Measurements of Concentration	79
B.3 References	84
C. STRATOSPHERIC WATER VAPOR: ANALYSIS AND INTERPRETATION OF FIELD MEASUREMENTS	88
Abstract	88
C.1 Introduction	89
C.2 Measurement Techniques	93
2.1 Contamination	93
2.2 Frost-point Hygrometer	94
2.3 Optical Techniques	95
2.4 Other Techniques	101
2.5 Instrumentation	102
C.3 Vertical Profiles	103
3.1 Results of Field Measurements	103
3.2 Average Profile	126
3.3 Natural Fluctuations	128
3.4 Temporal Variations	131
C.4 Latitudinal Variations	143
C.5 Experiments for Source Determination	153
5.1 Intertropical Convergence Zone	153
5.2 Thunderstorm Injection	155
5.3 Polar Jet Stream	155
C.6 Sources and Sinks	159
6.1 Global Mass	159
6.2 Sources and Their Strength	159
6.3 Sinks	169
C.7 References	172

LIST OF FIGURES

	<u>Page</u>
A-1 Ozone Measurements During a Day	6
A-2 Aperiodic Variations During a Day	6
A-3 Histogram of Interdiurnal Variation	10
A-4 Monthly Mean Values	12
A-5 Monthly Mean Values	14
A-6 Averages of Monthly Means, July-September	15
A-7 Monthly Mean Values 1932-1977	18
A-8 Annual Mean Value	20
A-9 Variability of Trends	20
A-10 Variation of Seasonal Mean Values	25
A-11 Total Ozone and Pressure Distribution	28
A-12 Tentative Models of General Circulation	28
A-13 Isopleths of Total Ozone	34
A-14 Probability Distribution	35
A-15 Average Global Distribution	37
A-16 Hemispherical and Global Averages	42
B-1 Meridional Cross-section	52
B-2 Meridional Cross-section	53
B-3 In-situ Measurements at 21 km	56
B-4 Time Cross-sections	58
B-5 Time Cross-sections	58
B-6 Meridional Cross-section	60
B-7 Annual Mean Density	60
B-8 Range of Vertical Ozone Profiles	64
B-9 Range of Vertical Ozone Profiles	65
B-10 Range of Natural Fluctuations	65
B-11 Time Cross-section	66
B-12 Transfer of Stratospheric Air	74
B-13 Ozone Overburden	80
B-14 Flight Record	82
C-1 Data from Frost-point Hygrometers	117
C-2 Data from Band Absorption	118
C-3 Data from Line Absorption	119
C-4 Data from Thermal Emission and Filters	120
C-5 Data from Thermal Emission and Spectroscopy	121
C-6 Vertical Profile	127
C-7 Average Mixing Ratio	127
C-8 Vertical Profile, Average and Range	129
C-9 Histogram of Mixing Ratio, Washington, D.C.	130
C-10 Histogram of Mixing Ratio, England	130
C-11 Time Series Analysis	133
C-12 Time Sequence of Mixing Ratio, England	134
C-13 Long-term Trend	137
C-14 Latitudinal Distribution	146
C-15 Latitudinal Distribution	151
C-16 Overburden Over Thunderstorms, ITCZ	154
C-17 Overburden Over Polar Jet Stream	156
C-18 Tropopause Conditions for Singapore	165

LIST OF TABLES

	<u>Page</u>
A-1	9
A-2	9
A-3	17
A-4	22
A-5	22
A-6	23
A-7	31
A-8	41
A-9	43
A-10	43
 B-1	 68
C-1	92
C-2	104
C-3	113
C-4	132
C-5	139
C-6	141
C-7	144
C-8	145
C-9	160
C-10	162
C-11	163

SUMMARY

S.1 PURPOSE AND SCOPE

In this report the field measurements of atmospheric ozone and water vapor in the stratosphere are critically reviewed, using information available as of summer 1978. Our data sources are the results of field measurements published in the journal literature. Preliminary data have been excluded. We also eliminated some of the older data after a critical analysis had shown that their accuracy is very low or that an unreliable technique had been used.

The available data have been analyzed to derive periodic and aperiodic variations, such as natural variability, diurnal and seasonal variations, and long-term trends. Latitudinal variations exist, caused by transport within the stratosphere from the source regions to the sinks. The results of transport through the tropopause are evaluated and described although no independent studies have been conducted by the author. Global inventories have been derived from the vertical profiles of concentrations. No comparison has been made between field measurement data and models.

The purpose of this review has been to gather and assemble all field measurement data considered pertinent to HAPP. Based on what we already know about the distribution of these gases, we can find out where the gaps in our knowledge are and suggest areas which appear to be in need of further measurements.

S.2 TOTAL AMOUNT OF OZONE

The total amount of ozone above any given location determines the UV-B flux. Of course other parameters modify the irradiance, such as solar altitude, the scattering by molecules and aerosols, the ground albedo, and the cloudiness.

Since ozone is the principal absorber of UV-B, we investigated its often neglected natural fluctuations. We selected as a primary data base the excellent measurements made at Arosa ($\delta = 47^\circ$ N) first by Götz and later by Dütsch, because it is the longest series in existence starting in 1926 with some minor interruptions. Similar studies should be made for the U.S. network. The Arosa data are characteristic for midlatitudes and should apply to most of the U.S.; I presume Florida belongs to the tropical regime.

During some days a diurnal variation, an increase or decrease but not a sine-type cyclic variation, may occur. It is related to changes in the stratospheric weather pattern during a 24-hour period; such variations are large in winter and spring and smallest in fall and they increase with latitude. In general, diurnal variations are small, although they may reach ± 10 to 20% on some days.

The change from one day to the next, or the interdiurnal variation has been computed for Arosa and Tromso. Its average variability is about 4 to 7% for Arosa and about 4 to 27% for Tromso. The largest changes occur in winter; in the tropics the changes are small.

The daily variability is the standard deviation of all daily measurements used in computing a monthly mean value. Expressed in percentage of the mean the daily variability is small in the tropics, about ± 1.5 to 3%, reaching about ± 6 to 14% in mid and high latitudes. Such a large variability should not be neglected in estimating UV-B effects on the biosphere.

Next we looked at the monthly mean values for a 45-year period. For an individual month, e.g. January, the amount of ozone can be large in one year and small in the next; there is no obvious periodicity in this sample, although a spectral analysis may be worthwhile. The natural fluctuations result in a standard deviation of about $\pm 3\%$ in summer and about $\pm 6\%$ and 14% in mid and high latitudes, respectively, in winter. Such fluctuations are related to the general circulation, which changes in an unpredictable manner from one year to the next. Winters with a strong (or sudden) stratospheric warming result in large positive anomalies of ozone because they are causing rising motions over the pole and sinking motions in mid latitudes. For the January 1958 sudden warming, the onset of the warming was accompanied by the appearance of a region with 40% higher than normal ozone concentration at the 30 to 35 km level.

Computing yearly mean values and looking at the 45-year-long series, we detect some outstanding large amounts in 1940-41 and in 1969-70. The various trend analysts agree on a negative trend for 1960-62 and 1970-76, a positive trend for 1962-70 in the Northern Hemisphere, and a negligible trend in the Southern Hemisphere from 1955 to 1972. The most recent trend analysis is based on seasonal and not on annual averages and therefore shows more detail than previously detected. The large increase from 1962 to 1970 is now shown to have been interrupted by a decrease from 1966 to 1967 in Europe as well as in North America. The ozone variations for the last 20 years now show a number of increases and decreases, very aperiodic, each lasting from 1 to 3 years and differing from one area of the globe to the next, although North America and Europe show a similar behavior. Such regional differences are expected from shifts in the general circulations.

The seasonal variation dominates all periodicities and its magnitude of about $\pm 30\%$ or more in midlatitudes is very large and increasing with latitude. The biennial variation (a 26-month cycle) influences

midlatitudes in winter only and the sunspot cycle with its small or negligible amplitude is questionable.

We conclude that fluctuations of the total amount of ozone appear in time and space. They are related to the stratospheric weather patterns and the general circulation, which undergo unpredictable changes. Generally the fluctuations are small in the tropics, reasonable in midlatitudes, but often very large in high latitudes. Numerical values are given.

One should realize that any presentation of "average" or "standard deviation" in space and time is not usually "representative" of the state of the atmosphere at any other time and place. However, such parameters can be used as a "guide." Also, frequency distributions usually give a better insight into expected occurrence than the standard deviation from the mean, especially when it has not been proved that the properties can be treated as gaussian.

There is no question that the stratospheric weather patterns determine the distribution of ozone and its anomalies. Unfortunately, good and reliable numerical computations are lacking. As long as the exact magnitude of the stratospheric vertical motions is not well known, progress in this area will be slow.

We investigated the global inventory, carefully computed by several investigators from observational data, and find good agreement. On the average, the ozone mass is about 3.0 to 3.4×10^{12} kg; the extrema characterize years with low and high ozone and correspond to 0.274 to 0.309 atm cm ozone as a worldwide average. Interestingly, the global and hemispherical inventory changes slightly from month to month as is reasonable. As expected, there exists a large seasonal trend for total ozone in each hemisphere, about $\pm 10\%$ in the Northern and $\pm 7\%$ in the Southern Hemisphere. On an annual basis, the Southern Hemisphere contains 2.5% less ozone than the Northern Hemisphere.

To assure the UV-B irradiance at the earth's surface, one should know not only the average amount of ozone but also its natural fluctuations in time and space. We have discussed the magnitude of such fluctuations based on available long-term series.

We suggest and recommend:

- (1) To conduct a detailed recomparison and recalibration of historical ozone data and previous significant reviews of such data and tabulation of recalibration coefficients required to bring these into agreement with current calibration standards.
- (2) To determine in a systematic way the magnitude of these natural periodic and aperiodic fluctuations for all North American ozone stations using Dobson spectrometers as a small sample in a world-wide trend analysis. The stations operate now for 10 to 20 years so that reasonable statistics can be obtained.
- (3) To assess the fluctuations of global ozone (day-to-day, monthly, yearly). This study may have to wait for the full evaluation of all the errors and the calibration of the satellite data and the publication of at least some of those data. Many investigations with satellite data from Nimbus 4 are possible and desirable. It is not obvious to us at this time what studies NASA plans to conduct in-house or by contracts. Therefore no specific recommendations are made.
- (4) To determine the correlations between total ozone and changes in the general circulation for the North American network. The known relationship between total ozone and weather should be explored and verified for the North American network. Comparisons with satellite data should be carried out once the Nimbus-4 data are fully reduced and made available.
- (5) To investigate in time and space the fluctuations of other parameters which influence UV-B irradiance, such as cloudiness,

aerosol scattering, ground and cloud albedo. This topic becomes important if the effects of man-made pollution on ozone are small, e.g. $\pm 2\%$, and small-scale fluctuations of the above mentioned parameters could compensate the man-made reductions of ozone.

S.3 THE VERTICAL DISTRIBUTION OF OZONE

The vertical profile of ozone concentration is being measured at several selected locations. The data base is smaller than for total ozone; nevertheless, the general distribution and its variation have emerged and no great surprises are expected from future measurements. What remains to be done are simultaneous measurements of as many trace gases as possible so that correlations between trace gases can find a firm footing useful for model atmospheric composition. The application of the actual three-dimensional ozone distribution to derive transport parameters is still in its infancy and more work in this direction is needed and recommended.

Reliable techniques have been developed to measure ozone; for balloons and aircraft as carriers the wet chemical techniques are favored. For rockets and satellites, optical techniques are preferred.

Average seasonal profiles exist for all latitudes, although large gaps exist for the Southern Hemisphere. The meridional cross-sections show the well-known maximum in concentration at 26 km over the equator, sloping downward to about 17 km over the poles. The maximum in mixing ratio, about 10 ppmv, is situated in the tropical middle stratosphere at about 30 km; polar irregularities remain small, yet they are the outstanding feature in concentration.

The seasonal variation in local concentration dominates all other periodic variation in the stratosphere at all latitudes and altitudes; it is largest (about $\pm 25\%$ in relative local concentration) from 12 to 22 km, where transport processes dominate. The biennial variation, large in the tropics ($\pm 15\%$), can be found at the level of the ozone maximum even in midlatitudes. A solar cycle variation, though very small ($< 2\%$), is noted above 30 km. Some long-term trends, well established in total ozone, are found. Preliminary

data exist so far only for Australia and for the 34 to 42 km regime in some other areas.

Satellite data suggest that a negative correlation exists between ozone concentration and temperature in the middle stratosphere. As expected, cold areas in the upper stratosphere produce more ozone than warm regions.

The natural aperiodic fluctuations are largest between about 5 and 12 km in middle latitudes. These fluctuations are caused by the change in the tropopause height, so that a particular altitude may experience stratospheric ozone concentrations on one day and tropopspheric conditions the next day. Thus the standard deviation reaches values of $\pm 90\%$ or more for the "tropopause layer." The tropopause layer is defined as that region within which the tropopause oscillates up and down and in which multiple tropopauses occur. The standard deviations are below $\pm 50\%$ in the lower troposphere and $\pm 10\%$ to 20% above 20 km.

The troposphere contains about 8 to 15% of the total ozone, depending on latitude and season; the global average lies at 8%. The ozone sink is at the ground, so that a constant flux of ozone of $(28 \pm 9) \times 10^{28}$ molec/sec or $(7 \pm 2) \times 10^{11}$ kg/year passes from the stratosphere through the tropopause to the ground with a residence time in the troposphere of 62 and 83 days for the Northern and Southern Hemisphere, respectively. The average tropospheric concentration is about $40 \mu\text{g}/\text{m}^3$. The local microclimate dominates its concentration in the boundary layer where the annual average varies between 20 and $50 \mu\text{g}/\text{m}^3$. Day-to-day variations, especially under strong inversions and near local pollution sources can reach much larger concentrations. The results obtained at one locality can not be simply applied to other places. Therefore environmental impact statements require a detailed knowledge of the local microclimate. General inferences can lead to erroneous conclusions.

The exchange through the tropopause is accomplished mostly in middle and high latitudes at the tropopause gaps through large-scale eddy transport. A flux of stratospheric air into the troposphere also occurs poleward of 70° latitude. All other forms of transport add only minor amounts. Some numerical estimates of the magnitude of this flux exist although more measurements are needed to derive reliable flux values for each transport process. In addition, measurements in the Southern Hemisphere are needed.

Field measurements using aircraft in the 8 to 21 km altitude range have been carried out since about 1972. Optical measurements give the overburden, a quantity we do not find especially useful. The many concentration measurements in the tropopause region gave the expected wide variations between, for example, 10 and 800 ppbv in midlatitudes, depending on the altitude of the tropopause and whether the aircraft was below or above the tropopause. The only sensible result is obtained if the data are arranged according to the distance from the tropopause, and that information is available from balloon ascents which can reach 30 km, whereas airplanes, especially commercial aircraft, are limited to a ceiling of 12 km and the position of the tropopause can be obtained only indirectly with a wide margin of error. Thus we find that only those aircraft measurements where the flight plan has been well prepared and adapted to a particular objective have contributed to our knowledge of the three-dimensional distribution of ozone.

We suggest and recommend:

- (1) To continue balloon, rocket, and satellite measurements to derive the three-dimensional distribution of ozone and its variations.
- (2) To derive statistical parameters for selected localities by operating stations for several years. For ozonesondes (balloons), one measurement per week seems sufficient; for tropical stations one or two measurements per month seem adequate. Satellite measurements conducted in previous years are presently being

reduced and I assume proper evaluation of all aspects has been planned by the cognizant agencies.

- (3) To conduct airplane measurements only if as many trace gases as possible are collected simultaneously, so that correlations can be established and transport parameters derived. Measurements of ozone alone are not recommended. The actual height of the tropopause has to be determined by better methods than are presently in use to be useful for a proper evaluation of such flights.
- (4) To investigate the transport of ozone through the tropopause and especially near the tropopause gaps so that the magnitude of each transport process can be determined. In such studies, the synoptic situation has to be selected very carefully under the guidance of weather forecasters.
- (5) To determine three-dimensional transport parameters from the measured 3-D ozone distribution. These parameters should vary with season and latitude. The meridional and vertical transport parameters need improvements.
- (6) To derive reliable stratospheric transport models based on the ozone balloon network. We urgently need information on the efficiency of the Hadley cell, the magnitude of meridional transport in the middle stratosphere, and the magnitude of vertical transport in low, middle, and high latitudes.
- (7) To investigate thoroughly all possible ozone sources in the troposphere above the boundary layer. Recent investigations of chemical reactions have led some investigators to propose such sources, while others have disputed such mechanisms.

S.4 WATER VAPOR

In the troposphere, water vapor is the most important gas; without it, there would be neither life nor weather. By contrast, the stratosphere is dry, yet water vapor plays a decisive role in radiative transfer and atmospheric chemistry. Its global stratospheric mass of 2 to 2.5×10^{12} kg is about the same as for ozone. With the exception of CO_2 and O_3 , all other trace gases have a smaller global stratospheric mass than H_2O .

Over the years several diverse techniques have been developed to measure water vapor. Contamination around the platform and within the instrumentation package is one of the most difficult obstacles. The frostpoint hygrometer is the "simplest" and most direct instrument and has given reliable and consistent data since the mid-40's. Optical IR techniques have been widely used by measuring either solar absorption or atmospheric emission in bands or selected lines, employing spectroscopic or radiometric devices. The transfer from a measured transmittance to molecular number density (concentration), described in Section C.2, involves numerous steps fraught with the possibility of errors. The systematic errors are difficult to assess, being uncomfortably large for most optical techniques and leading to differences of the order of a factor of 2 between investigators. The precision of a single measurement is generally estimated to be only ± 10 to $\pm 30\%$. The technique and analytical parameters change from one investigator to the next, and several active groups have changed both every few years, making a comparison of the results impossible. So far, no simultaneous measurements using different techniques have been carried out or even planned. This is, however, a very important part of the assessment of the various measurement techniques. It should be high on a priority list of any future measurement program.

The field measurements of vertical profiles have been assembled in tables and graphs in Section C.3 after eliminating all those results with mixing ratios greater than 15 ppmv above 15 km.

The tables list 32 data sets. Some consist of approximately 100 single balloon flights (Mastenbrook), while most of them represent just one flight. Measurements in the 30 to 50 km range are scarce. More field measurements up to 40 km should be attempted to see if the average mixing ratio increases slightly above 30 km or remains constant, because the limited measurements point to a slightly larger mixing ratio than below. This information is crucial for a reliable estimate of the contribution by CH_4 oxidation.

For theoretical studies and for models one needs a set of good average profiles. The optical measurements and the frostpoint hygrometer measurements yield a mean value of 3.5 and 4.3 ppmv, respectively. We suggest an average of 4.15 ppmv, valid for the period 1969-70 and midlatitudes. The average mixing ratio is constant with altitude; individual profiles, however, show fluctuations which are real and in harmony with results for other trace gases. Whenever these fluctuations are smaller than the precisions of the measurements, it is best to assume a constant mixing ratio. The fluctuations for Washington, D.C., yield a standard deviation of about ± 1.1 ppmv, with extreme values of 1.5 and 10 ppmv recorded over a 10-year period. Subtracting the large long-term trend, the standard deviation amounts only to $\pm 15\%$ (± 0.6 ppmv) for Washington, D.C. and ± 10 to 20% for southern England. This value is smaller than the precision of most optical techniques.

The seasonal variations of the mean mixing ratio are of the order of ± 10 to 20% at 15 km and ± 5 to 10% at 17 to 20 km and even smaller than $\pm 5\%$ above 20 km. The annual cycle is significant for altitudes below 20 km only and of approximately the same magnitude as its aperiodic fluctuations. Long-term trends were first discovered by Mastenbrook. A continuous increase in mixing ratio occurred from 1964 to 1973, followed by a steep decrease thereafter. The increase from 1964 to 1973 amounts to 1.2 ppmv/decade (or 30%) followed by a decrease of 1 to 2 ppmv/decade from 1972 to 1976 if we use linear regression analysis. Assuming

the 1954-55 data are correct, the increase from 1954 to 1973 amounts to 86% over England. The speculative linear trend is probably not realistic; a cyclic trend seems more reasonable to us, although we have no information about the length of such a cycle. It may be longer than 12 years. We have fitted a sine curve to the data, yet future field measurements are certainly needed to determine its period and amplitude. The parallel trends in total ozone and water vapor mixing ratios from the mid 1960s to the mid 1970s may be coincidental but we believe them to be related. Consequently, it seems necessary to continue Mastenbrook's measurement program if the need arises to monitor water vapor concentrations.

Profiles up to 30 km for the tropics and polar caps are practically nonexistent. Thus, neither an average profile nor its fluctuations or temporal changes can be derived yet. Measurements of a latitudinal variation exist only for relatively low levels, quite insufficient for the tropics, where the tropopause is situated at 16 to 17 km. There exist just 6 series for limited latitude ranges, with no data at all south of about 40°S. Some sets show hardly a change, but others show changes. All mixing ratios agree fairly well at high latitudes, but diverge over the low latitudes. Around 17 km there is a maximum of 10°N and in some data sets also a decrease of perhaps 30% between 30 and 60°N. Other sets, however, yield a negligible gradient between 30 and 75°N. We believe its magnitude to be less than 20%, smaller than the seasonal and long-term variation as well as its aperiodic fluctuations. It may be buried in the noise. Thus we believe a small latitudinal gradient to be realistic in the 17 to 19 km altitude range. Above 20 km, no conclusion can be offered because the field measurements are practically nonexistent.

Measurements of water-vapor injections have been made for the intertropical convergence zone, thunderstorms, and polar jet streams. The measurements have given numerical data for a few isolated samples, namely, the influx of water vapor at the ICZ, and probably some very minor injections through thunderstorms and

large-scale eddy transport in midlatitudes. The role of hurricanes, still unexplored, should be minor because their occurrence is rare. Unfortunately, the results are incomplete because an unknown amount of the injected water vapor will be carried downward during the decay phase of the phenomena. At least we have obtained some preliminary information.

The global mass of stratospheric water vapor is estimated to be 2 to 2.5×10^{12} kg in fair agreement with earlier estimates. There exists probably a seasonal and a long-term variation of unknown magnitude.

Despite the reasonably accurate field measurements, our understanding of its sources and sinks remains incomplete. So far no more plausible explanation of the dry stratosphere has been advanced than the original one made by Dobson in 1946, who proposed that all the air entering the stratosphere is forced through the cold trap of the tropical tropopause. The Hadley cell circulation transports about 3.3×10^{17} kg air/year into the stratosphere. This value, arrived at by Ellsaesser, seems plausible, although others arrive at smaller or larger values from 0.76 to 9.7×10^{17} kg air/year. So far there is no agreement on a consistent model for the "average" Hadley cell. The temperature and pressure of the tropical tropopause undergo an annual cycle. Characteristic values are: $T = -76$ to -86°C , $P = 95$ to 115 mb. The saturation pressure of water vapor varies accordingly. This leads to a mixing ratio of 2 to 7 ppmv at the cold trap. The input of H_2O through the Hadley cell is about 1.1×10^{12} kg/year or slightly larger. Other sources, like methane oxidation and extratropical thunderstorms are estimated to add only small amounts. Some investors assume that CH_4 oxidation plays a larger role than our assessment shows. Therefore, more measurements of CH_4 should be carried out, especially in the tropical troposphere but also in the stratosphere in various latitudes up to 40 km to derive the actual CH_4 flux and determine its contribution to stratospheric water vapor concentration.

The sinks of stratospheric water vapor have been elusive. While the return Hadley cell should transport water vapor downward into the troposphere, it can handle only about 70% of the injected mass. Ellsaesser proposed that additional water vapor can freeze out during the winter months over Antarctica, where temperatures reach -80 to -100C and ice crystals fall to the ground. A search for additional sinks hinges on reliable models for the stratospheric circulation. At present they are not as good and trustworthy as we require them to be to estimate sink strength.

If it is recognized that water vapor plays a decisive role on modeling the stratospheric chemistry and in predicting changes in the atmospheric composition which are deemed detrimental to life, we recommend:

- (1) To conduct a few simultaneous measurements using balloons or aircraft by selecting a few techniques to assess the reliability of the best optical techniques and compare the results with those obtained by the frostpoint hygrometer technique.
- (2) To assess long-term variations, the frostpoint hygrometer balloon program near Washington, D.C. should be continued. A continuous series of water-vapor measurements by a proven and reliable instrument is required.
- (3) To conduct measurements to at least 40 km, preferably between 30 and 50 km in midlatitudes. They are needed to derive a reliable average mixing ratio above 30 km. This knowledge is important for estimates of the contribution by CH_4 oxidation.
- (4) To conduct latitudinal measurements of an in-situ technique at 20 km, well above the tropical stratosphere, to obtain the meridional gradient for two extreme seasons.
- (5) To carry out balloon flights in the tropics and polar cap to derive an annual average profile close to the center of the

Hadley cell and for a true polar cap condition. This is important for assessing source and sink strength.

(6) To attempt to carry out measurements in the Southern Hemisphere. The minimum would be a program to measure water vapor over Antarctica during the winter months. This is needed to assess the Antarctic sink.

(7) To carry out CH_4 measurements in the troposphere and stratosphere at various latitudes. Such measurements are important to assess the CH_4 and its contribution to the stratospheric water vapor concentration.

A. ATMOSPHERIC OZONE: THE TOTAL AMOUNT AND ITS FLUCTUATIONS

ABSTRACT

The fluctuations of the amount of total ozone are manyfold. Ozone can undergo unsystematic changes during a particular day in mid and high latitudes of up to 10%; from one day to the next up to 25 to 30% in polar regions in winter. The daily and monthly variability, low in the tropics, reaches about 6 to 14% in midlatitudes. Annual means have a standard deviation of about $\pm 3\%$. Trend analysis is reported for the period 1955 to 1976. Most of the fluctuations can be explained by changes in the stratospheric weather pattern. The global inventory, with a total mass of 3.0 to 3.4×10^{12} kg, shows good agreement among several investigators. Global and hemispherical inventories undergo some systematic variations.

A.1 INTRODUCTION

1.1 THE ROLE OF OZONE IN THE HAPP PROGRAM

In all stratospheric pollution programs, the central role is played by ozone because the ozone concentration can be modified by the addition of oxides of nitrogen (NO_x) engine effluent in the flight corridors of the lower stratosphere or by fluorocarbons diffusing into the stratosphere, where they are photochemically dissociated. The present model computations, using a very large number of chemical reactions and projected number of aircraft and projected production of fluorocarbons, show that such additions could lead to a reduction in stratospheric ozone and consequently to an increase in ultraviolet light (UV-B) reaching the ground. Recent refined model computations, however, lead to estimates of drastically smaller ozone changes than previous CIAP estimates. It is more or less accepted that an increase in UV-B can cause some types of skin cancer in man and, therefore, any decrease in total ozone from man-made pollution is considered deleterious to the biosphere.

The assessment of such perturbations caused by high flying aircraft has been discussed in detail in the Report of Findings of the Climatic Impact Assessment Program (CIAP) of the U.S. Department of Transportation (Grobecker et al. 1974) and in the Report of the National Academy of Sciences (1975); on the effects of fluorocarbons the National Academy of Sciences issued a report in 1976.

The theoretical work of CIAP has been published in the form of monographs (1975). What is known about atmospheric ozone from direct measurements can be found in Monograph 1, primarily in Chapter 3, although some facts can be found in Chapter 2 and the ozone chemistry in Chapter 5. There is no need to repeat these descriptions.

The assessment of such perturbations caused by aircraft is still going on under the High Altitude Pollution Program (HAPP) of the Federal Aviation Agency (FAA) (HAPP program plan 1976; Oliver et al. 1977). Several other government agencies are now involved in the measurements and also in the assessment of man-made pollution in the stratosphere.

We present here a discussion of the periodic and aperiodic variations and fluctuations of the amount of ozone, an aspect critical to the HAPP program and not fully or not at all discussed in the CIAP Monographs.

1.2 A BRIEF SURVEY OF ATMOSPHERIC OZONE

Ozone strongly absorbs solar UV radiation. It is also a strong emitter in the atmospheric window at $9.6 \mu\text{m}$, and both UV absorption and infrared (IR) emission play dominant roles in determining the thermal structure of the stratosphere, i.e., the temperature rise from the tropopause to the mesopause.

Routine observations of total ozone have been conducted at a large number of places all over the world since 1926 and observations of its vertical distribution at a few places since the mid 1930s. Information of the distribution of total ozone with latitude and season and of ozone distributions with height have been summarized by Dütsch (1971, 1974) and others. While the total ozone reaches a maximum at polar and subpolar latitudes during spring in each hemisphere, it drops to a minimum in equatorial regions with negligible seasonal variations.

The ozone mixing ratio is about 10^{-8} near the ground; it is reasonably constant in the troposphere, due to strong mixing, and increases in the lower stratosphere to a maximum of about 10^{-5} at a height of 30 to 35 km in the tropics. Above 35 km the volume mixing ratio decreases steadily with altitude to about 2×10^{-6} in 50 km. There the variations with latitude and season are

small and ozone is in photochemical equilibrium. Below 35 km, however, the ozone has a relatively long photochemical relaxation time, or time of half restoration, perhaps a week, increasing to several years at the tropopause. Consequently, photochemistry determines the global ozone distribution above 35 km and transport processes below that altitude.

The concentration reaches its maximum at much lower altitudes than the mixing ratio, at about 27 km in the tropics with a concentration of about 150 nb ($400 \mu\text{g}/\text{m}^3$) and about 17 to 20 km in polar regions with a concentration of 140 to 200 nb (375 to $530 \mu\text{g}/\text{m}^3$). Thus, most of the ozone mass is under the influence of atmospheric transport phenomena: horizontal large scale transport, vertical transport, and small scale turbulence, leading to large day-to-day variations. The changes in its vertical distribution and thus of its mass are associated with large scale weather patterns in the lower stratosphere (12 to 25 km). Ozone variations are largest in the subpolar regions during winter when temperature and wind variations are large. There is also a quasibiennial variation of about 26 months, mainly in the tropics, but of smaller magnitude noticeable also in winter in midlatitudes. The very large seasonal variation dominates all fluctuations. Finally, the long term variations are somewhat unsystematic, of the order of 5 to 10% over periods of decades and probably related to the changes in the general circulation.

The literature on atmospheric ozone is extensive. We have selected only the most noteworthy contributions and the best examples of careful data evaluation based on the longest available series of measurements. Often the investigators returned to the same subject after accumulating more relevant measurements. In this case only the most recent publications are cited. We realize of course that other investigators may have occasionally selected or added another paper or report. The reader should be aware of these selection rules when using this report and its list of references.

A.2 VARIATIONS IN TOTAL OZONE

Measurements have shown a multitude of variations in total ozone, although good statistical investigations have been made only sporadically. We believe, however, that they are very important in relation to model computations, which normally select only an average without regard to its standard deviation.

2.1 DIURNAL VARIATION

During the course of a day, the total amount of ozone remains more or less constant. On some days, however, especially in spring, drastic changes occur, related to the stratospheric weather pattern.

It has been proven that the solar altitude did not influence the determination of total ozone using the Dobson spectrophotometer. This is a very important point. Despite the strong variation of the effective thickness of the ozone layer with the change in zenith distance of the sun from sunrise to noon, as shown in the upper part of Figure A1, the total ozone stays constant for all three pairs of wavelengths, with a deviation of about $\pm 0.5\%$ before noon (lower part of Figure A1) and a total variation from minimum to maximum of about 1.4%.* Such high internal accuracy can be obtained at a high altitude station like Arosa, 1900 m, where the aerosol scattering plays such a minor role. Hence it does not matter at what time of day the measurements are made.

Of course, there are days when the total ozone undergoes some changes, and Götz (1940) published three good examples of diurnal variations; these examples are reproduced in Figure A2. The following text gives the amounts in the new scale.* On 30

*Figures 1 and 2 give the ozone data in the old scale; thus, multiply all data in the figure by 1.35 to obtain the results in the presently used scale (since 1957).

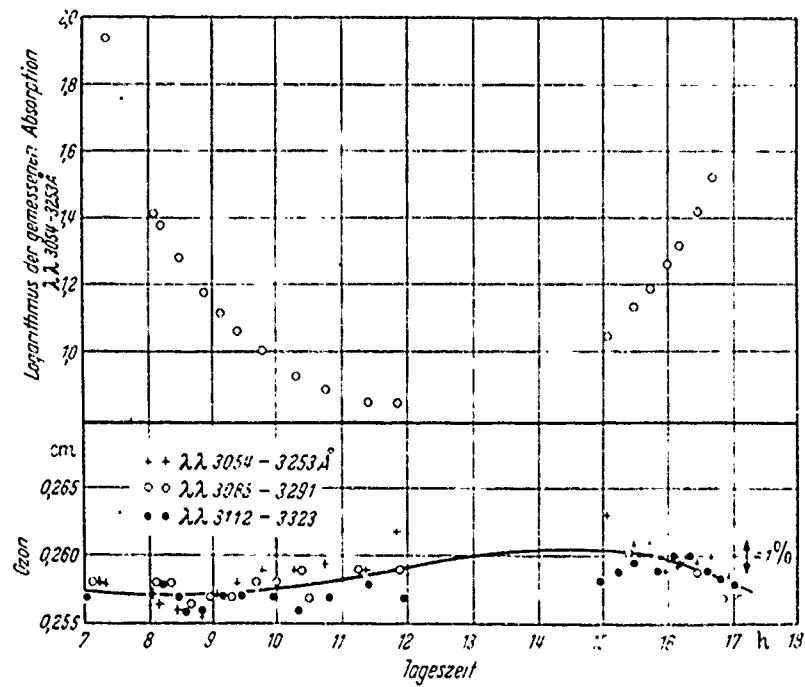


Figure A1 Ozone Measurements During a Day at Arosa Using the Dobson Spectrophotometer. (Source: Götz.) Upper curve: Logarithm of measured absorption. Lower curve: total ozone in atm cm, old scale. This proves total ozone measurements are independent of the solar altitude, or airmass.

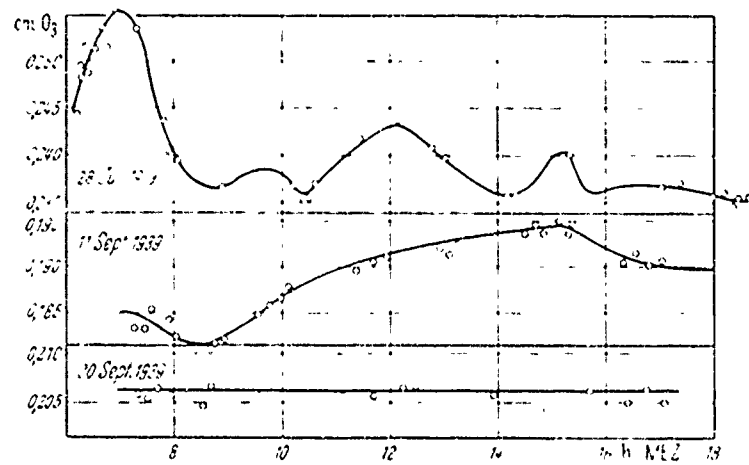


Figure A2 Aperiodic Variation of Total Ozone During a Day in Arosa. Three days are selected with quite different diurnal variation. (Source: Götz 1940.) They are typically aperiodic variations. Note the old scale.

September 1939, the total ozone of 0.278 atm cm does not change at all during the day within the accuracy of the measurements. The second example, for 11 September 1939, shows a steady increase of about 7% from 8:30 A.M. to 3:00 P.M. and a slight decline thereafter. The extrema are 0.244 and 0.263 atm cm or a diurnal variation of 0.019 atm cm. The third case, of 28 July 1939, shows a strong variation during the day, as if "ozone clouds" passed over the station. The extrema of 0.317 and 0.344 atm cm correspond to a variation of 8.5%, although some of the "clouds" show increases of only 1 to 3%. Such changes are probably related to the passage of weather fronts or to the advection of polar air in the lower stratosphere.

A more recent example has been published by Dütsch (1974) for 16 April 1962. On that day ozone decreased during the sunlit hours from 0.455 to 0.375 atm cm, amounting to about 18%. The rapidity with which ozone can change has also been well documented by Kerr (1973). During 1971-72 he used the Dobson instrument at Toronto, Ontario, Canada, to study such sudden diurnal changes. As the most extreme case, he found a change of 0.05 atm cm in one hour, with short-term changes of 0.01 atm cm to occur often within 30 to 60 minutes.

Such examples indicate that a single measurement, usually at 11:00 A.M. (as prescribed by the ozone handbook), may not represent the true ozone value for this day, yet the deviations will amount to just a few percent in midlatitudes and much less in tropical latitudes. Such aperiodic diurnal fluctuations may, however, hamper comparisons between ground-based and satellite measurements if both are taken several hours apart, more so in spring than in fall.

We can summarize the knowledge about diurnal variations as follows: they can occur; they are aperiodic, related to changes in the general weather pattern, large in spring and small in fall, and they increase with latitude. On most days the variations are

small; only occasionally may they reach 10% or more in middle and high latitudes.

2.2 INTERDIURNAL VARIABILITY

The first ozone measurements by Fabry and Buisson in 1920 showed surprisingly large variations from one day to the next. The magnitude of such interdiurnal variations is now well documented for at least two locations. Table A1 shows the interdiurnal variability for Tromsø after Penndorf (1950a) and for Arosa after Götz (1950). The average increases and decreases for each month are based on several years of observations, namely 1926-42 for Tromsø and probably a similar length for Arosa. The average variability is about 4 to 7% for Arosa and about 4 to 27% for Tromsø, and its seasonal variation is well pronounced.

Figure A3 is an histogram of the interdiurnal variation for Tromsø using class intervals of 5×10^{-3} atm cm. Since the number of pairs varied from month to month, relative frequencies are shown. The area of each rectangle is a measure of the frequency for each class in percent of the monthly total. During winter, the distribution is flat and looks more like a random distribution, but from March to October a more or less "normal" distribution emerges. The class interval is based on the old scale and corresponds to 6.7×10^{-3} atm cm in the new scale. The numbers in the table, however, are in the new scale.

In summary, the interdiurnal variability is small in the tropics and largest in polar regions in winter, perhaps up to 25 to 30% on the average, and during the summer it is small, about 4% on the average. There are no data for U.S. stations, but such statistics could easily be obtained from the records.

2.3 DAILY VARIABILITY

A statistical examination of the daily ozone values leads to a monthly average and its standard deviations (σ), which is the

TABLE A1
INTERDIURNAL VARIABILITY IN TOTAL OZONE*
(10^{-3} atm cm)

LOCATION	J	F	M	A	M	J	J	A	S	O	N	D
Tromsø	56	32	24	22	17	16	14	13	13	21	44	67
Arosa	23	23	20	20	15	14	14	12	11	12	14	18

*The monthly average of the increases and decreases is given.

TABLE A2
DAILY VARIABILITY OF TOTAL OZONE
(10^{-3} atm cm)

LOCATION	8	J	F	M	A	M	J	J	A	S	O	N	D
Resolute	75	-	-	44	38	23	17	14	27	17	25	-	-
Tromsø	69	65	45	30	25	23	18	13	14	14	25	50	76
Arosa	47	44	50	43	36	29	23	20	18	20	23	26	33
Kodaikanal	10	6	7	5	5	6	7	4	5	5	3	2	3
Ozone gradient	30-50	50	70	70	70	60	50	45	38	25	25	30	25

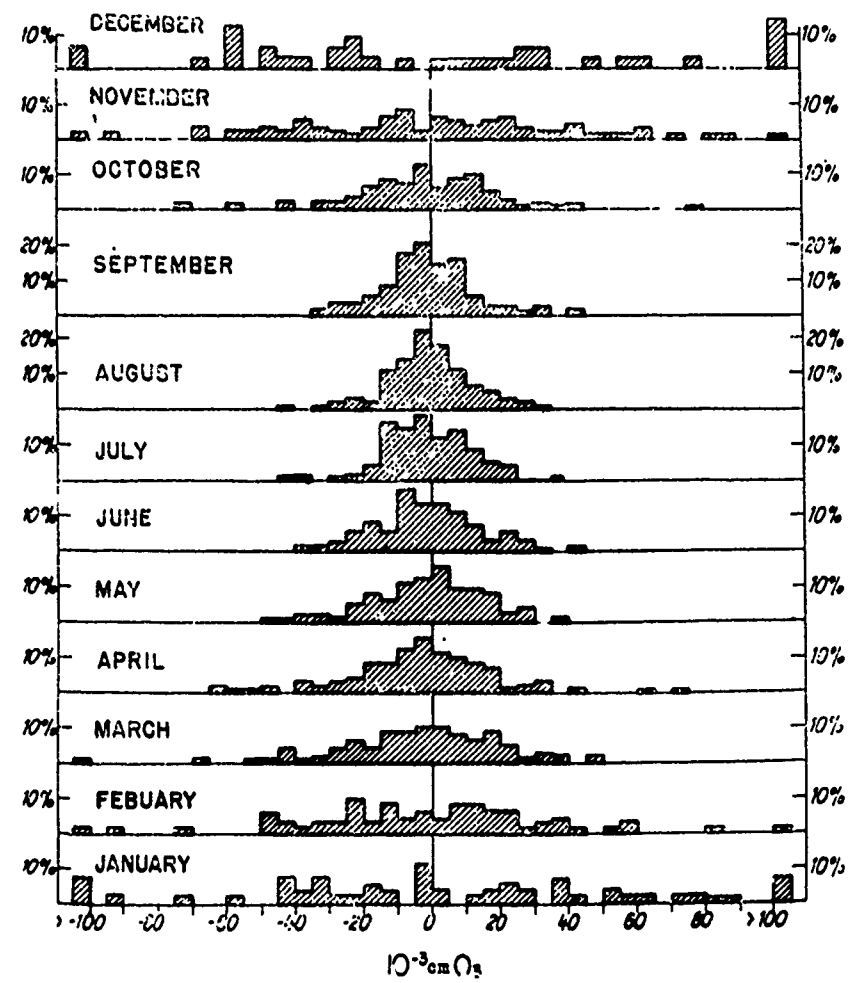


Figure A3 Histogram of Interdiurnal Variation of the Amount of Ozone Over Tromsø, Norway, for Each Month of the Year for the Period 1926-1942. Relative frequencies are given in percent for class intervals of 5×10^{-3} cm ozone. (Source: Penndorf 1950a.)

best measure of the scatter of data, or of its daily variability. From the literature, we select in Table A2 a few of the results taken from Khrgian (1973, p. 190); those for Tromsø are from Penndorf (1950a) and those for Arosa from Dütsch (1974). Khrgian lists results for a few more stations, not reproduced here, because we find our listing sufficient to draw the general conclusions. Most of his data are based only on the short IGY series; those for Tromsø are for the period 1926-42 and for Arosa from 1926-73.

The daily variability is small in the tropics, 1.5 to 3%, but large in mid- and high latitudes. For Arosa, it declines from 14% in February to 6% in July and August, and similar values apply to the polar region, with somewhat higher values in winter. The gradient in total ozone between 30 and 50°N, taken from the isopleths constructed by Dütsch (1971, see Figure A13), is given in the last line and shows a similar trend as the daily variability. Between these latitudes the ozone gradient is largest. The daily variability is a clear sign of the role of transport and the relationship between total ozone and weather.

The uneven ozone distribution with longitude along a particular latitude can best be seen on the monthly maps produced by London et al. (1976) for the years 1957-1967. They also show this variability for January and July in map form for both hemispheres, amounting to about 2% in the tropics and 15 to 20% in polar regions, especially during the winter season. For the U.S., the variability is, in general, smaller than 5%. The results, based on a 10-year sample, should apply for any period.

For Arosa and Tromsø, we have given, in Figure A4, the monthly average and its standard deviation. Thus, 68% of all daily observations are within the upper and lower curves. The band of the most probable ozone values is wide in winter and narrow in summer and fall; for Tromsø the widening starts in October and is largest in December and January. It is important to note that 32% of all data still fall outside of this band.

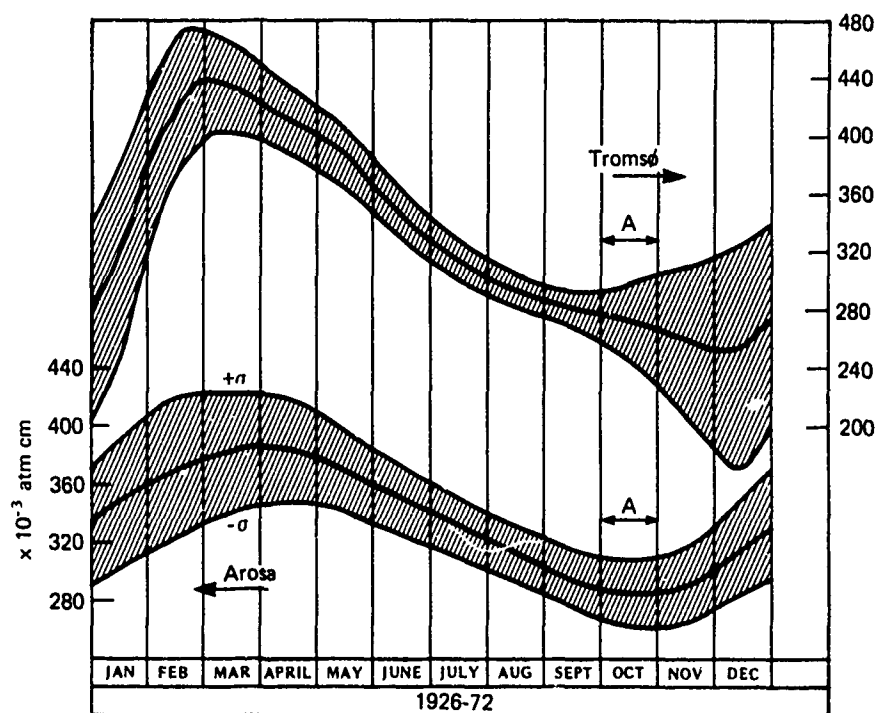


Figure A4 Monthly Mean Values of Total Ozone and Standard Deviation. Forty-five years of observation for Arosa. (Source: Dütsch 1973.) Tromsø data from 1926-1942. (Source: Penndorf 1950a.) The seasonal variation is very pronounced. The variability of the monthly mean is large. "A" stands for long-term annual average.

The latitudinal and seasonal variation of the standard variation of the monthly averages is consistent with similar variations of other meteorological elements in the upper troposphere and lower stratosphere. This similarity supports the view that the major fluctuations in total ozone are closely associated with meteorological processes.

2.4 MONTHLY AVERAGES, THEIR VARIABILITY AND TRENDS

It is customary to compute monthly averages, and Figure A5 displays the data for January, March, July, and October for Arosa since 1926. There appears no obvious "trend" but an unsystematic change from one year to the next. Smoothing by hanning (1-2-1) seems to result in a more acceptable curve, although it hides the true year-to-year change. We computed it but do not show it, because it would smear the curves too much. But we do show the \pm limits together with the long-term average to indicate the variability of such monthly averages for a single station. Extremely high values appear in the years 1940-42, and also in the 1960s, but the most outstanding peak is the 1940 anomaly, which was also observed at other European stations.

An inspection of the figure shows that, for a particular year, ozone may be high in one month but just about normal in another month, for example, in 1944; and for 1971-74 the March values fall rapidly while the October values rise. Such results strongly suggest not to use the data for one particular month for a trend analysis.

We also computed averages from July, August, and September for Arosa; these are the months in which people are exposed to a lot of UV radiation, and we show the results in Figure A6. The long-term average is 307 ± 11.0 atm-cm. The year to year changes still appear, reaching $\pm 10\%$ in 1940 and 1958, although the average variability is $\pm 3.5\%$. To detect a trend of (for example) -5% will require several years of observations to be certain that the decrease is larger than the normal variability.

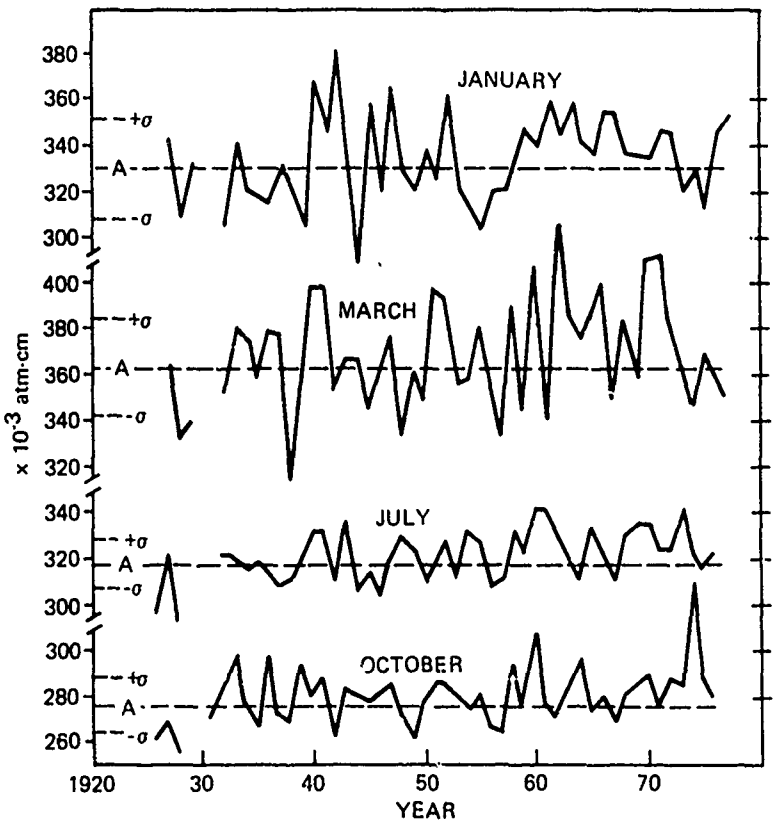


Figure A5 Monthly Mean Values of Total Ozone at Arosa for the Period 1926-1976; January, March, July, and October. Raw data, no smoothing applied. "A" stands for long-term average, one standard deviation is indicated by σ .

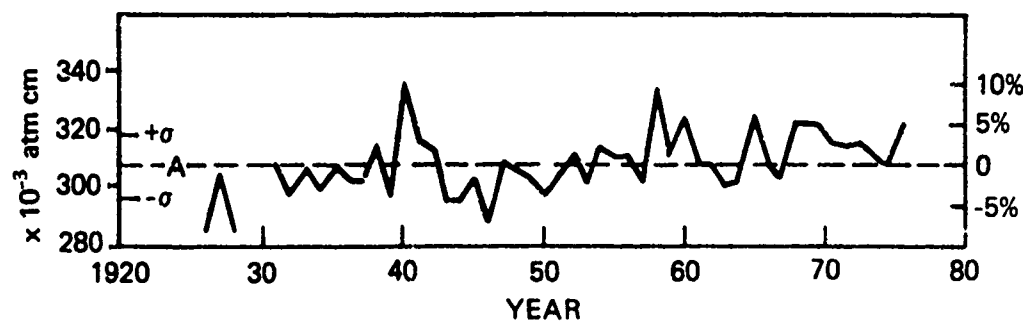


Figure A6 Average of Three Monthly Mean Values, July to September at Arosa for the Period 1926-76. "A" stands for long term average, one standard deviation σ is indicated. At the right hand side deviation in percent.

The standard deviation, σ , or variability, of the monthly averages is listed in Table A3 for Tromsø and Arosa. The seasonal trend of σ is, as expected, larger in Tromsø than in Arosa: 14 and 6%, respectively, during winter and spring, but during the summer they are of the same magnitude, about 3%.

According to Dütsch (1974, his Figure 20), the biennial variation shows up in midlatitudes only in winter when its amplitude can add a few percent to the monthly average value; the rest of the year its amplitude is negligible. Analyzing total ozone data from 1957 to 1972, Wilcox et al. (1977) found the maximum of the annual wave along the east coast of Asia with an amplitude of 0.12 atm cm. The quasibiennial oscillation reaches a maximum in eastern Siberia with an amplitude of 0.02 atm cm, and the semi-annual wave reaches a maximum at high latitudes with an amplitude of 0.025 atm cm.

Predicting the monthly averages depends on a forecast of the general circulation, and long-range weather forecasts are notoriously unreliable. Hill and Sheldon (1975) model statistically the monthly ozone values for Arosa by using past data and a time series analysis, including a 25-month (biennial) and 22-year (sunspot) cycle. Their predictions are, however, meaningless, because the predicted monthly values have an uncertainty of $\pm 29 \times 10^{-3}$ atm cm.* From Table A3, we can see that the standard deviation for all months is smaller than their uncertainty. Normally a "prediction" within the limits of one standard deviation is not considered useful, but, in the case of Hill and Sheldon, their uncertainty is 2 to 3 times one standard deviation.

A well known graph of the monthly averages for Arosa for the period 1932-64, by Newell, has been extended to 1976 in Figure A7. These are the raw data from which many trend analyses have been made, and this is the longest series in existence.

*At the 95% confidence level.

TABLE A3
 VARIABILITY OF THE MONTHLY AVERAGES OF TOTAL
 OZONE AT TROMSØ AND AROSA
 (10^{-3} atm cm)

LOCATION	PERIOD	J	F	M	A	M	J	J	A	S	O	N	D
Tromsø	1935-59	70	54	33	23	78	14	12	14	9	16	28	50
Arosa	1926-59	21	22	21	19	14	11	10	10	12	11	9	15

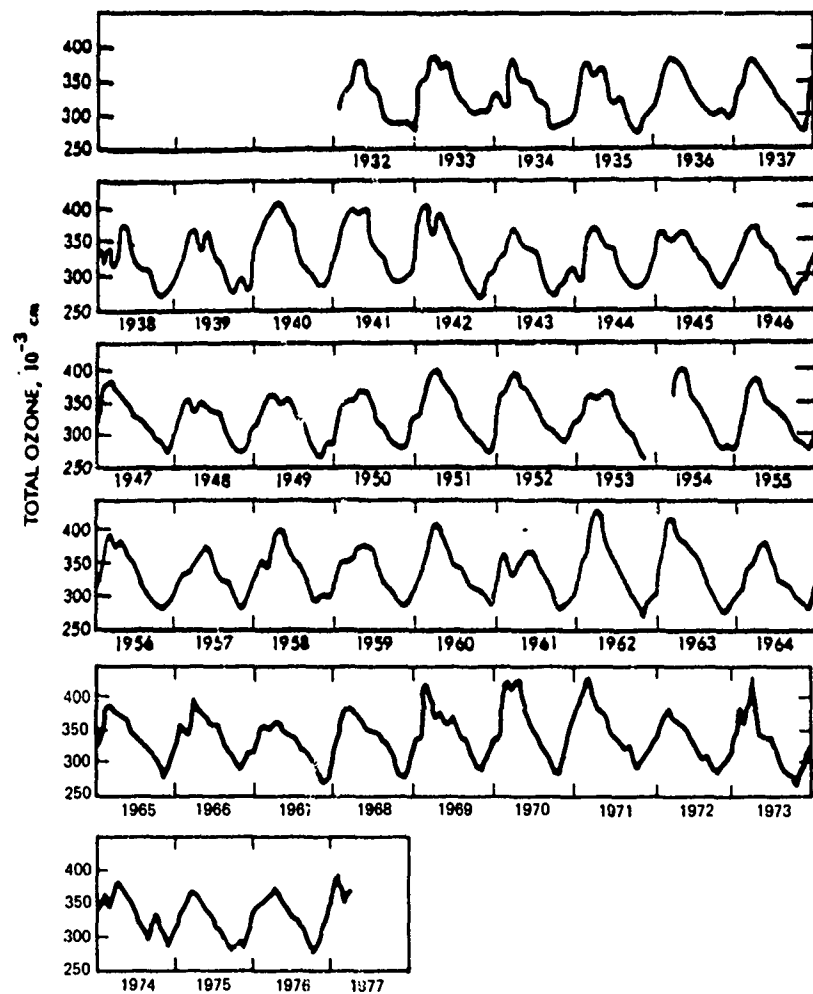


Figure A7 Monthly Mean Values of Total Ozone at Arosa. The figure clearly shows the dominant seasonal variation. Source: Wallace and Newell (1966) for the period 1932-1964. Completed to 1977 by the author.

2.5 ANNUAL AVERAGES AND THEIR LONG-TERM TRENDS

The annual averages for Arosa are displayed in Figure A8 for the period 1927-1976. The long-term average of 47 years is $326 \pm 10.2 \times 10^{-3}$ atm cm for this period. For shorter periods it is $322 \pm 9.3 \times 10^{-3}$ for the period 1927-58 and $333 \pm 7.9 \times 10^{-3}$ for the period 1958-76. In this figure, we indicate the 1926-58 average and standard deviation on the right. The standard deviation, approximately $\pm 3\%$, is fairly large. Averages for single years can be low or high; for example, 1928 was 6.7% below and 1940-41 as well as 1969 and 1970 were about 6% ($= 2\sigma$) above the longterm average. The 1960's were, in general, well above the average, but abruptly decreased thereafter and are now around the longterm average.

Khrgian (1973, p. 189,191) published some curves of annual averages for selected stations. Unfortunately, his list is based on 1- to 13-year averages and therefore the data are not strictly comparable. For any serious investigation, the data must be for the same period or the conclusions are meaningless.

Dütsch (1974) investigated "trends" for the Arosa data by computing 5-, 7-, 10-, and 20-year running means. The magnitude of observational trend, as one can see in Figure A9, is rapidly decreasing with the increasing length of the period for which the trend is computed. The largest trends occurred around 1940, but the steady increase in the 1960s is also obvious. The last period has been investigated fairly extensively, and is described below.

The amount of total ozone was large in the 1960s, as we have discussed above for Arosa, but also at many other places, and it aroused great interest in connection with the CIAP program and nuclear explosions producing large amounts of nitric oxide (NO).

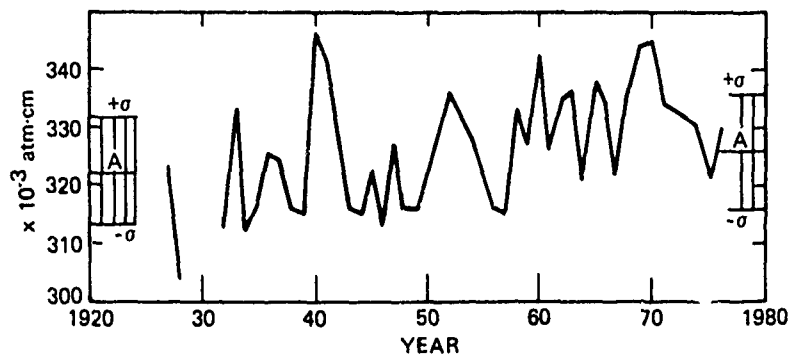


Figure A8 Annual Mean Value of Total Ozone at Arosa in 10^{-3} atm cm for the Period 1927-76. Raw data, no smoothing applied. Left hand side, A = Average and ± 5 for the period 1926-58. Right hand side: same but for period 1926-76.

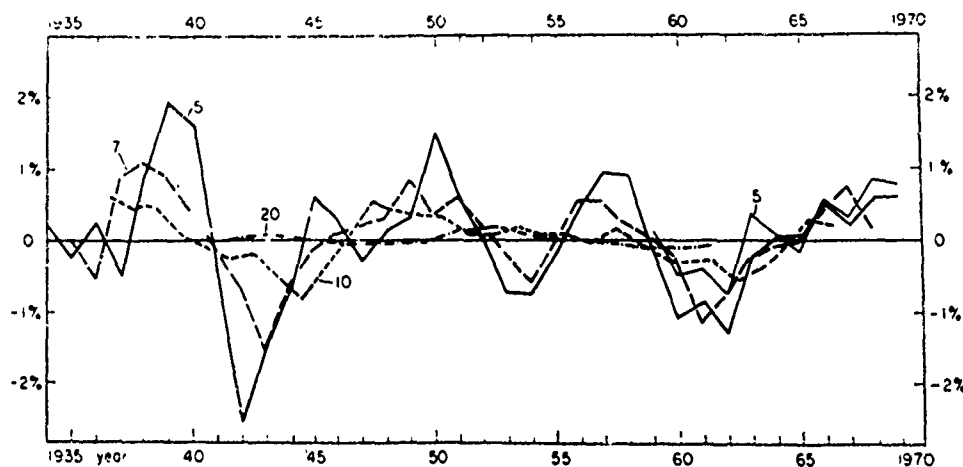


Figure A9 The Variability of "Trends" in Ozone Content With Time and the Dependence of the Trend Intensity on the Length of the Chosen Trend Period (the center date of the period is shown) Computed from the Observational Series at Arosa. C wavelength data were used; after 1959 trends (5 year period) for AD data are shown for comparison (Source: Dütsch 1974).

Thus, the question of total ozone reductions during the 1962 test series was raised and its effects on global ozone over a long time span. However, extrapolations of short time series are always full of pitfalls and this case is no exception.

An increasing trend in total ozone for the decade 1960-1970 was first reported by Komhyr et al. (1971) and was based on a few selected stations. The trend was then thoroughly investigated by several authors (Angell and Korshover 1973, 1976, 1978; London and Kelley 1974; Johnston et al. 1973). The method of these investigations differs, but each one is described in detail in CIAP Monograph 1 (Chapter 8.2). The results are of great interest and are given in Tables A4 and A5.

The trend analysis for selected groups of stations, by Angell and Korshover in 1976, using dates from 1955 to 1974, is reproduced in Table A5. In general, the trend in the Northern Hemisphere is negative for 1960-1961 and 1970-74, but positive from 1962-70. Their percentage changes apply for the given period only and are not reduced to a decade as in Table A4. Obviously, the magnitude of such trends differs markedly from one geographic area to another and seems to be related to changes in the general circulation; see also Birrer (1974).

For the Southern Hemisphere, Kulkarni (1976) found a decreasing trend at Aspendale, Australia, but not at other stations, to be statistically significant. His results for the years 1957-74 are given in Table A6 after conversion to percents and reducing to one decade. The decrease in total ozone at Aspendale amounts to 4.4% over an 18-year period. The temperature at 100 mb shows the same amount of cooling at all four stations during those 12 years.

TABLE A4
TRENDS IN TOTAL OZONE*

Investigators	Time Period	Northern Hemisphere	Southern Hemisphere	Globe
Angell & Korshover (1973)	1955-70	+ 3.9	- 1.2	+ 1.5
London & Kelley	1957-61	- 2.4 ± 1.1		
	1962-70	+11. ± 3.5		
Johnston et al.	1957-62	- 2.7 ± 1.0		
	1963-70	+ 4.5 ± 0.6		

*The numbers are percent increase or decrease per decade in total amount of ozone for the whole globe or in each hemisphere.

TABLE A5
PERCENTAGE CHANGE IN TOTAL OZONE IN THE
GIVEN REGIONS (ORDERED BY MEAN LATITUDE) FOR THE GIVEN PERIOD INTERVALS*

Region	1960-62	1962-70	1970-72	1955-70
Russian Arctic (72°N)		4	-2	
West Arctic (70°N)	-1	6	-1	
European Russia (51°N)	-2	8	-1	4 (1958-70)
Asiatic Russia (51°N)		5	0	
East Europe (51°N)		3 (1963-70)	-2	
West Europe (48°N)	-2	4	-1	7
North America (45°N)	-1	3	-1	
Japan (37°N)	1	1	-1	0 (1958-70)
India (21°N)	2	4	-1	8
South Tropics (8°S)		3 (1964-70)	0	
Pretoria-Buenos Aires (30°S)		-2 (1966-70)	-1	
Australia (40°S)	0	0	-1	-2
Antarctica (78°S)	-1	0 (1962-68)		

*The numbers in parentheses indicate the slightly different period intervals for some regions.

TABLE A6
TRENDS IN TOTAL OZONE, SOUTHERN HEMISPHERE, 1957-1974*

Station	Geogr. Lat.	1963-74	1957-74	ΔT at 100 mb 1963-74 ($^{\circ}$ C)
Darwin	12	+0.3 \pm 1.4		-1.6 \pm 0.4
Brisbane	27	-1.1 \pm 1.1	-0.4 \pm 0.8	-1.5 \pm 0.7
Aspendale	38	-3.4 \pm 1.0	-2.4 \pm 0.9	-1.1 \pm 0.7
Macquarie Island	54	-1.7 \pm 6.7		-1.5 \pm 1.0

*The numbers are percent increases or decreases per decade in amount of total ozone.

An updated investigation by Angell and Korshover (1978) includes data up to 1976 and is based on seasonal mean values smoothed by standard procedures. These results are shown in Figure A10 as the latest in these trend investigations for the Northern Hemisphere. There exists a sharp rise for the Soviet Union stations between 1967 and 1970. For North America, there are peaks in 1965 and 1970 with a strong minimum in the spring of 1976, about 3% below the average. The European stations, excluding Russia, indicate behavior similar to those for North America. Results for Japan are totally different. There is no longer a clear long-term trend either upward or downward as suggested in the 1973 publications by various authors. Angell and Korshover relate these seemingly aperiodic variations to such phenomena as the biennial oscillation; there exists perhaps a very minor solar cycle variation. Some of the variations are related to changes in the general circulation, but have not been identified in any concrete way.

Angell and Korshover also derive some zonal averages by giving each geographic area a particular weight, a process with which others probably disagree. In their zonal averages they find no proof for any anthropogenic influence, nor for nuclear effects, solar proton events, or volcanic eruptions, a result with which we agree.

The first reports, sounding an alarm of steadily rising amounts of ozone and based on a few years of data, have now been proven wrong. What we had seen in the long series of data for Arosa, Figure A8, is found in the 20 years of observations on a global scale, i.e., that the amount of total ozone is undergoing aperiodic increases and decreases of a few percent, larger in some areas of the world than in others and seemingly similar in Europe and North America but dissimilar in other areas. It shows how difficult it will be to prove a 1 or 2% change in total ozone from man-made pollution within a period of a few years.

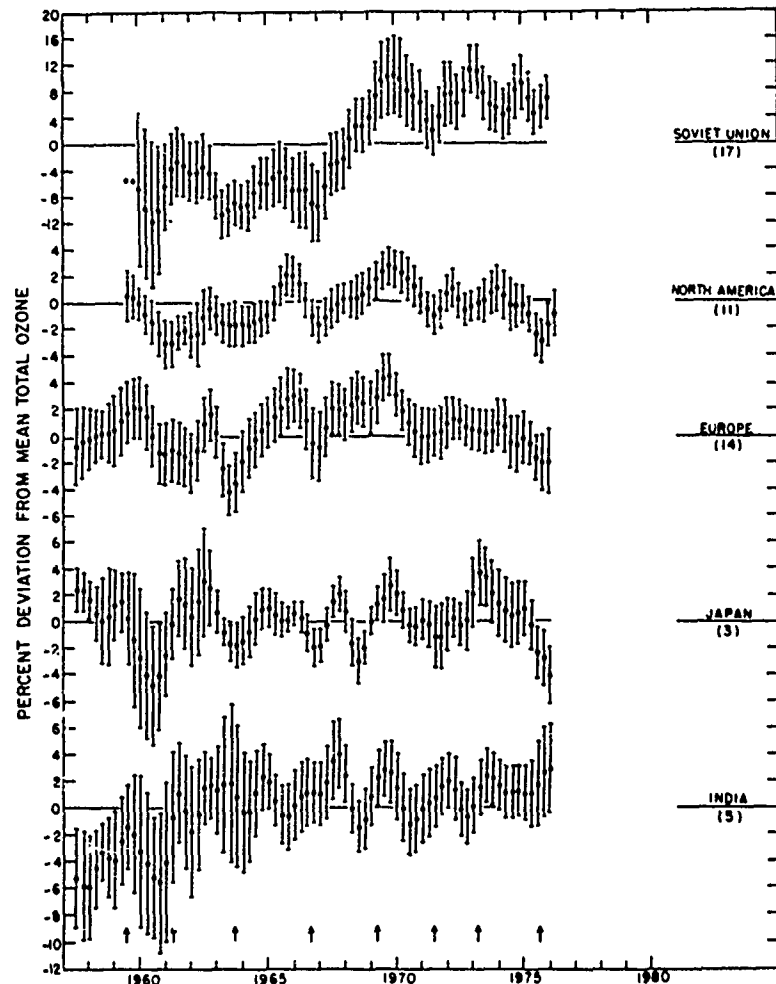


Figure A10 Variation in Seasonal-mean Total Ozone (expressed as a percentage deviation from the mean) for the Five Data Regions in North Temperate Latitudes (Source: Angell and Korshover 1978). The vertical bars extend two standard deviations of the mean either side of the mean, and the usual number of stations on which the analysis is based is given in parentheses at right. A 1-2-1 smoothing (divided by 4) has been applied twice to the successive seasonal values (1-1 at beginning and end of record. The vertical arrows indicate the time of quasi-biennial west wind maximum at 50 mb in the tropics, while the tick marks are in summer of the given year.

This section on trends is a classical example demonstrating that one ought not to get overly excited if ozone increases or decreases for a few years, to extrapolate "trends", and to assign unproven causes to such "trends."

The amplitude of the sunspot cycle, if it exists at all in the total ozone, is very small. Many investigations have been conducted on this subject over the years with conflicting results. Nevertheless, investigators agree that its amplitude is very small indeed and may be close to zero. For the ozone concentration above 30 km, such a sunspot cycle effect has been proven (Paetzold 1973, Dütsch 1976); but there is very little ozone at these altitudes and its contribution to the total ozone is definitely small.

A few words should be added about the value of historical data. As stated before, the first measurements of total ozone at Marseille, France were made by Fabry and Buisson in 1920 (May and June), and they obtained and published (Fabry 1950) values between 0.275 and 0.335 atm cm with an average of 0.303. This result is in the same range as those we find today. However, the accepted absorption coefficients of ozone in the UV have changed slightly from time to time. Fabry and Buisson used their absorption coefficients measured in 1913. There have been many investigations after that, and each one is slightly different from the others. For many years, those by Ny and Choong (1933) were regarded as standard; later, measurements by A. and E. Vassy came into use; and finally those by Vigroux (1953) were adopted as standard by the International Ozone Commission for 1957 and after. The older scales are, of course, used in the various publications and the following table should be helpful in interpreting such old data. To obtain data in the present scale, the old data should be multiplied by the following factors:

Before 1939	1939-1957	After 1957
1.19	1.35	1.0

If old data look strange, one should check to determine if they fit after the correction to the present scale has been used.

Perl and Dütsch (1958) have reanalyzed all ozone measurements in Arosa from 1926 to 1958 and published daily measurements in the 1939-57 Dobson scale. The quality of these data is as good as those obtained today, because Götz was a very careful and competent experimenter.

2.6 OZONE AND WEATHER

From the first ozone network in Europe in 1926-27, Dobson et al. (1927) deduced a distribution of total ozone related to surface pressure systems, i.e., cyclones and anticyclones. At that time Dobson published selected weather maps for 1926 with the measured ozone values. Dobson came back to this idea from time to time (1973) fortifying his basic findings: low total ozone is correlated with high pressure and high ozone with cyclones. In Figure A11, we show his basic results, i.e., that in the rear of a moving cyclone the total ozone is 120% and west of an anticyclone the total ozone is decreased to 70% of its "normal" value. Big jumps can occur with the passage of fronts. Normand, in 1953, extended the results to pressure troughs (high ozone) and ridges (low ozone), where increases and decreases of about 15% are found for Western Europe.

In 1937 Meetham found correlations between variations in total ozone and height of the tropopause and similar parameters of the low stratosphere. Others have added to his basic findings, but all the numerical results apply to Europe and not to America. Tønsberg and Olsen (1944) found good correlation of changes in ozone and surface fronts for Northern Norway; Moser (1949) and Penndorf (1950b) obtained good correlations of ozone with upper air trajectories at 11 and 16 km, respectively.

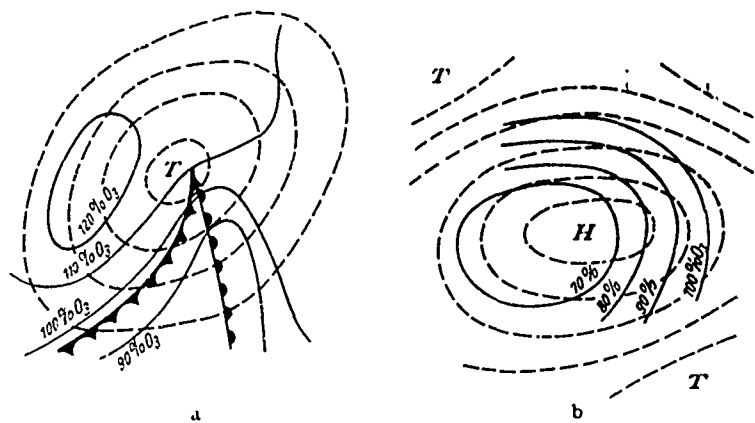


Figure A11 Total Ozone and Pressure Distribution After Dobson. Left cyclone, right anticyclone. The ozone increase or reduction is given in percent of the normal mean value for the undisturbed condition of this month.

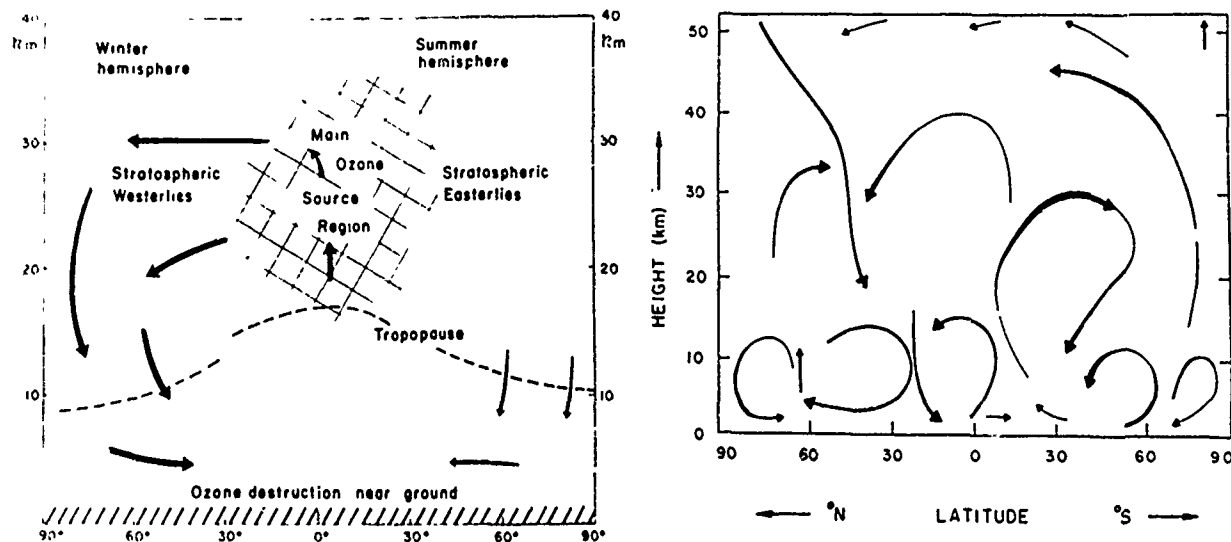


Figure A12 Tentative Models of the General Circulation as it Affects the Ozone Flux in the Stratosphere. Left: model proposed by Dutsch, 1974. Right: model proposed by London, 1975.

All this information points to the dominant role of advection at the height of the ozone maximum (concentration) and midlatitudes. Since the ozone shows a large meridional variation, especially during winter and spring, the advection from the north will bring in air with high ozone, and an advection from the south will bring in the opposite. Besides advection there is an influence of vertical motion and convergence and divergence. Although it has been discussed by several investigators, no real numerical calculations have been published. The reason is simple: the network of ozonesondes is not dense, and the magnitude of stratospheric transport parameters is not well known.

There are some general schemes for such stratospheric transport, and we select, in Figure A12, the models proposed by Dütsch (1971) and by London (1975). The Hadley cell circulation must play a role in transporting ozone from its source region at 30 km and above into the polar regions, but there are also downward components acting in the polar region. The circulation has to be closed.

The finding that anticyclones correlate with low total ozone is important. In this type of weather, people spend a lot of time outside because cloudiness is very low. On the other hand, cyclones are connected with cloudy and rainy weather and that is the time when people do not go to the beach or enjoy the outdoors. Thus, people will actually be exposed to low total ozone, i.e., high values of UV radiation. Consequently, the monthly average ozone values overestimate the ozone shield for outside activities. For skin cancer studies, one should arrange the ozone values according to cloudiness to obtain the actual effective mean values.

2.7 PERTURBATIONS

Predicted changes in total ozone following such perturbations as nuclear tests, cosmic-ray intensity variations during a solar

cycle, polar cap absorption events, and volcanic eruptions cannot be clearly identified in the ozone observational network. This indicates that although small local short-time changes may occur, the diffusion acts to obliterate them in a relatively short time and none of these has any influence on global ozone.

2.8 DENSITY OF NETWORK

What is the necessary density of a ground network to detect possible trends in total ozone? This question is important in relation to the discussion of monitoring ozone for possible influences caused by man-made changes in the stratospheric chemistry. The significance of a trend, or, equivalently, the standard error of point or area means is properly derived from temporal and spatial auto-correlations. Wilcox (1978) derived them for midlatitudes from 15 years of daily Dobson data. The characteristic time between effectively independent observations is about 4 days and for spatial distances about 20° in longitude. Such investigations are necessary to plan a proper network of stations.

2.9 AMPLITUDE COMPARISON

This section on variations in total ozone can best be summarized in Table A7. The amplitudes of the periodic variations are given first with the "U.S." values applying for the "lower 48," and they are, of course, somewhat smaller than those found in polar regions, which show the maxima. Clearly the annual wave stands out. Among the aperiodic fluctuations, the largest amplitudes are measured for the changes caused by the passage of active weather systems, and this is, of course, also the main contributor to the daily standard deviation. The last two and the annual wave are each of the order of $\pm 25\%$ or more in high latitudes and $\pm 12\%$ or more in the U.S. The solar cycle variation, if it exists at all, is buried in the noise, and the long-term variations are also small in most parts of the world. Both have received too much

TABLE A7
MAGNITUDES OF PERIODIC AND APERIODIC VARIATIONS
(amplitudes in % of mean values)

<u>A. Periodic</u>	Max. Amplitude Northern Hemisphere	Amplitude in U.S.
Annual wave	± 33	± 12
Semiannual wave	± 8	± 2
Quasibiennial wave	± 6	± 2
Solar cycle	± <2	± <2
<u>B. Aperiodic</u>		
Daily standard dev.		
January	± 25	± 8 to 12
July	± 15	± 4 to 6
"Weather" (Pressure pattern)	± 25	± 15
Long-term variation		
Areas	± 10	± 3
Global	± <3	-

attention and study, but are not very significant in comparison to the major variations. Obviously, the detection of small trends can be quite difficult.

A.3 GLOBAL DISTRIBUTION OF OZONE

3.1 LATITUDINAL DISTRIBUTION

Maps of average distribution of ozone over the globe have been constructed by several investigators, starting with Dobson in 1926. The first isopleth representation by Götz in 1934 correctly showed the basic pattern, i.e., low tropical values and high values in the polar region with maxima in March. The present data are best represented by the map constructed by Dütsch (1971), replotted with $\sin \delta$ as ordinate and shown on Figure A13. From this map the global ozone can be correctly estimated (see Section 3.2). It tells us that more than 50% of the globe (the low latitudes) experience only small seasonal variations of ozone and that large seasonal variations are restricted to the mid- and polar latitudes. The hemispherical differences are very marked, with a maximum near the North Pole in March/April, and between 50 and 70°South in September/October. These differences are due to the differences in stratospheric circulation for both hemispheres, because the Antarctic continent, being very cold and high, modifies the Southern Hemisphere circulation south of 50°.

An interesting distribution is derived from this map and displayed as Figure A14. The percentage of global area, where the total amount of ozone is equal or smaller than the ordinate, is given. In a probability scale, a straight line represents a "normal distribution." For values greater than or equal to 0.34 atm cm, such a straight line exists, but for low ozone values it does not. Fifty percent of the globe has only about 0.29 atm cm or less, and 75% of the globe less than 0.32 atm cm.

3.2 MAPS

A valuable atlas of global distribution of ozone has been prepared by London et al. (1976). It presents monthly maps separately for both hemispheres from July 1957 to June 1967, and those

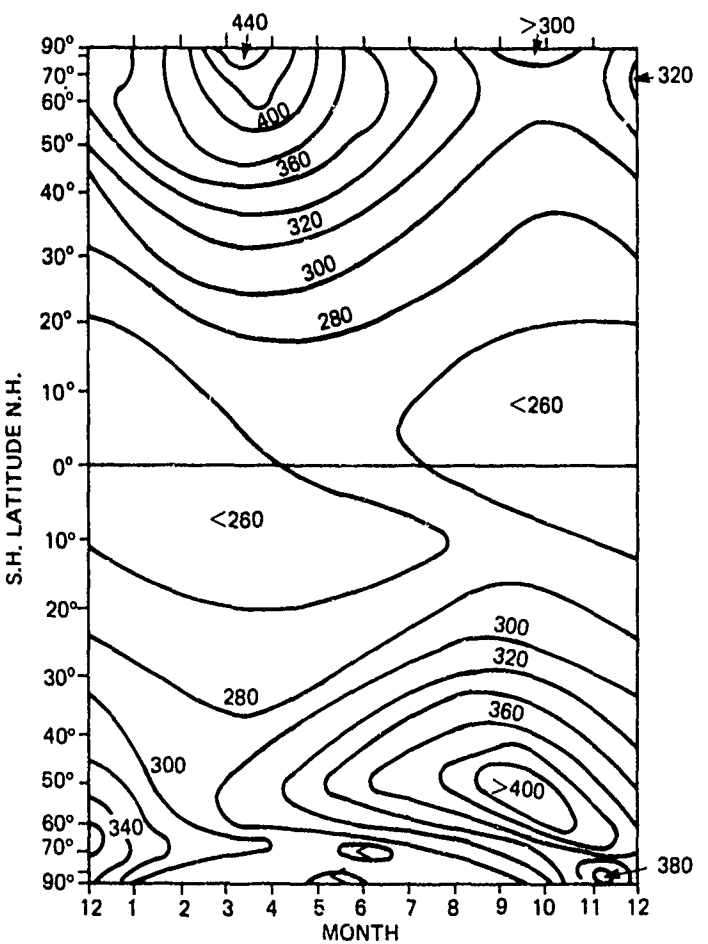


Figure A13 Isopleths of Total Ozone. The seasonal and latitudinal variations are shown. Replotted after Dütsch 1971, using $\sin \theta$ as ordinate. Units are 10^{-3} atm cm.

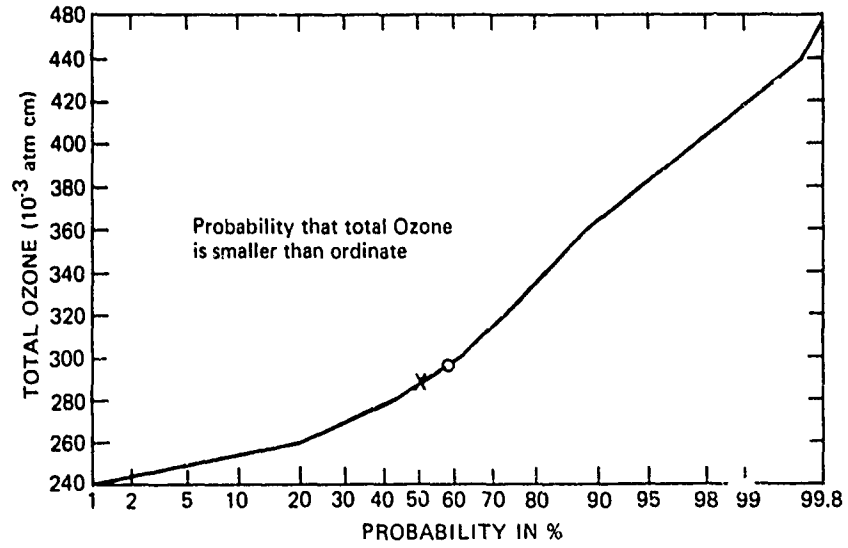


Figure A14 Cumulative Probability Distribution of Total Ozone. The abscissa gives the percentage of global ozone for which the total ozone (in 10^{-3} atm cm) is less than the ordinate. A straight line means a Gaussian distribution. Cross = 50%, circle = mean value of global inventory.

for the following 10 years are being prepared. They are based on all available observations from ground stations using the Dobson spectrophotometer or filter instruments. The sparse network in the tropics and over the oceans and instrument calibration errors may lead to some inaccuracies of which the authors are well aware.

The average global distribution during those 10 years is shown in Figure A15, unfortunately in a Mercator projection. The monthly maps should be studied because they show the actual changes from one month to the next and also the changes from one year to the next; for example, one should look at one particular month for each year to see how variable the distribution is. Such a consultation leads to an inside view of the "real" ozone distribution, so different from some computer-produced models. We find three maxima in the Northern Hemisphere and one in the Southern Hemisphere between 50 and 60° undergoing seasonal changes closely related to changes in the lower stratospheric general circulation pattern.

The authors computed yearly ranges, and their maps indicate them to be small in the tropics and largest near the poles with a maximum value of 180×10^{-3} atm cm found over Siberia; this value is probably too high as a result of the nature of the inaccuracies of the filter instrument. However, a value of 160×10^{-3} atm cm occurs over a wide area in the polar region and is probably correct, while in the Southern Hemisphere the maximum reaches only 80×10^{-3} atm cm over Antarctica, another hemispherical difference which is real.

Satellite observations can yield global maps; they can cover the globe evenly if launched into a polar orbit and provide an enormous amount of data per day, thus requiring extensive and costly data processing and reduction to a manageable level. Global ozone data were first derived from Nimbus 3 IR interferometer spectrometer (IRIS) measurements. Later, Nimbus 4 (launched in

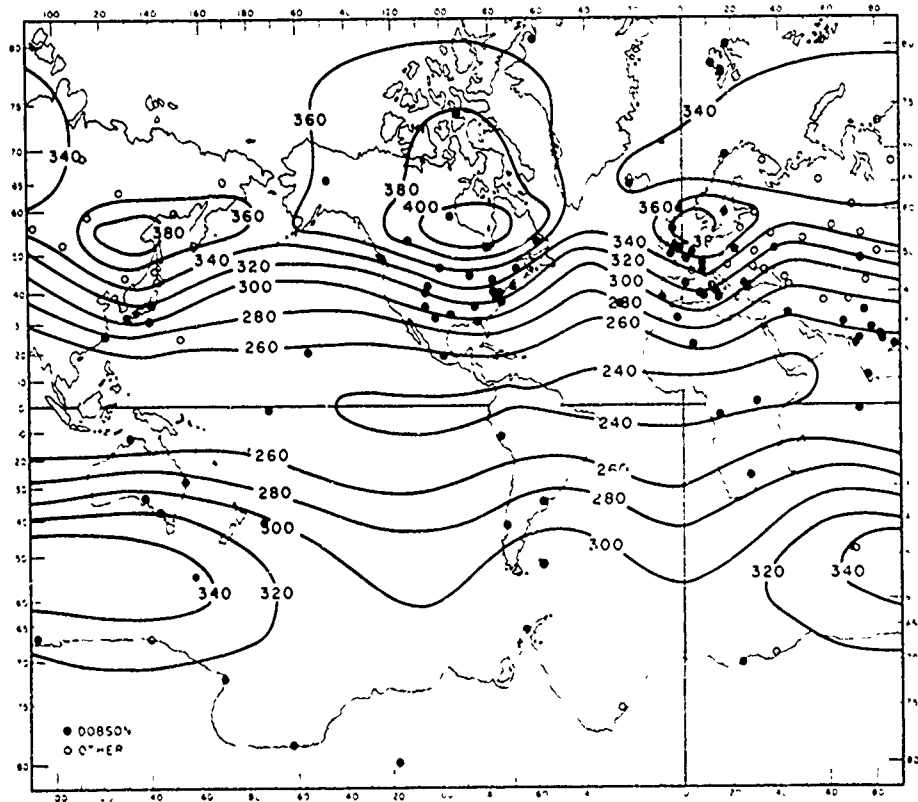


Figure A15 Average Global Distribution of Total Ozone for the Period 1957-1967) (Source: London 1976).

April 1970), IRIS and BUV (backscatter ultraviolet spectrometer) experiments also provided global coverage. The first publications, however, contain inaccuracies in the data processing, and, finally, in 1976, NASA formed an ozone processing team to provide a uniform and validated data base for BUV measurements. No maps have been published as yet, although the first year's data have been archived (NASA 1978).

Lovill et al. (1978) published 20 daily maps between 12 May and 5 July 1977. They are derived from radiance data in the 9.6 μm ozone band measured by a satellite (USAF, 5D-series, altitude 835 km, nearly polar orbit, sun-synchronous orbit, cross track scanning), and by a multifilter-multichannel radiometer. A good global coverage is obtained, although heavily clouded and very cold surface areas do not lead to reliable results and are therefore excluded. The maps show more or less uniformity over the tropics, but many small- and large-scale irregularities in middle and high latitudes. During those days, the centers of maximum and minimum amounts can be observed to change in intensity and move with variable speed and direction. Since these extrema are closely correlated with stratospheric temperatures, their intensity changes and their movements can be interpreted as the locations where changes in stratospheric radiative heating occur.

From 13 daily maps, Lovill et al. also compiled an average June 1977 map, which agrees in principle with those prepared by London, although many striking differences appear and need further clarification. For example, the Siberian contours are now much smoother and therefore the extrema are lower, the gradients in total ozone more constant over wide areas and the isolines more parallel to the latitude circles with smaller undulations. It is hoped that more of such maps will be forthcoming in the near future.

Comparing satellite data with ground-based measurements is very important. For the same place and time both should give identical results, at least for cloudless conditions. NASA conducted

such a comparison between BUV and Dobson for the first year (1970-1971) (NASA 1978) and found a correlation coefficient for the entire year of 0.938, with monthly variations between 0.973 and 0.792. The average BUV total ozone was 5.4×10^{-3} atm cm less than that measured by the Dobson instruments. For the filter instruments used in Russia, the correlation coefficient was as poor as expected, namely, 0.685 for the yearly average, proving the well known deficiency of this instrument. The comparisons were made for the time of fly-over.

Lovill et al. (1978) also conducted a comparison with simultaneous Dobson data from selected stations, with particular emphasis on actual timing to avoid diurnal variations. They also found the same difference as NASA, i.e., that the satellite gives about 5×10^{-3} atm cm less ozone than the Dobson.

Another, but coarser, comparison was made by Prior and Oza (1978) using IRIS and BUV data from Nimbus 4 for 1970. They averaged all data obtained by each technique for 10°-wide latitude belts. The IRIS and BUV techniques gave similar results at low latitudes, but, with increasing latitude, the IRIS data led to higher ozone amounts than the BUV observations, reaching 23% at 75°North during the months July to October. The ground-based Dobson data agreed fairly well with BUV, but poorly with IRIS. Although their investigation shows the gross features very well, we prefer to compare individual measurements during fly-over as done by the previously discussed investigators.

3.3 INVENTORY

Estimates have been made of the total global amount of ozone. The early estimates are all based on measurements from the Dobson network and therefore restricted in accuracy. Satellite monitoring systems permit us to obtain a fairly even global distribution. However, the error analysis of the satellite monitoring has not been completed as yet and the 1974 results by Lovill and Heath

may have to be revised. Nevertheless, the earlier estimates are not much different from the most recent data. Table A8 lists some of the published data.

Junge's estimate was correct, although on the high side. Khrgian's result for the Southern Hemisphere is incorrect because all later investigations clearly show that there is less ozone in the Southern than in the Northern Hemisphere. The values by Heath and Lovill are obtained from satellite measurements, those by London are based on his monthly global maps and those by Penndorf are derived from the isopleths constructed by Dütsch and replotted here as Figure A13.

We computed monthly hemispherical and global averages from the atlas of London et al. (1976) and present the results in Figure A16 and in Tables A9 and A10. The curves show the 10-year average amount and the extreme values during this period. For another 10-year period, the absolute values but not the general character may be somewhat higher or lower. It is important that opposite trends of the seasonal variation in each hemisphere do not completely cancel each other, so that a seasonal variation of about $\pm 3\%$ remains mainly caused by the lower concentrations of 2.5% in the Southern Hemisphere. This value is somewhat higher than those found by Brewer and Wilson ($\pm 2\%$) and by Heath ($\pm 2.6\%$). For each hemisphere, the ranges are 2 to 3 times as large as for the global range, as can be seen in Table A9. Besides these seasonal variations in global ozone, there is also the long-term variation of about the same magnitude, $\pm 3\%$.

TABLE A8
GLOBAL AMOUNT OF OZONE

Author	Period	Molecules $\times 10^{37}$	Mass $\times 10^{12}$ kg	Ozone 10^{-3} atm cm		
				Globe	N.H.	S.H.
Junge 1963		4.4	3.5			
A. Vassy 1965			3.0			
Brewer & Wilson 1968	1964	4.06	3.24	296		
Khrgian 1973	1957-69	3.99	3.18	290.9	290.1	291.7
Heath 1974	1970/71	4.24	3.38	309	314	304
Penndorf 1976		4.08	3.25	298.1	300.6	295.7
London 1976	1957-67	3.90	3.11	284.5	288	281
Lovill 1974	1969 SU	4.19	3.34	305.6		
Lovill 1978	1977 June	4.06	3.24	296	315	278

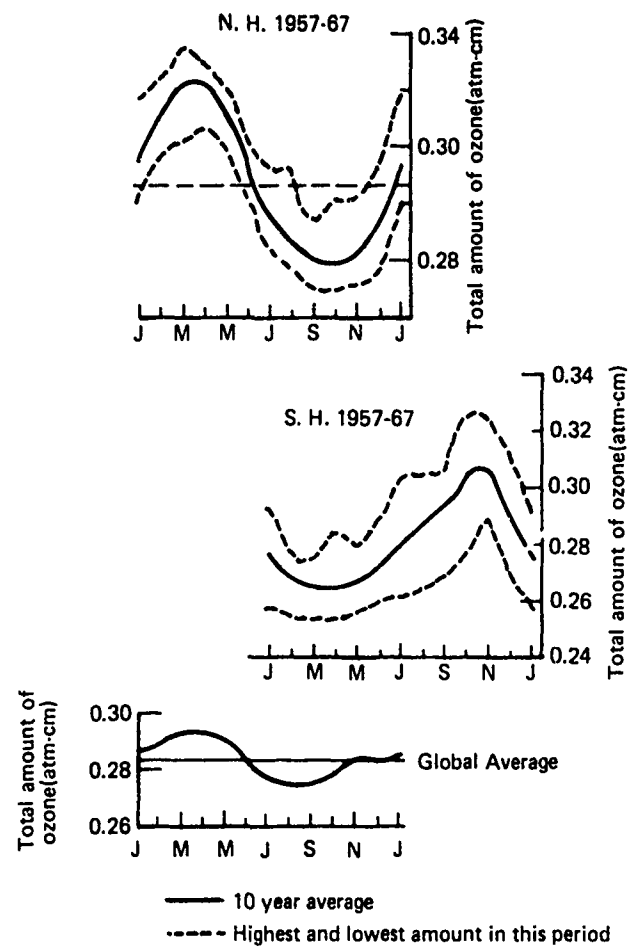


Figure A16 Hemispherical and Global Average of Total Ozone for Each Month and the Period 1957-67.

TABLE A9
EXTREME MONTHLY OZONE AMOUNTS*
(10^{-3} atm cm)

Average	Northern Hemisphere	Southern Hemisphere	Globe
Highest	335	326	304
Lowest	250	253	266

TABLE A10
RANGE OF AVERAGE MONTHLY OZONE AMOUNTS*

Area	10^{-3} atm cm	Percent	Mass 10^{12} kg	Molecules 10^{37}
Northern H.	259-322	-9.9 to +12.2		
Southern H.	265-303	-5.6 to + 8.0		
Globe	275-294	-3.1 to + 3.3	3.01-3.20	3.77-4.02

*Computed from the atlas of London et al. (1976)

From these tables, it follows that the global mass varies between 3.0 and 3.4×10^{12} kg (3.75 and 4.26×10^{37} molec.), with seasonal and long-term variations causing these limits. An average value of 3.2×10^{12} kg seem to represent present conditions fairly well.

Day-to-day changes of the global ozone amount should be small. Such information can be obtained from satellite observations and so far only those computed by Lovill et al. (1978) for a short time period in June 1977 are available. They found the change was less than 0.5% in any 24-hour period. Even that may be too large and caused by errors in data processing and calibration.

A.4 REFERENCES

Angell,J.K., and J.Korshover, Quasi-biennial and long-term fluctuations in total ozone, Monthly Weath.Rev., 101, 426, 1973.

Angell,J.K., and J.Korshover, Global analysis of recent total ozone fluctuations, Monthly Weath.Rev., 104, 63, 1976.

Angell,J.K., and J.Korshover, Recent trends in total ozone and ozone in the 32-46 km layer, WMO Symposium, Toronto, 1978.

Birrer,W.M., Some critical remarks on trend analysis of total ozone data, Pure and appl. Geophys., 112, 523, 1974.

Brewer,A.W., and A.W. Wilson, The regions of formation of atmospheric ozone, Quart.J.Roy.Meteor.Soc., 94, 249, 1968.

CIAP, Monograph 1, The natural stratosphere, DOT-TST-75-51, 1975.

Dobson,G.M.D., Atmospheric ozone and the movement of air in the stratosphere, Pure Appl. Geophys., 106-108, 1520, 1973.

Dobson,G.M.D., D.N. Harrison, and J. Lawrence, Measurements of amount of ozone in the earth's atmosphere and its relation to other geophysical conditions, Part II, Proc. Roy. Soc, London, A 114, 521, 1927.

Dütsch,H.U., Ozone distribution and stratospheric field over Europe during the sudden warming in Jan/Feb. 1958, Beitr. Phys. Atm., 35, 87, 1962.

Dütsch,H.U., Photochemistry of atmospheric ozone, Adv. Geophys., 15, 219, 1971.

Dütsch,H.U., The ozone distribution in the atmosphere, Can. J. Chem., 52, 1491, 1974.

Dütsch,H.U., private communication, 1976.

Fabry,Ch., L'ozone atmosphérique, CNRS, Paris, 278 pp, 1950.

FAA, High Altitude Pollution Program (HAPP), Program Plan, 1976.

Götz, F.W.P. Ozonwolken, Helv. Phys. Acta, 13, 3, 1940.

Götz, F.W.P., Ozone in the atmosphere, in: Compendium of Meteorology, 275, AMS, Boston, 1950.

Grobecker,A.J., S.C. Coroniti, and R.H. Cannon, CIAP Report of Findings, DOT-TST-75-50, 1974.

Heath,D.F., Recent advances in satellite observations of solar variability and global atmospheric ozone, Proc. Intern. Conf. on struct.,..., Melbourne, IAMAP, 2, 1267, 1974.

Hill,W., and P.N. Sheldon, Statistical modeling of total ozone measurements with an example using data from Arosa, Switzerland, Geophys. Res. Lett., 2, 541, 1975.

Johnston,H.S., G.Whitten, and J.Birks, The effect of nuclear explosions on stratospheric nitric oxide and ozone, J. Geophys. Res., 78, 6107, 1973.

Junge,Ch., Air chemistry and radioactivity, Acad. Press, New York, 1963.

Kerr,J.B., Short time period fluctuations in the total ozone, Pure Appl. Geophys., 106-108, 977, 1973.

Khrgian,A.Kh., The physics of atmospheric ozone, Leningrad, 1973, Translation TT 74-50027 (NTIS), 262 pp, Jerusalem, 1975.

Komhyr,W.D., E.W.Barrett, G.Slocum, and H.K. Weickmann, Atmospheric ozone increases during the 1960', Nature, 232, 390, 1971.

Kulkarni,R.N., Ozone trend and stratospheric circulation over Australia, Quart.J.Roy. Meteor.Soc., 102, 697, 1976.

London,J., The thermal structure and dynamics of the stratosphere, Intern. J. Chem. Kinetics, Symposium No 1, 85, 1975.

London,J., and J. Kelley, Global trends in atmospheric ozone, Science, 184, 987, 1974.

London,J., R.D.Bojkov, S.Oltmans, and J.I.Kelley, Atlas of the global distribution of total ozone July 1957 - June 1967, NCAR Techn.Note, NCAR/TN/113, 1976.

Lovill,J.E., A comparison of the Southern and Northern Hemisphere general circulation characteristics as determined by satellite ozone data, Proc. Intern. Conf. on struct.,..., Melbourne, IAMAP 1, 340, 1974.

Lovill,J.E. et al. (8 authors), Total ozone retrieval from satellite multichannel filter radiometer measurements, Lawrence Livermore Lab., UCRL 52473, 1978.

Meetham,A.R., The correlation of the amount of ozone with other characteristics of the atmosphere, Quart.J. Roy.Meteor. Soc., 63, 289, 1937.

Moser,H., Ozon und Wetterlage, Ber. deutsch. Wetterd., US zone,
No.11, 28,1949.

National Academy of Sci., Environmental impact of stratospheric flight, 348 pp, Washington,D.C., 1975.

National Academy of Sci., Halocarbons: Effects on stratospheric ozone, Washington,D.C., 1976.

NASA, Ozone Processing Team, User's guide to the Nimbus 4 BUV experimental data set, NASA TMX-78069,1978.

Normand,Ch., Atmospheric ozone and the upper air conditions, Quart. J.Roy.Meteor. Soc., 79, 39,1953.

Ny Tsi-Ze, and Choong Shin Piau, Sur l'absorption ultra-violette de l'ozone, Chin.J. Phys., 1, 38,1933.

Oliver,R.C., et al., Aircraft emissions: Potential effects on ozone and climate, FAA-EQ-77-3,1977.

Pätzold,H.K., The influence of solar activity on the stratospheric ozone layer. Pure Appl.Geophys., 106-108,1308,1973.

Penndorf,R., The annual variation of the amount of ozone over Northern Norway, Ann. Géophys., 6,4,1950a.

Penndorf,R., Ozon und Wetter II, Meteorol.Rundsch., 3,49,1950b.

Perl,G., and H.U.Dütsch, Die 30-jährige Arosa Ozonmessreihe, Ann. schweiz. Meteorol.Zentr.Anst., Appendix 8, 1958.

Prior,E.J., and B.J.Oza, First comparison of simultaneous Iris, BUV, and ground-based measurements of total ozone, Geophys. Res. Lett., 5,547,1978.

Tønsberg,G., and K.Olsen Investigations of atmospheric ozone at the auroral observatory Tromsø, Geofys.Publ., 13,No 12, 1944.

Vigroux,E., Contributions a l'étude experimentale de l'absorption de l'ozone, Ann.Phys., 8,709,1953.

Vigroux,E., Détermination des coefficients moyens de l'absorption de l'ozone en vue des observations concernant l'ozone atmosphérique a l'aide du spectrophotomètre Dobson, Ann.Phys., 2,209,1967.

Wallace,J.M., and R.E.Newell, Eddy fluxes and the biennial stratospheric oscillation. Quart.J.Roy.Meteor.Soc., 92,481,1966.

Wilcox,R.W., Total ozone trend significance from space and time variability of daily Dobson data, Appl.Met., 17,405,1978.

Wilcox,R.W., G.D.Nastrom, and A.D.Belmont, Periodic variations of total ozone and of its vertical distribution, J. Appl. Meteor., 16, 290, 1977.

B. ATMOSPHERIC OZONE: THE VERTICAL DISTRIBUTION AND ITS FLUCTUATIONS

ABSTRACT

The ozone concentration reaches a maximum in the lower stratosphere at about 26 km over the tropics and sloping downward from the equator to the poles. Its mixing ratio reaches a maximum over the tropics at about 30 km altitude. At midlatitude stations, the seasonal variation is dominant and pronounced at all altitudes, and other periodicities are of small magnitude. The natural aperiodic fluctuations are largest between 5 and 12 km in midlatitudes so that the standard deviation reaches values of 90% or more.

The troposphere contains only about 8% of the total ozone with an average concentration of about $40 \mu\text{g}/\text{m}^3$. Ozone moves from the stratosphere downward predominantly by mass exchange in the gap between the tropical and polar tropopause. The ground is a sink for ozone. Airplanes are being used as carriers to measure ozone concentration between 8 and 21 km altitude, often over very large meridional or longitudinal distances, yielding large fluctuations in concentration.

B.1 VERTICAL PROFILES AND MERIDIONAL CROSS-SECTIONS

At present we have a reasonable concept of the three-dimensional ozone distribution and its seasonal variation. The data have been accumulated over a span of many years, yet are limited to a selected number of places and often to a very short series of 3 to 5 years. The most up-to-date list of stations is given by Dütsch (1978); the longest series has been obtained in Switzerland.

1.1 TECHNIQUES

The vertical distribution of ozone has been measured using various carriers and techniques. It is considerably more difficult to obtain reliable data of concentrations than of total ozone; the accuracy is also often lower than the inventor assumed. One extensive data base is obtained by the indirect Umkehr-method when measuring the scattered zenith light during sunrise or sunset with the Dobson spectrophotometer. It has the advantage of giving averages for about 8 broad altitude ranges up to 50 km, but the disadvantage of smearing out details (Götz 1931, Mateer 1965).

The second method uses balloons as carriers and wet chemical instruments based on the potassium iodide-ozone ($KI-O_3$) reaction (Brewer 1960, Komhyr 1969). Such instruments are Brewer-Mast, Komhyr-Electrochemical concentration cell, Italian, Indian, and DDR-Brewer types, and Japanese Carbon Iodine. The chemiluminescent instrument developed by Regener (1960) uses Rhodamine-B and has serious calibration problems. It is no longer in use. Optical techniques, the earliest, are also no longer in use; they give only overburden and the concentration must be obtained by differentiation. Recently the in-situ UV absorption cell (Dasibi) has been used. Properly calibrated it is a very reliable instrument. Altitudes of 30 to 35 km are routinely reached. The higher the accuracy the more fine structure appears in the profiles, although minor fluctuations within the accuracy of the technique may not

be real. This method now provides the most extensive data base, although the majority of stations operated for only a few years.

The third method uses aircraft reaching 21 km. They obtain meridional cross-sections at constant altitudes, which is especially important across oceans. Techniques are those used primarily for balloons but adapted to the high ram pressure of airplanes. The wet chemical techniques prevail, followed by the Dasibi UV absorption-cell technique. UV and IR optical techniques are also used for determining the overburden.

The fourth method uses rockets and satellites, which employ optical techniques to obtain concentrations up to 60 to 70 km altitude. Rockets can be launched at only a few locations; they are expensive but, if well calibrated, lead to reliable profiles. An average profile of ozone concentration for midlatitudes, based exclusively on rocket data, has been derived by Krueger and Minzner (1976). Satellite measurements have used various techniques. The backscatter UV radiation technique (BUV) gives worldwide distribution of ozone over the illuminated atmosphere. No data for the polar caps in winter (polar night) can be derived, and, in addition, the sunrise-sunset areas have to be excluded. Further problems are the regular calibration during the lifetime of the satellite. The total amount of ozone and its vertical distribution can be obtained, but the latter only for broad altitude ranges above 30 km. Hence, as with the Umkehr-method, it will smear out details. Such data will describe the concentration in the region where photochemical reactions dominate and transport phenomena play a minor role. I doubt very much that they will replace the balloon program because the information between the ground and 30 km is so essential to all ozone problems.

1.2 MERIDIONAL CROSS-SECTIONS

Dütsch (1971, 1974, 1978) computed average profiles and time cross-sections for selected stations and derived from them average meridional profiles (pole to pole) for the seasons. They are based on profiles obtained by the Umkehr-method and from balloon measurements; the most recent profiles, however, shown below, are based predominantly on balloon measurements.

There is no need to repeat all the published material and the discussions, most of which can be found in CIAP Monograph 1, section 3.3.1 and the references cited there. The meridional cross-sections of the partial pressure of ozone in nb are shown in Figure B1 for four selected months. Clearly the equatorial minimum of total ozone is mainly due to the high tropical troposphere, which has a rather low ozone concentration at altitudes where the absolute maximum in concentration occurs in polar regions.

The level of the peak ozone concentration slopes strongly downward from the low to the high latitudes, namely from 26 km over the equator to 17 km at the poles. In this representation the polar maxima appear more dramatic than they really are, because the linear latitude scale is used, while we prefer a $\sin\varphi$, which gives the true mass distribution. The polar anomalies cover only a small part of the total ozone mass.

Next, we show in Figure B2 the volume mixing ratios

$$w_{3v} = p_3/P$$

for the same meridional profiles as in Figure B1. Certainly the volume mixing ratio looks very different from the meridional profile for concentration, due to the exponential decrease in air density with altitude. The isopleths of mixing ratio are fairly smooth, with a maximum in the tropical middle stratosphere at or slightly above 30 km centered over the equator. The polar maxima disappear because they are situated at a much higher pressure

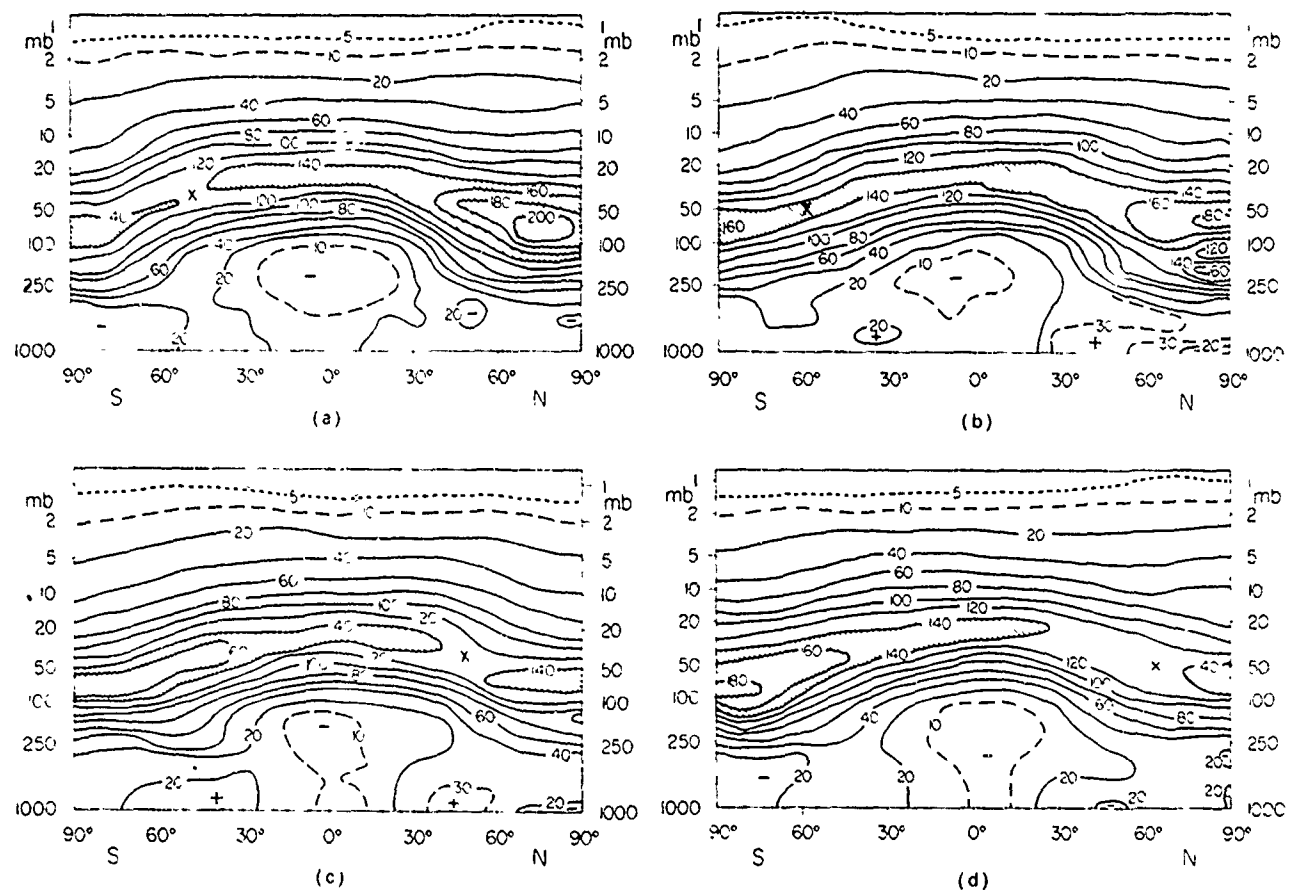


Figure B1 Meridional Cross Sections of Ozone Partial Pressure (isoline in nb). The x marks the position of the lowest value within the maximum layer. (a) February, (b) May, (c) August, (d) November (Source: Dütsch 1978).

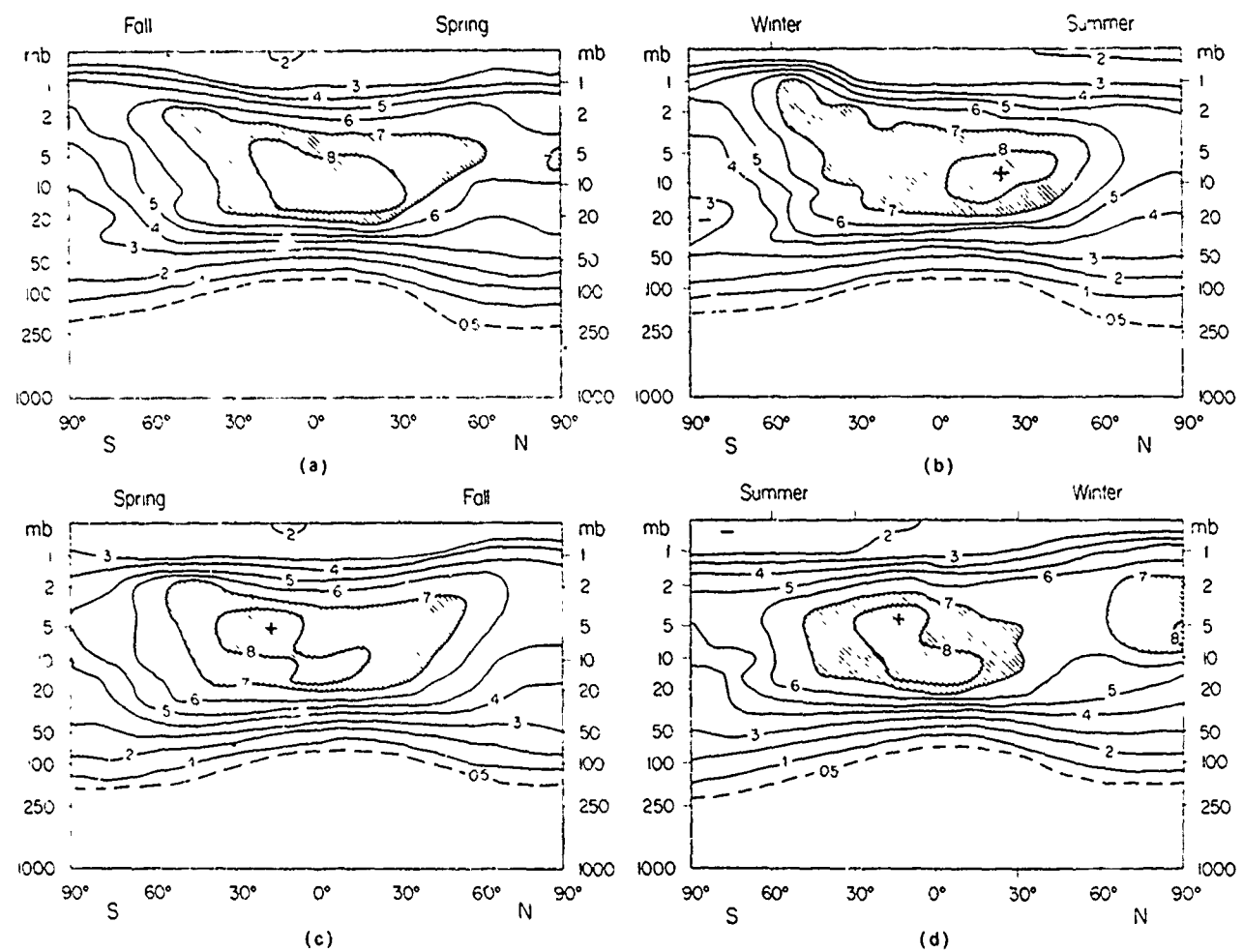


Figure B2 Meridional Cross-sections of Ozone Air Mixing Ratios (isolines in ppmV) (a) April, (b) June, (c) October, (d) December (Source: Dütsch 1978).

than the tropical maximum; only a minor irregularity is left in December above 30 km and north of 60°. This anomaly, however, is not a major event at all compared to the rest of the meridional distribution.

The gradient in mixing ratio dw/dx or dw/dh (horizontal or vertical) determines the location of sources and sinks. In Figure B2 we see the contours of equal mixing ratio sloping downward from low to high latitudes below 22 km but sloping upward above this altitude. The gradient of mixing ratio clearly points to the tropical middle stratosphere as the main source region.

Using ozone as a tracer (because it is not in photochemical equilibrium below 20 km in the tropics), stratospheric transport models have been inferred from the observed ozone distribution as shown in Figure B2 (e.g. Dütsch 1971, 1974; London 1975; Mahlman in CIAP Monograph 1, p.6-110). They all prove that ozone is moved poleward and downward by the meridional circulation and large-scale eddies. Looking at the literature we find this problem to be treated in general terms only; it is very complex and therefore difficult. Some recent model efforts try to obtain the average ozone distribution (Figure B1) by assuming fairly simple diffusion coefficients to represent transport. However, such coefficients can not explain the actual intricate transport systems proposed by the above-named investigators.

It has been suggested (International Ozone Conference 1976) to obtain actual transport parameters (type, magnitude, and direction) from a carefully planned and reliable field measurement program.

Satellite BUV measurements can be used to derive ozone concentration between 30 and 60 km. However, preliminary Nimbus 4 data may be incorrect and a final data processing is still incomplete. Thus none will be discussed here.

Monthly mean mixing ratios up to 34 km and their standard variation have been derived by Wilcox and Belmont (1977) for the latitudes 0 to 80°N and 80°W based on American soundings. This data evaluation in graphical and tabular form is designed for operational problems and will be very useful.

In-situ observations at 18 and 21 km have been made on U-2 flights and evaluated by Loewenstein et al. (1975 a,b; 1978). Recently, a chemiluminescent detector with a systematic error of \pm 20% was used. The data show the expected trends with latitude, altitude, and season. As an example, we present in Figure B3 measurements obtained during September-November 1976 at 21.3 km. Such measurements are valuable and necessary in relation to simultaneous measurements of other trace gases. This particular series shows some variability along the meridional flight path from the west coast of the U.S. to Alaska.

The altitude regime around 40 km has recently become very important because model computations indicate the fluorocarbon effect to be most pronounced near 40 km. Trends at this altitude have been investigated by Angell and Korshover (1978) for the period 1957-76. They find an 8% increase in the North temperate zone between 1962 and 1973, whereas models predict a 2% decrease during that time. The authors state: "the increase in ozone concentration implies any fluorocarbon effect on ozone is being overwhelmed by natural processes, assuming the Umkehr data are representative and basically correct." Balloon measurements to 45 km are rare and expensive, and we have to wait for rocket measurements to shed light on this problem. I would not be surprised if future actual measurements support Angell and Korshover's finding and the model computations turn out to be another fruitless scare.

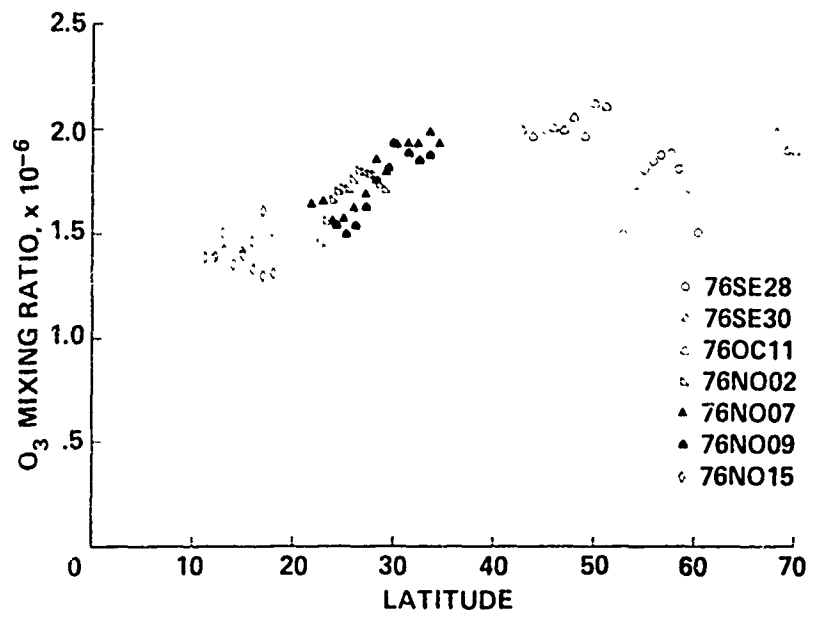


Figure B3 In-situ Measurements of Ozone. Altitude 21.3 km, September to November 1976 (Source: Loewenstein 1978).

1.3 TEMPORAL VARIATIONS

Just as for the total amount of ozone, there are temporal and spatial variations in each altitude regime, such as a large seasonal variation, a minor solar cycle variation; longitudinal dependence (often called continental effect) with differences between east and west coasts of America and Eurasia; hemispherical differences, especially in high latitudes. Such variations have been described, e.g. by Dütsch (1974).

For the dominant seasonal variation, we select the time cross-section for Zurich, Switzerland, Figure B4. It is based on 6 years of observations (Dütsch and Ling 1973) and differs in some details from earlier publications (Dütsch 1969). The altitude of the peak concentration reaches a minimum at about March/April and a maximum in late summer when the concentration reaches a minimum. The latter increases rapidly by about 30% to a maximum which lasts from January to March. This augmentation in ozone concentration propagates into the lower stratosphere with some time delay and finally into the troposphere. This fact is shown best in Figure B5 by the increase in partial pressure (in nb) per month; it details visibly the magnitude of the monthly change and its delay through downward propagation. The absolute magnitude of the seasonal variation at fixed pressure levels is largest from 200 mb (12 km) to about 40 mb (22 km). Above 25 km it decreases to very small values because photochemical processes compete with the transport by the general circulation. Such presentations are not only very important but also instructive in elucidating the role of transport.

Japanese balloon and rocket flights indicate that winter concentrations are larger than those in summer (Watanabe and Tohmatsu 1976). While the seasonal variations below 35 km are of the same magnitude as over the U.S. and Europe, the winter concentrations above 35 km are a factor of 2 larger than in summer.

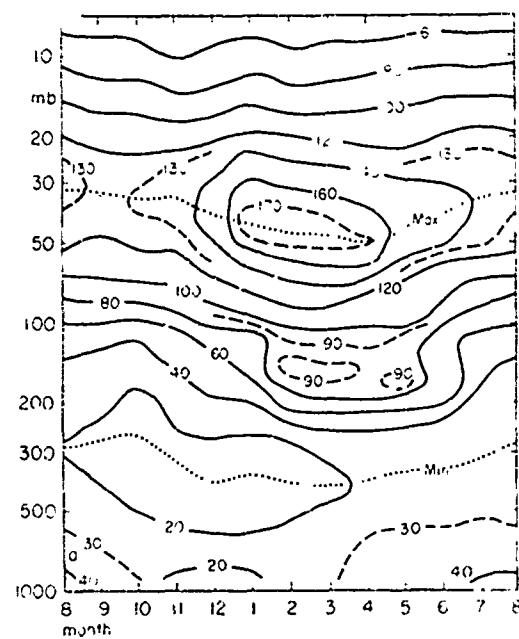


Figure B4 Time Cross-section of Vertical Ozone Distribution. Partial pressure in nb over Switzerland from 6 years of observation (Source: Dütsch 1974).

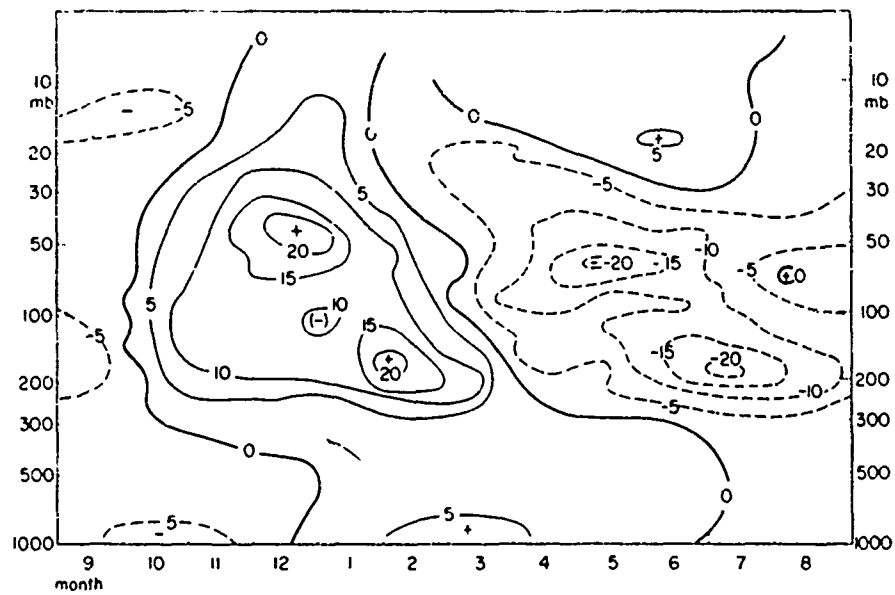


Figure B5 Time Cross-section of Month-to-Month Variation of Ozone Concentration Over Switzerland. Partial pressure changes in nb (Source: Dütsch 1971).

Wilcox et al. (1977) conducted a Fourier analysis for the American network and found the maximum of the annual wave to be situated near 16 km with an amplitude of about 54 nb at 80°N, decreasing to 12 nb at 30° and to 6 nb at the equator. The maximum occurs in February/March north of 40°N. Dütsch (1978) depicts the range (twice the amplitude) of the annual wave from pole to pole, Figure B6, in great detail based on his worldwide network discussed before. Both representations are similar. In the Southern Hemisphere the maximum amplitude is smaller than in the Northern Hemisphere and it is split as a result of the difference in stratospheric circulation.

The semiannual wave is of about equal amplitude as the annual wave in the tropics. In absolute values it is largest between 50 and 80°N, yet amounts to only a 7% variation in the concentration at 20 km. The first maximum occurs in January at low latitudes and progresses northward, reaching the pole in March.

No periodicities longer than one year become evident in the lower stratosphere while the biennial variation occurs in the middle stratosphere. In the 6-year series of Switzerland it has been found at the level of the ozone maximum between 60 and 30 mb (20 to 25 km) in the first half of the year. From 1967 to 1974 the peaks in late winter show a clearcut biennial variation, which, however, fails to appear in 1975 and 1976. Pittock (1977) finds no evidence for a quasibiennial variation over Australia (38°) in 8 years of observations. Wilcox et al. (1977) also derive amplitude and phase for the biennial variation by assuming a constant period of 29 months. We question this result because the period has varied between 22 and 33 months during the last 15 years and their analytic technique does not allow variable periods. The amplitude of this variation should be of the order of 5 to 10% of the average concentration in the middle stratosphere.

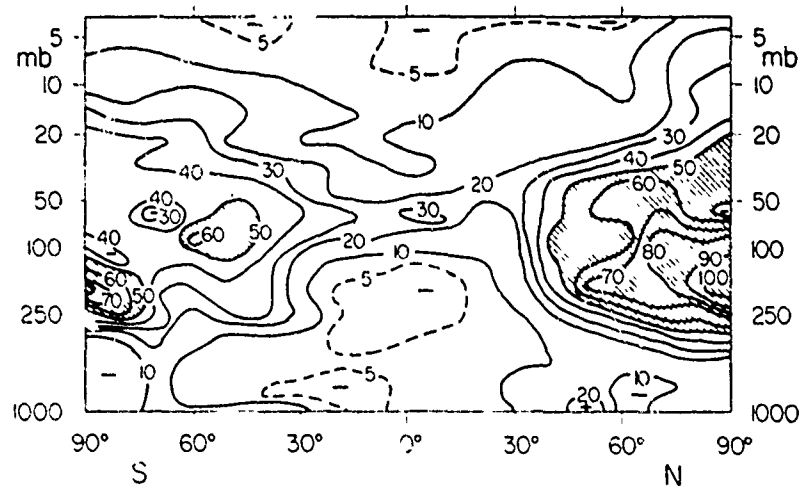


Figure B6 Meridional Cross-section of the Range of the Seasonal Variation of Ozone Partial Pressure (Δp_3 in nb) without Regard to Phase (Source: Dütsch 1978).

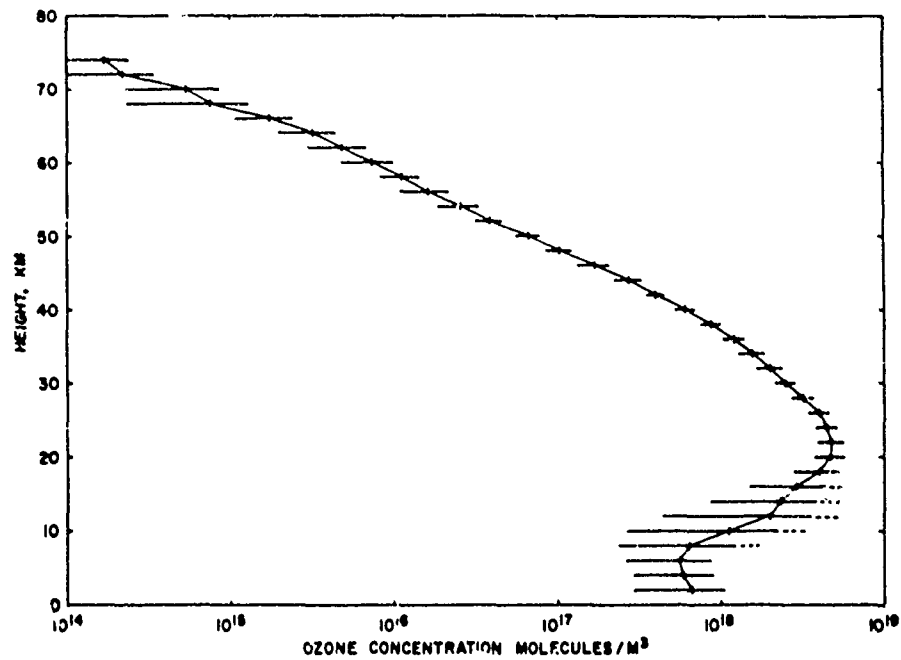


Figure B7 Mean Annual Midlatitude Ozone Number Density Versus Height. Horizontal lines correspond to ± 1 standard deviation (Source: Krueger and Minzner 1976).

The question of a solar cycle variation has been raised from time to time; for the total ozone we discussed it in Section A.2.5. For the ozone concentration in or just below the production region, such a variation seems plausible, provided the solar UV flux undergoes such a systematic variation. Although a solar variation has not been proven conclusively, it is anticipated, and satellite experiments should establish its magnitude in the tropical photochemical production region. Its amplitude must be small, probably not more than 2%, so that it is buried in the noise and would require a very large amount of data for a reliable extraction.

Dütsch et al. (1969) tentatively reported such long-term variations in the ozone concentration above the 30 km level based on Umkehr-effect data. Recently, Dütsch (1976) stated that his data support his earlier findings. Pätzold et al. (1972) reported a similar variation, but for the 20 to 30 km region, based on European optical ozonesonde data. They find a significant positive correlation between ozone concentration and sunspot number with a suggestion of a sign change above 30 km.

Trends in ozone concentration have been investigated by Pittock (1974) for the 8-year series (1965-1973) of ozonesonde data for Aspendale, Australia. He finds a decrease of 10 to 20% per decade in the troposphere, of 15 to 25% per decade in the lower stratosphere, of 10% per decade at the peak of the ozone concentration and an increase of up to 15% per decade above 28 km. A more complete investigation of just one altitude regime, 34 to 42 km, based on Umkehr-measurements, was carried out by Angel and Korshover (1978), as mentioned previously. They believe the increases in concentration in this layer after the Agung eruption at the two Australian stations indicate at least a 10% reduction in ozone concentration and a 4% reduction in the Northern Hemisphere at the time of the Fuego eruption. So far these are just two possible coincidences; they may be real effects, but the big question remains whether the neglect of aerosol scattering in the stratosphere may have just such an effect on the evaluation of the Umkehr measurements.

Good and reliable trend investigations for all altitudes based on a large network are still lacking. It makes sense that long-term trends vary with altitude or even reverse sign, because of the complex interplay between production and transport.

1.4 NATURAL FLUCTUATIONS

The natural aperiodic fluctuations of total ozone have been described in Section A.2 where we define such fluctuations as the range of one standard deviation ($\pm\sigma$). The data base of ozone concentration, however, is much smaller than that for total ozone and extends only over a few years with balloon ascents of about once a week. Consequently, our knowledge of fluctuations is rather limited. For example, over a 3-year span, Hering's American network made only about 50 ascents at some locations but up to 173 at others. With such a small sample, statistics by seasons are possible only for the stations with the largest data base. Wilcox and Belmont (1977) derived monthly values of the standard deviation of the concentration in $\mu\text{g}/\text{m}^3$ and of volume mixing ratio in tabular and graphical form. However, they state that the data were difficult to analyze. I believe the small number of cases per month makes such a representation less accurate than statistics based on seasons, although in the latter case the annual and semiannual wave contributions are included. Dütsch published monthly statistics for his balloon ascents at Boulder, Colorado, and Zurich, Switzerland. I am not aware of similar statistical studies for other places, yet they are vital for understanding these natural fluctuations.

Krueger and Minzner (1976) have averaged the U.S. rocket data to derive an annual model for 45°N as in Figure B7. Between the ground and 14 km the standard deviation varies between ± 50 and 109%, decreasing to $\pm 21\%$ at 20 km and remaining between ± 10 and $\pm 20\%$ up to 50 km. As we will see, these magnitudes of aperiodic fluctuations are characteristic for midlatitudes.

To present the conditions over the U.S., we select stations with the largest number of ascents, Albuquerque, New Mexico, and Bedford, Massachusetts. Data for four seasons at each 2 km interval were published by Hering and Borden in 1964. They list the average concentration in $\mu\text{g}/\text{m}^3$ and its standard deviation, which we converted into units of molec/ m^3 and volume mixing ratio. Figures B8 and B9 show for each season the range of the standard deviation ($\pm \sigma$), e.g.; 67% of all measurements fall within the hatched area and 33% fall outside. Most instructive is the graphical presentation of the range of fluctuations in isopleths, Figure B10, where just a few contours are selected. These fluctuations amount to about ± 30 to 50% in the lower troposphere, increasing towards the tropopause where they vary between ± 50 and 100%, an extraordinarily large value, and decrease to ± 5 to 20% above 20 km. The range $\geq \pm 50\%$ is situated between 4 and 16 km in winter and between 10 and 16 km in summer over Albuquerque and between 4 and 12 km in winter and 8 to 12 km in summer over Bedford. Values of $\geq \pm 90\%$ are observed only in the tropopause layer.

Dütsch (1971, 1974), using a larger sample, derived monthly averages and standard deviation for Zurich and Boulder. The 6-year average is presented in Figure B4 for Zurich. Dütsch computed the relative standard deviation of the partial pressure as percentage from the average. The latter is given as Figure B11, because it can be compared with Figure B10. His results for Boulder and Zurich are very similar to those we obtained for Bedford and Albuquerque and reported above. A standard deviation $\geq 60\%$ occurs all year round in the tropopause region with maxima of $\geq \pm 100\%$. In Zurich, the lower boundary varies between 5.5 and 8 km, the upper boundary between 12 and 14 km; for Boulder the respective values are 8 and 12 to 16 km. In the lower troposphere, excluding the boundary layer, the range is ± 20 to 40%. Above the tropopause layer the fluctuations decrease to less than 10% in the 20 to 30 km region, but seem to increase in the middle stratosphere. This increase may not be real because the concen-

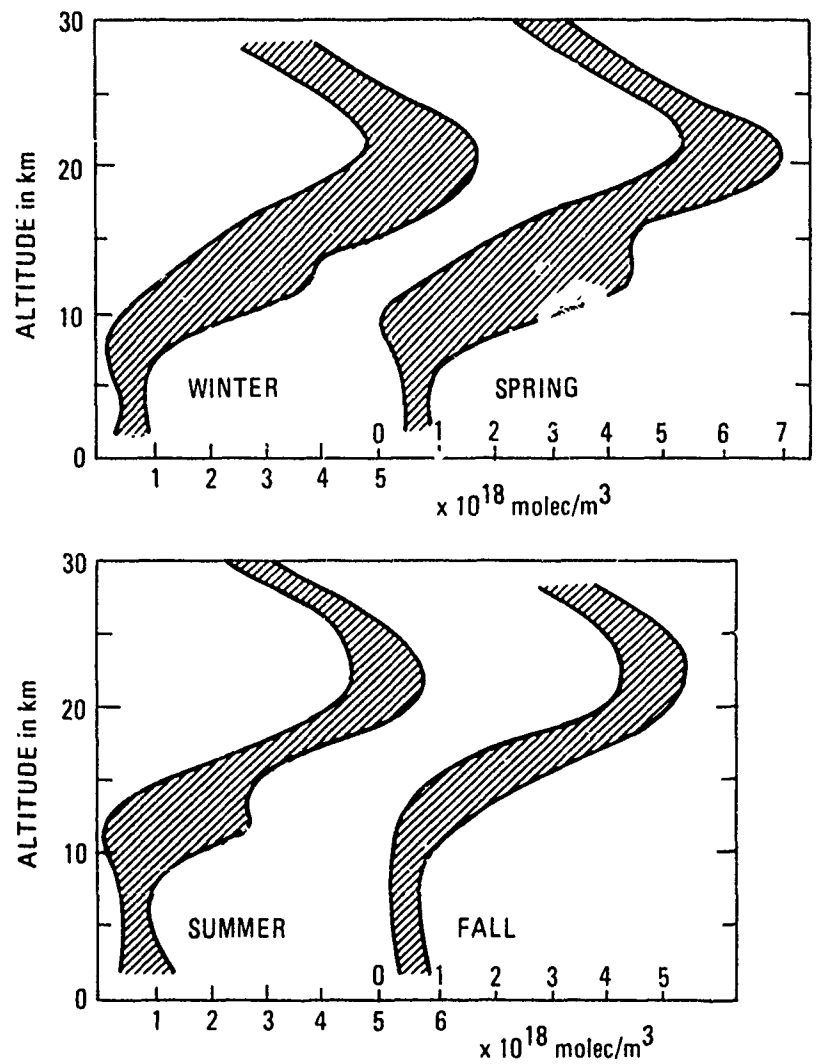


Figure B8 Range of Vertical Ozone Profile Over Bedford, Massachusetts. Contours represent $+ \sigma$ and $- \sigma$, units are 10^{18} molec/m 3 .

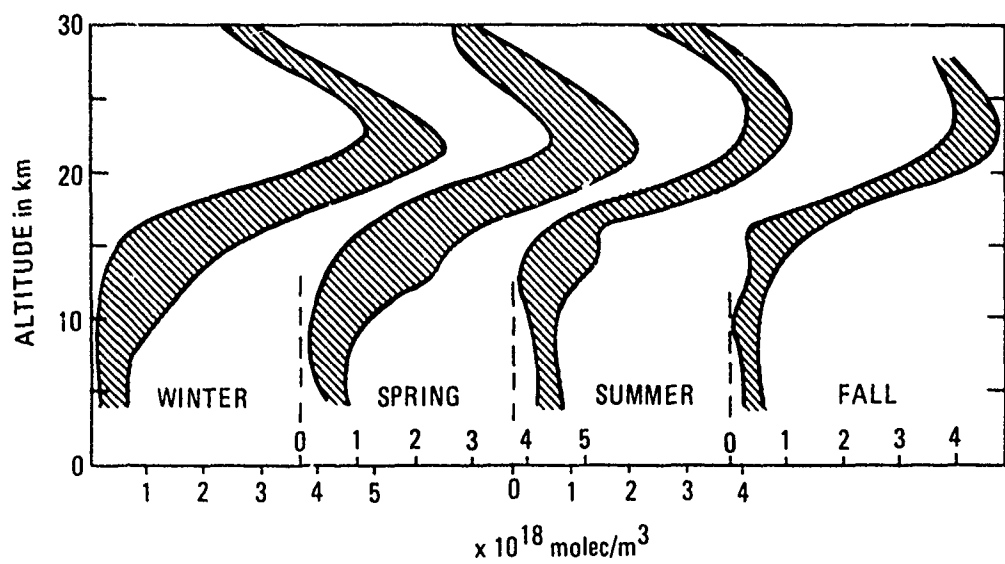


Figure B9 Range of Vertical Ozone Concentration Over Albuquerque, New Mexico. Contours represent + σ and - σ ; units are 10^{18} molec/m³.

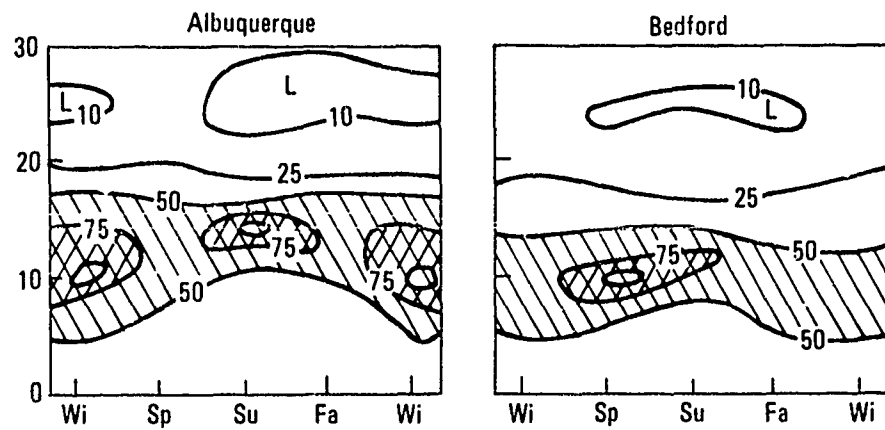


Figure B10 Range of Natural Fluctuation in Ozone. Numbers give the standard deviation in % of the mean.

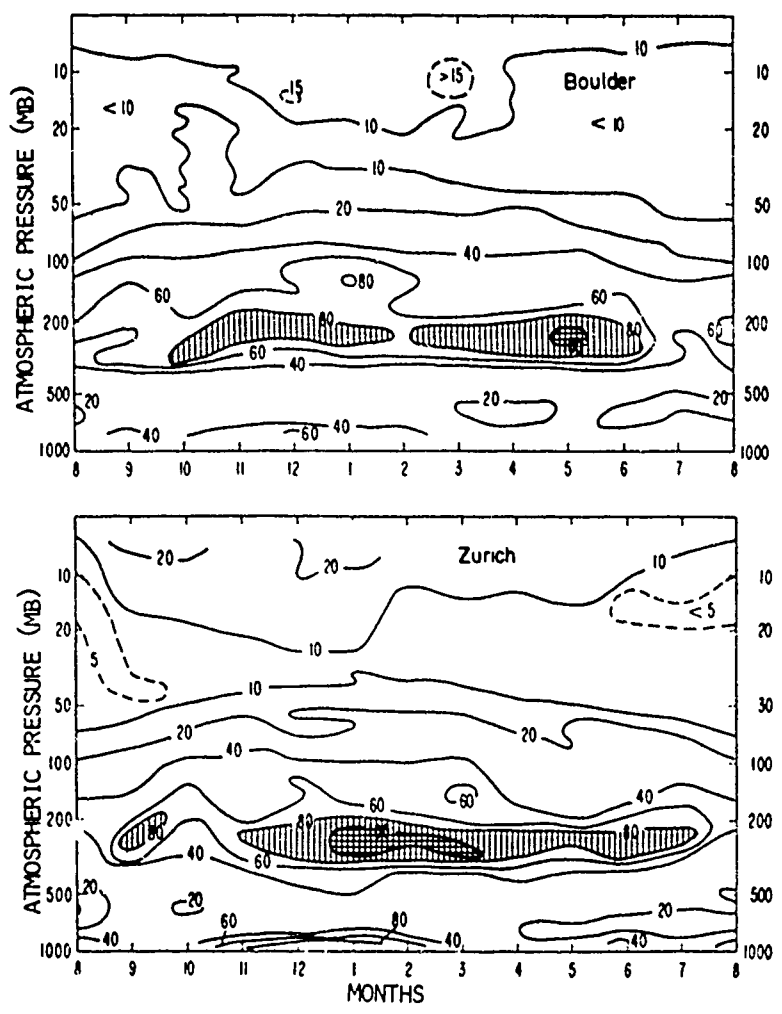


Figure B11 Time Cross-sections of Relative Standard Deviation Over Zurich and Boulder (in percentage of mean concentration) (Source: Dütsch 1971).

tration and the accuracy of the measurements are low. Some of the fine structure shown by Dütsch in Figure B11 may not be real; in a longer time series it should vanish.

The variance of ozone concentration in the Australian measurements (at 38°S) has been analyzed by Pittock (1977), using 8 years of observations from 1965 to 1973. The short-term variance is low above the 50 mb level, but exceeds the seasonal contribution below the 70 mb level. Thus, Pittock concludes, at 100 mb the variance is caused predominantly by synoptic events.

We conclude from these investigations that the natural ozone fluctuations are small in the lower troposphere, $\leq \pm 40\%$, and in the middle stratosphere above 20 km, $\leq \pm 20\%$. However, they reach extraordinary large values of ± 50 to $\pm 100\%$ in the altitude region in which the tropopause moves up and down, i.e., from 8 to 14 km in midlatitudes and perhaps 6 to 11 km in polar regions. The large fluctuations are a consequence of low tropospheric concentrations and the rapidly increasing concentrations above the tropopause.

1.5 MAGNITUDE OF TEMPORAL VARIATIONS AND FLUCTUATIONS

This section can best be summarized in giving orders of magnitude for the amplitudes of periodic variations and for the standard deviations of aperiodic short- and long-term fluctuations. This summary is shown in Table B1.

Our knowledge of the relative standard deviation of fluctuations is limited to midlatitudes. These fluctuations represent the "noise" level of regular observations and are, unfortunately, much larger than most of the periodic variations, reaching values of ± 50 to 100% for the short-term fluctuations in the tropopause region and decreasing to $\pm 10\%$ in 20 to 30 km. They are an obvious consequence of the influence of "weather" in the lower stratosphere, where ozone concentrations are controlled by atmo-

TABLE B1

VERTICAL DISTRIBUTION OF AMPLITUDES OF PERIODIC VARIATIONS
AND OF RELATIVE STANDARD DEVIATIONS OF APERIODIC
SHORT- AND LONG-TERM FLUCTUATIONS

A. Relative Standard Deviations of Aperiodic Fluctuations in Midlatitudes (percent)

Altitude	Short-term	Long-term	
		Australia	Midlatitude
Troposphere	± 20 to 40	-	-
Tropopause layer	> ± 50 to 100	± 15 to 25	-
20-30 km	± 10	± 15	-
> 30 km	± 20	-	-10 to + 5(?)

B. Annual Wave*

Parameter	Latitude		
	0°	40°	80°
Altitude (km) } of maximum	20	12-20	16
Amplitude } of maximum	± 10	± 25	± 33
Amplitude 25-30 km	± 5	± 8	± 30

C. Semi-annual Wave*

Altitude (km) } of maximum	20	20	18
Amplitude } of maximum	± 10	± 6	± 7
Amplitude at 25-30 km	± 3	± 2	± 8 (?)

D. Quasibiennial Variation*

Amplitude above 20 km	± 15	± 4	± 9 (?)
-----------------------	------	-----	---------

E. Solar Cycle Variation*

Amplitude above 30 k	<± 2(?)	<± 2(?)	?
----------------------	---------	---------	---

*Amplitudes in B through E expressed in percent of mean

spheric transport processes. The long-term fluctuations have hardly been investigated because of the relatively short series of in-situ measurements. Those based on Umkehr-measurements lead to seemingly large fluctuations. However, we cannot accept them at face value so long as the question of taking aerosol scattering into account (in applying the inversion technique) is not settled.

Among the periodic variations, only the annual wave has large amplitudes that reach a maximum well above the tropopause and in high latitudes. Its magnitude in the upper stratosphere (35 to 50 km) is not yet established. The semi-annual wave possesses the largest amplitude in the tropics, where it attains a magnitude similar to that for the annual wave. Its magnitude at 25 to 30 km seems to us less certain because it is small and probably buried in the noise. Nothing is known about its magnitude in the upper stratosphere.

The quasibiennial variation exists only at altitudes well above 20 km and may reach ± 5 to 10%, but further careful investigations are needed. The present results seem questionable.

Finally, the solar cycle variation, if it exists at all and then only above 30 km, is very small and may be less than $\pm 2\%$, so that it is buried in the noise.

B.2 TROPOSPHERIC OZONE

2.1 TROPOSPHERIC CONTENT

Using the balloon measurements, the tropospheric ozone content can be determined. Unfortunately, very limited use is made of the measurements to derive this information. The main problem of tropospheric ozone is the magnitude of its flux from the stratosphere through the tropopause to the ground and the magnitude of its destruction at the earth's surface. Junge (1963) investigated it with limited data and derived a flux of $1 \text{ to } 2 \times 10^{-7} \text{ g}/(\text{m}^2 \text{ sec})$ with a residence time of 1.1 to 2 months. Present estimates are of the same order of magnitude. Fabian and Pruchniewicz (1977) derive tropospheric residence times for 30° latitude intervals from which we obtain, after weighting according to the area, 62 ± 14 days for the Northern and 83 ± 18 days for the Southern Hemisphere. This difference is caused by the land/ocean distribution of the two hemispheres and by land having a larger destruction rate than ocean. Tropospheric mean residence time is therefore only 2 to 2.7 months.

At any place, about 6 to 15% of the total ozone is confined to the troposphere; its magnitude depends on the latitude and season (Khrgian, p. 146). For example, the annual average for Boulder, Colorado, is 7%, for England (Kay et al. 1956) 8.5%, and for India (Sreedharan et al. 1974) 8 to 10%.

The global average content, estimated first by Junge (1963), is $2.6 \times 10^{11} \text{ kg}$, or about 8% of the total ozone. We derive from Pruchniewicz's data (1974) practically the same value. The content undergoes seasonal variations with a maximum during the summer and an amplitude of about ± 20 to 25% of its mean value.

There are no ozone sources in the troposphere except pollution sources in the ground. Its production by lightning and in polluted cities (e.g., Los Angeles) contributes practically nothing to the

global budget. The tropospheric sink is its destruction on the ground, which has been computed by several investigators; their results are listed in CIAP Monograph 1, p. 342. Reactions of OH with ozone could be a very minor tropospheric sink. From extensive ground and aircraft measurements, Fabian and Pruchniewicz (1977) derive for the ozone sink in the Northern Hemisphere $(17 \pm 5) \times 10^{28}$ molec/sec, and a global total of $(28 \pm 9) \times 10^{28}$ molec/sec corresponding to $(7 \pm 2) \times 10^{11}$ kg/year. From all recent investigations, it follows that a reasonable value for the global destruction rate is 5 to 10×10^{11} kg/year, or 2 to 4×10^{29} molec/year. The combination of destruction rate, tropospheric content, and tropospheric lifetime have to agree.

2.2 TROPOSPHERIC CONCENTRATION

Average tropospheric concentrations in $\mu\text{g}/\text{m}^3$, based on airplane measurements, have been derived by Pruchniewicz (1974) as follows.

Hemisphere	Latitude Belt		
	0 - 30°	30 - 60°	60 - 90°
Northern	38	42	49
Southern	35	44	42

From these values, we derive 2.56×10^{11} kg as the tropospheric global content using our tropopause heights. Finally, this value corresponds to an average global mixing ratio of about 36 ppbv, or a concentration of $40 \mu\text{g}/\text{m}^3$.

In the troposphere, the partial pressure is, in general, constant with altitude. Consequently, the mixing ratio and the concentration in $\mu\text{g}/\text{m}^3$ increase with height by at least a factor of 2, and at some places more. This is best seen in the extensive tabulations prepared by Wilcox and Belmont (1977).

The ozone concentration in the atmospheric boundary layer (thickness variable, about 1 km) is influenced by the mass exchange through its boundary, the strength of the sink at the ground, and, of course, by the strength of the pollution sources; in short, it is dominated by the local microclimate. The average undisturbed (unpolluted) concentration in this boundary layer is about 20 to 50 $\mu\text{g}/\text{m}^3$, about 10 to 24 ppbv, with the highest values on coastal places, because ocean water is less destructive to ozone than continental soils are. For example, while automobile traffic increased ozone concentration in Los Angeles, the concentration decreased in Paris from 1954 to 1963 from 22.7 to $3.1 \mu\text{g}/\text{m}^3$ or from 10.6 to 1.45 ppbv (Vassy 1965, p. 135). Although there have been many systematic measurements of ozone near the ground (see the extensive discussion by Khrgian, p. 157 and, especially, the extensive German network from Northern Norway to South Africa with most stations operating since 1969/70, as reported by Fabian and Pruchniewicz 1977), no simple relationships have evolved because the ozone concentration is tied to the meteorology of the particular location and it is unwise to apply results obtained at one place to any other place.

Since the FAA is concerned about airport pollution, the results obtained from the worldwide network of stations, although based on individual interests, should be consulted to see where the results of the multitude of such studies may apply.

2.3 EXCHANGE THROUGH THE TROPOPAUSE

Generally, the ozone concentration increases rapidly above the tropopause. There its gradient for an average winter profile is perhaps 25 to $70 \mu\text{g}/(\text{m}^3 \text{ km})$ and, in individual cases, $100 \mu\text{g}/(\text{m}^3 \text{ km})$. At times the gradient is smaller than these averages, but the increase is always distinct.

An ozone concentration with a mixing ratio in the upper troposphere of 100 ppbv will always indicate stratospheric ozone. Only rarely does an increase begin in the troposphere as shown in Figure B12, where the temperature profile implies a tropopause at 9 km, but the ozone increase starts at 6.5 km and the dark area indicates stratospheric air to be found in the troposphere. It must have entered the troposphere in the tropopause gap between the tropical and polar tropopause because such a massive infusion cannot be accomplished by a simple downward diffusion process. When this air mass moves further downward, it leads to spikes in the vertical ozone profiles, but the spikes disappear fairly fast because of strong horizontal and vertical mixing in the troposphere.

The whole question of stratospheric-tropospheric exchange, ozone intrusions into the troposphere, and its possibility of reaching the ground received a lot of attention during the last few years because EPA set a federal standard of 80 ppbv for 1 hour per year at the ground (now proposed to be revised upward to 100 ppbv) as a limit for an ozone alarm. A number of measurements shows such high concentrations to occur naturally away from pollution sources. In addition, the results of some extensive field measurements with airplanes are now available (Fabian and Pruchniewicz 1977; Holdeman et al. 1977 a, b).

The ozone reservoir for injections into the troposphere is situated in the 125 to 250 mb layer, where large seasonal variations occur, with a maximum in late spring. From its tropical source region, ozone is transported poleward in the stratosphere by the general circulation. The lower stratosphere also participates in the large-scale weather processes (cyclones-jet stream).

For the tropospheric-stratospheric mass exchange, several processes are involved, often simultaneously, yet of different magnitude. They are, according to Reiter (1975):

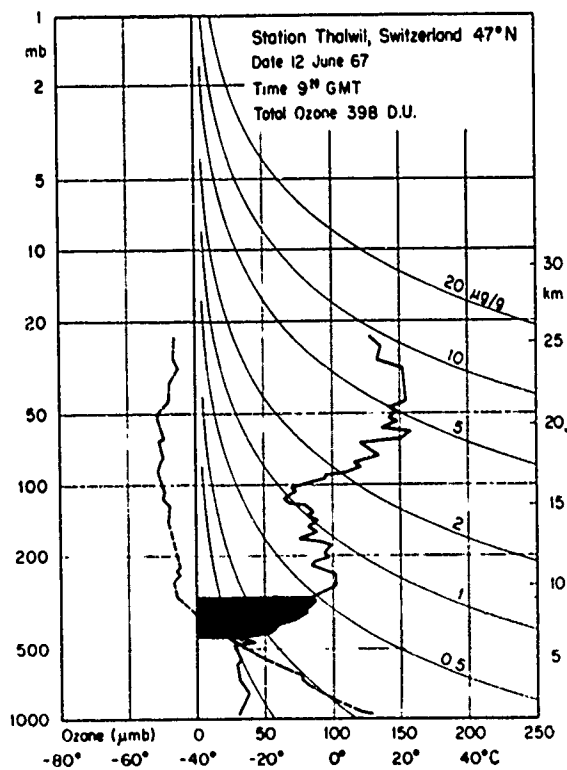


Figure B12 Transfer of Stratospheric Air (dark mass between 6.5 and 9 km) into the Troposphere. This infusion is manifested by the strong increase of ozone concentration with height in the upper troposphere (solid line: ozone concentration, dashed line: temperature) (Source: Dütsch 1971).

- (a) large-scale eddy transport, mainly in the jet stream region,
- (b) seasonal height variations of the tropopause level,
- (c) mesoscale and small-scale eddy transport across the tropopause, and
- (d) organized large-scale quasi-horizontal and vertical motions in the mean meridional circulation.

In process (a), transport occurs during the deformation of the tropopause in the jet stream, the so-called tropopause gaps. While this process is in progress, a net outflow of stratospheric air occurs. This outflow has been computed by Danielsen and by Reiter for a few selected synoptic cases leading to an outflow of 20 to 90% of all of the stratospheric mass in the course of one year. There are several assumptions involved for which we must refer to the original papers. If the ozone concentration in its reservoir is taken as 1 ppmv, the outflow amounts to 0.8 to 4.3×10^{11} kg in the Northern Hemisphere. These numbers already indicate that this must be the dominant process. Examples of the field measurements and their interpretation can be found in Danielsen (1968) and Danielsen and Mohnen (1977). It is also worth mentioning that the Japanese ozonesonde data show larger ozone concentrations in the region of the polar tropopause than in the region of the tropical tropopause (Watanabe and Tohmatsu 1976).

Another indicator of the dominance of process (a) is the relationship between the vertical ozone profile and the wind curvature, the latter being obtained from windfield measurements. During cyclonic curvature of the windfield, the tropopause layer contains much more ozone (350 ppbv) than for the cases of anti-cyclonic curvature (130 ppbv at the tropopause). This difference of up to about 200 ppbv between the two mixing-ratio profiles seems unambiguous from 40 mb below to 40 mb above the tropopause with little overlap in the standard deviations of the two data sets. The basic data have been obtained on the numerous GASP flights by Holdeman et al. 1977b and are another example of the importance of process (a).

After intruding into the troposphere, mixing with the surrounding air dilutes the ozone concentration during its descent toward the ground. While the border areas undergo a rapid mixing process, the core dilutions amount to about a factor of 5 (Danielsen 1964). If this is the case, values of 150 ppbv at the ground are conceivable.

Process (b) describes the annual variation of the tropopause height, transforming stratospheric air into tropospheric air by the gradual rise in tropopause height, especially in late winter. This process, for example, clears the stratosphere of a large amount of aerosols, as Hofmann et al. have shown convincingly. It amounts to about 10% of the stratospheric mass and operates only north of 30° , while height changes in the tropics are negligible. This process could add 4 to 8×10^{10} kg of ozone to the Northern Hemisphere troposphere.

Process (c) has been investigated by Reiter (1975). It amounts to only 1 to 5% of the total flux from the stratosphere, and a similar small magnitude has been derived by Fabian from his airplane measurements between Norway and South Africa.

Process (d), the mean meridional circulation, is mainly the Hadley cell circulation in the tropics. In the inner tropics, it transports tropospheric air, poor in ozone, into the stratosphere and, after some enrichment due to mixing, brings it back into the troposphere in the descending branch of this circulation around 15 to 30° N, depending on season. Its magnitude is not known, but its contribution to enrich the tropospheric ozone concentration should be very small indeed. However, this process is the most important one for water vapor and is discussed in Section C6.2.1.

The estimates of the magnitudes of each individual process and the derivation of yearly magnitudes are difficult to make. Often it is easier to estimate the total injection by all processes combined. Nastrom (1977), using GASP data, took the ozone gradient

in a layer from 50 mb below to 50 mb above the tropopause and assumed a downward wind component of 0.5 cm/sec based on estimates from other investigations. From this ozone gradient and the wind speed follows an average annual injection rate of 7.8×10^{10} molec/(cm² sec) north of 30°, corresponding to 4.9×10^{11} kg. Fabian and Pruchniewicz (1977) obtained 3 to 10×10^{10} molec/(cm² sec) or 2 to 6.3×10^{11} kg.

Such estimates point to process (a) as the main injection process, all others being of minor importance. Certainly neither process (a) nor any of the others is a diffusion process to be described by a single diffusion coefficient as most model computations do.

Extremely large concentrations from such stratospheric intrusions have been recorded on mountain stations. Attmannspacher (1973) reports recording at a few occasions 150 to 300 ppbv values for periods longer than 10 minutes connected with cold fronts and snowfall at a station at a 1000 m high mountain top. Some specific cases of large ground concentrations are discussed by Mohnen (1977); they are rare but should not be overlooked.

Some puzzling data have been obtained on some airplane flights crossing the equator. Nastrom (1978) finds some high values (> 60 ppbv) around 3 to 10°N in November 1976 on CASP flights, and Fabian reported two cases in late 1972. Nastrom believes them to be related to the occurrence of clouds. This rare phenomenon need some further investigation, although it does not seem to play any major role.

Although tropospheric measurements using the chemiluminescent technique have not been used in this Section B.2 to derive numerical values, it should be added that recent investigations by Chatfield and Harrison (1977) and Wilcox (1978) have shown that this technique consistently underestimates ozone concentrations in the troposphere. Such data should be raised by about 50%.

B.3 FIELD MEASUREMENTS BETWEEN 8 AND 12 KM ALTITUDE

3.1 OVERBURDEN

Using UV or IR optical techniques, the overburden of ozone above flight altitude can be measured. Nobody has used a Dobson spectrophotometer on such a flight; that might be a bit too complicated. Simpler instruments have been used, and a proper but involved reduction program yields the overburden. Such data are useful only if the flight follows a constant pressure level, which it normally does not. For operational reasons or to fulfill the requirements of other experimenters on board, altitudes change along the flight routes. Thus, the overburden is less useful than concentration measurements. Data have been obtained by Sellers and Hanser (1975), Hanser et al. (1978), Barrett et al. (1973), and Shlanta and Kuhn (1974). The first authors used UV, the rest IR techniques. In the case of Barrett et al., the overburden at two flight altitudes over the tropical convergence zone and by Shlanta and Kuhn at several altitudes between 13.7 and 17 km around cumulonimbus clouds was used to derive the concentration within a layer and, together with the water vapor concentration, to estimate the vertical ozone flux. The changes in ozone concentrations in both cases are small and explanations are discussed in an earlier report by Penndorf (1975).

Sellers' and Hanser's earlier data are not too useful. The difficulty in reducing the data to a selected altitude lies in the steep ozone gradient of about a factor of 2 in this altitude region from 13 to 19 km. The same disadvantages apply to Murcray's data. However, Sellers' and Hanser's recent (1978) measurements in the upper troposphere permit us to calculate the total stratospheric amount because its tropospheric concentration is small. Flying at about 10 km above clouds gave about 0.9 to 0.95 of the total amount measured by Dobson instruments during overflights. Applying a correction for flight altitude and tropospheric ozone

B.3 FIELD MEASUREMENTS BETWEEN 8
AND 12 KM ALTITUDE

3.1 OVERBURDEN

Using UV or IR optical techniques, the overburden of ozone above flight altitude can be measured. Nobody has used a Dobson spectrophotometer on such a flight; that might be a bit too complicated. Simpler instruments have been used, and a proper but involved reduction program yields the overburden. Such data are useful only if the flight follows a constant pressure level, which it normally does not. For operational reasons or to fulfill the requirements of other experimenters on board, altitudes change along the flight routes. Thus, the overburden is less useful than concentration measurements. Data have been obtained by Sellers and Hanser (1975), Hanser et al. (1978), Barrett et al. (1973), and Shlanta and Kuhn (1974). The first authors used UV, the rest IR techniques. In the case of Barrett et al., the overburden at two flight altitudes over the tropical convergence zone and by Shlanta and Kuhn at several altitudes between 13.7 and 17 km around cumulonimbus clouds was used to derive the concentration within a layer and, together with the water vapor concentration, to estimate the vertical ozone flux. The changes in ozone concentrations in both cases are small and explanations are discussed in an earlier report by Penndorf (1975).

Sellers' and Hanser's earlier data are not too useful. The difficulty in reducing the data to a selected altitude lies in the steep ozone gradient of about a factor of 2 in this altitude region from 13 to 19 km. The same disadvantages apply to Murcray's data. However, Sellers' and Hanser's recent (1978) measurements in the upper troposphere permit us to calculate the total stratospheric amount because its tropospheric concentration is small. Flying at about 10 km above clouds gave about 0.9 to 0.95 of the total amount measured by Dobson instruments during overflights. Applying a correction for flight altitude and tropospheric ozone

leads to an agreement with Dobson measurements of 0.985 or about $\pm 2\%$. Such "low" flights can be useful to provide latitude and longitude structure of total ozone or seasonal variations, or data over the oceans as long as they are made below the tropopause.

There is one interesting case published by Sellers for a flight from Panama to Albuquerque shown as Figure B13. The outstanding feature is the area of high ozone overburden at 16.2 km between 28 and 32°N. The overburden increased from 0.22 to 0.252 atm cm or about 14% and decreased to 0.23 atm cm. This ozone cloud is 0.02 atm cm above the values experienced 9 days earlier at the same latitudes but at an altitude of about 17.4 km. This is a good example of the influence of a weather condition with a transport from higher latitudes. It is restricted to a cross-section of about 450 km with a lateral mixing extending over 200 km at the northern and southern boundary. While such changes are well known from ground measurements, their latitudinal extent can best be established during an aircraft flight.

Measuring the overburden in the stratosphere is not recommended, because such measurements do not tell us at what altitudes changes in concentration occur.

3.2 IN-SITU MEASUREMENTS OF CONCENTRATION

In Section 1.4, we discussed the large natural fluctuations in the tropopause region. This is exactly the region in which so many in-situ measurements are accomplished and which is described below.

Pruchniewicz et al.(1974) report measurements of ozone concentration using commercial aircraft between middle Europe and South Africa as well as northern Norway. The cruising altitude of 10 to 12 km was definitely in the troposphere for equatorial flights. Using a chemical technique, they obtained 32 profiles from Sep-

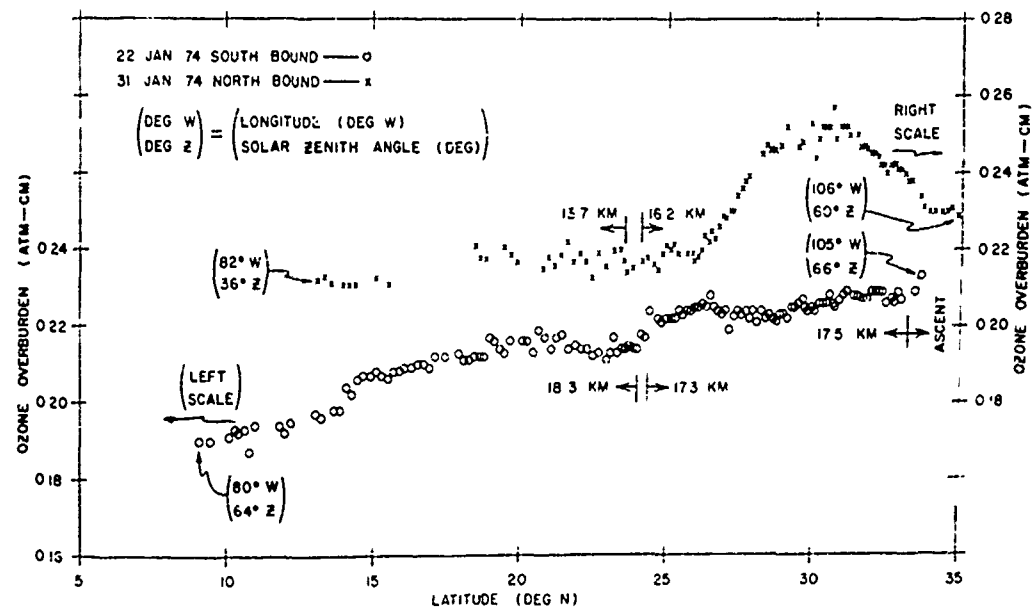


Figure B13 Ozone Overburden in atm cm Between Panama and Albuquerque. An ozone cloud is encountered near 30° N on 31 January 1974. The overburden increases by 14% (Source: Sellers and Hanser 1974).

tember 1970 to July 1973. Over low latitudes, 30°S to 30°N , no latitudinal variation in mixing ratio was measured, but a seasonal march with about 36 ppbv in March to August and 24 ppbv from September to February. Their large values over Norway seem questionable to us. If the measurements were made in the troposphere, as the authors claim, they represent large influxes of stratospheric air around 65°N . These data have been used by Fabian and Pruchniewicz (1977) to derive regions of injections, the injected mass, and their tropospheric residence time, topics discussed above in Section B.2.3. For these purposes the flights have been very useful and necessary.

Another measurement program using commercial aircraft is being vigorously carried out by NASA/Lewis (Holdeman and Falconer 1976 and Holdeman et al. 1977b). It started in March 1975, uses a UV ozone photometer (Dasibi) with a sensitivity of 3 ppbv and a flight altitude of the B-747 between 8.8 and 13.1 km, but most data are taken at 11 ± 1 km. The tropopause pressure is derived from the National Meteorological Center Library of gridded meteorological field-data, which are on tape. Results are stored on tape and available to interested investigators. Only a few flights have been interpreted so far. We select a sample in Figure B14, a flight from San Francisco to Japan, India, and Germany in March 1975. Above the Pacific Ocean the flight altitude was above the tropopause and the ozone mixing ratio of 600 to 800 ppbv was truly stratospheric. The maxima in ozone over the Pacific coincide with cyclonic wind flow. Between Hongkong and Germany the flight was in the troposphere with mixing ratios between 3 and about 40 ppbv (exact values cannot be read well). The ozone peak of 440 ppbv and the corresponding increase in static air temperature over the Middle East suggests a brief stratospheric penetration or an infusion of stratospheric air through a tropopause gap.

These data have been used extensively by Belmont et al. (1978) to derive information for flight planning when high stratospheric

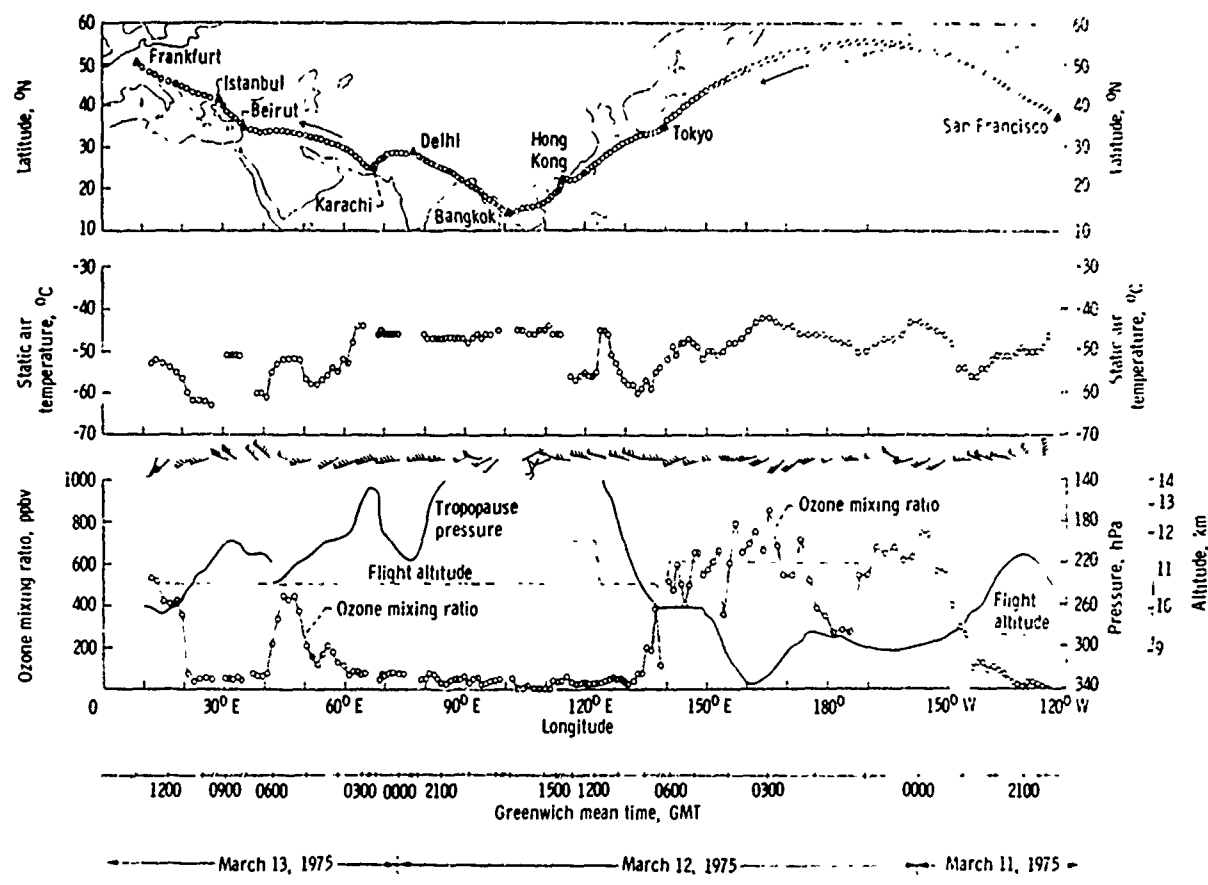


Figure B14 Flight Record of March 11-13, 1975 from San Francisco to Frankfurt, West Germany. Ozone mixing ratios, ambient air temperature, wind data, flight route and altitude are obtained from GASP and aircraft systems. Wind barbs follow standard National Weather Service plotting conventions. Tropopause pressures are obtained from National Meteorological Center data archives and are assumed to be valid for ± 6 hours about 0000 GMT and 1200 GMT (Source: Holdeman and Falconer 1976).

ozone concentrations can lead to unhealthy conditions inside the cabin. Other studies of the data by Nastrom (1978) include, for example, averages, standard deviations, and maximum values in zones 6° in latitude and 50° in longitude by season at 11 to 12 km altitude. What these data clearly indicate is the extremely large natural variability of ozone concentration in midlatitudes at 11 km. To me, this is about the worst altitude at which to measure ozone because any value is possible. I am not sure what we may learn from this exercise.

Briehl et al.(1974) report measurements of ozone (and NO and H_2O) using a Convair 990 between Hawaii and the U.S. west coast at flight altitudes from 8 to 12.4 km. The mixing ratios varied between 10 and 120 ppbv depending on altitude. Most of the values are low, typically tropospheric as expected for these altitudes and latitudes. No evaluation with regard to tropopause height and weather situation has been attempted.

In summary, there exist several measurements of ozone concentration using aircraft as carriers. Those flying in the 8 to 12 km altitude range show a wide variety of concentrations depending solely on the distance from the tropopause. In those cases, the mixing ratio can be used to identify the air mass. For flights around 20 km, the concentrations are strictly stratospheric with minor fluctuations.

3.4 REF E R E N C E S

Angail,J.K., and J.Korshover, Recent trends in total ozone and ozone in the 32-46 km layer, WMO Conference,Toronto, 1978.

Attmannspacher,W., and R.Hartmannsgruber, On extremely high values of ozone near the ground at the observatory Hohenpeissenberg, Pure Appl. Geophys., 106-108,1091,1973.

Barrett,E.W., P.M.Kuhn, and A.Shlanta, Recent measurements of the injection of water vapor and ozone into the stratosphere by thunderstorms, Proc.2nd Conf. on CIAP, DOT-TSC-OST-7304,34,1973.

Belmont,A.D., et al. (5 authors), Guidelines for flight planning during periods of high ozone occurrence, FAA-EQ-78-03,1978.

Brewer,A.W., and D.R.Milford, The Oxford-Kew ozone sonde, Proc. Roy. Soc,London, A 256,470,1960.

Briehl,D.C., E.Hilsenrath, B.A.Ridley, and H.I.Schiff, In-situ measurements of nitric oxide,water vapor, and ozone from an aircraft. 2nd Intern.Conf. environm.impact...,San Diego, Am. Meteor.Soc., 11,1974.

CIAP, Monograph 1, The natural stratosphere, DOT-TST-75-51, 1975.

Danielsen,E.F., Radioactivity transport from stratosphere to troposphere, Miner.Ind., 33,1,1964.

Danielsen,E.F., Stratospheric-tropospheric exchange based on radioactivity,ozone, and potential vertyicity, J.Atm.Sci., 25, 502,1968.

Danielsen,E.F., and V.A.Mohnen, Project Duststorm report, J. Geophys. Res., 82,5867,1977.

Dütsch,H.U., Atmospheric ozone and ultraviolet radiation, in: World survey of climatology, 4,383,1969.

Dütsch,H.U., Photochemistry of atmospheric ozone, Adv. Geophys., 15,219,1971.

Dütsch,H.U., The ozone distribution in the atmosphere, Can.J. Chem., 52,1491,1974.

Dütsch,H.U., private communication, 1976.

Dütsch,H.U., Vertical distribution of ozone on a global scale, Pure Appl. Geophys., 116,511,1978.

Wütsch, H.U., and Ch.C.Ling, Six years of regular ozone soundings over Switzerland, Pure Appl.Geophys., 107, 1139, 1973.

Fabian, P., and P.G.Pruchniewicz, Meridional distribution of ozone in the troposphere and its seasonal variations, J. Geophys. Res., 82, 2063, 1977.

Götz, F.W.P., Zum Strahlungsklima des Spitzbergen Sommers. Strahlungs- und Ozonmessungen in der Königsbucht, 1929, Gerl. Beitr. Geophys., 31, 119, 1931.

Hanser, F.A., B.Sellers, and D.C.Briehl, Ultraviolet spectrophotometer for measuring columnar atmospheric ozone from aircraft, Appl.Opt., 17, 1649, 1978.

Hering, W.S., and T.R.Borden, Ozone observations over North America, AFCRL-64-30, Vol 3 and 4, 1965, 1967.

Holdeman, J.D., and P.D.Falconer, Analysis of atmospheric ozone measurements made from a B-747 airliner during March 1975, NASA-TN-D-8311, 1976.

Holdeman, J.D., D.J.Gauntner, F.C.Humenik, and D.Briehl, NASA global atmospheric sampling program (GASP). Data report for tape VL 7 and 8, NASA-TM-73784, 1977a.

Holdeman, J.D., G.D.Nastrom, and P.D.Falconer, An analysis of the first two years of GASP data, NASA-TM-73817, 1977b.

Junge, Ch., Air chemistry and radioactivity, Acad. Press, New York, 1963.

Kay, R.H., A.W.Brewer, and J.M.B. Dobson, Some measurements of the vertical distribution of atmospheric ozone by a chemical method, Sci.Proc.IAM, 10th Gen.Assembly, Rome 1954, 189, 1956.

Khrgian, A.Kh., The physics of atmospheric ozone, Leningrad 1973, Translation TT-74-50027 (NTIS), Jerusalem, 262 pp, 1975.

Komhyr, W.D., Electrochemical concentration cells for gas analysis, Ann. Géophys., 25, 203, 1969.

Krueger, A.J., and R.Minzner, A mid-latitude ozone model for the 1976 US standard atmosphere, J. Geophys.Res., 81, 4477, 1976.

Loewenstein, M., H.Savage, and R.C.Whitten, Seasonal variations of NO and O_3 at altitudes of 18.3 and 21.2 km, J.Atmos.Sci., 32, 2185, 1975a.

Loewenstein,M., and H.F.Savage, Latitudinal measurements of NO and O_3 in the lower stratosphere from 5° to $82^{\circ}N$, Geophys.Res.Lett., 2,448,1975b.

Loewenstein,M., et al.(5 authors), Geographical variations of NO and O_3 in the lower stratosphere, J.Geophys.Res., 83,1875,1978.

London,J., The thermal structure and dynamics of the stratosphere, Intern.J.Chem.Kinetics, Symposium No 1,85,1975.

Mateer,C.L., On the information content of Umkehr observations, J.Atmos. Sci., 22,370,1965.

Mohnen,V.A., The issue of stratospheric ozone intrusion, ASRC, Publ.No 428,1977.

Nastrom,G.D., Vertical and horizontal flux of ozone at the tropopause for the first year of GASP data, J.Appl.Met.,16,740,1977.

Nastrom,G.D., Variability of ozone near the tropopause from GASP data, NASA-CR-135405, 1978.

National Academy of Science, Environmental impact of stratospheric flight, Washington, D.C., 1975.

Pätzold,H.K., F.Piscalar, and H.Zschörner, Secular variations of the stratospheric ozone layer over middle Europe during the solar cycles from 1951 to 1972, Nature, 240,106,1972.

Penndorf,R., The results of CIAP's stratospheric measurement Program, in: DOT-TST-75-106,1975.

Pittock,A.B., Ozone climatology,trends, and the monitoring problem, Proc. Intern.Conf. on struct.,...,Melbourne,IAMAP,1,455,1974.

Pittock,A.B., Climatology of the vertical distribution of ozone over Aspendale, Quart.J.Roy.Meteor.Soc.,103,575,1977.

Pruchniewicz,P.G., A study of the tropospheric ozone budget based on interhemispheric mass exchange, Proc.Intern. Conf. on struct.,...,Melbourne,IAMAP,1,429,1974.

Pruchniewicz,P.G. et al. (5 authors), The distribution of tropospheric ozone from worldwide surface and aircraft observ., Proc. Intern. Conf.on struct.,...,Melbourne,IAMAP 1,439,1974.

Regener,V.H., On a sensitive method for the recording of atmospheric ozone, J. Geophys. Res., 65,3975,1960.

Reiter, E.R., Stratospheric-tropospheric exchange processes, Rev. Geophys. Space Phys., 13,459,1975.

Sellers,B., and F.A.Hanser, WB57f-borne measurements of UV flux and ozone overburden, 4th CIAP Conf., DOT-TSC-OST-75-38,398,1975.

Shlanta,A., and P.M.Kuhn, Ozone and water vapor injected into the stratosphere from isolated thunderstorms, NOAA, Letter report to CIAP, 1973.

Vassy,A.T., Atmospheric ozone, Adv. Geophys., 11,116,1965.

Watanabe,T., and T.Tohmatsu, An observational evidence for the seasonal variation of ozone concentration in the upper stratosphere and the mesosphere, Rep.Ionosph.Space Res. Japan, 30,47,1976.

Wilcox,R.W., and A.D.Belmont, Ozone concentration by latitude, altitude, and month, near 80° W., FAA-AEQ-77-18,1977.

Wilcox,R.W., G.D.Nastrom, and A.D.Belmont, Periodic variations of total ozone and of its vertical distribution, J.Appl.Meteor., 16,290,1977.

Wilcox, R.W., Comments on tropospheric ozone, J. Geophys. Res., 83, 6263, 1978.

C. STRATOSPHERIC WATER VAPOR:
ANALYSIS AND INTERPRETATION OF FIELD MEASUREMENTS

ABSTRACT

The stratospheric field measurements of water vapor are critically analyzed and interpreted. Existing techniques are described. The results obtained for vertical profiles are given in tables and graphs, omitting obviously incorrect data. An average profile for midlatitudes is derived with a constant mixing ratio of 4.15 ppmv and a standard deviation of about 1 ppmv. There exists a seasonal variation of small magnitude and a long-term trend of about ± 1.5 ppmv per decade. Latitude variations seem to exist in the 15 to 19 km altitude range with maxima in the tropics, yet the data are somewhat contradictory. No clear picture emerges for altitudes above 20 km because of lack of measurements.

The main source of stratospheric water vapor is the upwelling in the Hadley cell, with about 11×10^{11} kg per year. Other sources contribute only minor amounts. The downwelling part of the Hadley cell provides the major sink, followed by some loss during the winter over Antarctica. The total water vapor mass is 2 to 2.5×10^{12} kg with some seasonal and long-term trends.

C.1 INTRODUCTION

From a meteorological point of view, water vapor is the most important atmospheric gas, although its concentration is small. A maximum volume mixing ratio of 4% occurs at sea level at some humid tropical areas of the earth, but mostly it is much less. For example, while many areas in tropical Africa and other tropical countries abound with 3 percent per volume (pcv), for Boston the monthly average of atmospheric water vapor is about 1.5% in July and 0.3% in January.

If there were no water vapor in the atmosphere, the radiative transfer and that part of the energy transport involving conversion from liquid to gaseous phase and vice versa, as well as some of the stratospheric chemistry, would be quite different. We would have neither clouds nor precipitation, resulting in simpler systems of atmospheric processes and of atmospheric chemistry and the "weather" would be completely different from the way it is now.

Fortunately, there is water vapor in the atmosphere, and the tropospheric weather is determined to a large extent by water vapor, water droplets, and ice crystals and the phase changes among them. The stratospheric radiative transfer involves only water vapor, carbon dioxide, and ozone while none of the "trace" gases plays any large role at the present time.

Up to the mid 1960s, we really did not know much about stratospheric water vapor concentration. There was more controversy than agreement, best expressed in Gutnick's (1961) paper, entitled: "How dry is the sky?". Although water vapor has been measured in the stratosphere since the late 1940s, our knowledge of its actual concentration and variation is more or less still limited to northern latitudes, and some controversies we discuss in this section have not been completely resolved. This problem can be readily explained by the enormous difficulties in measuring

the actual undisturbed natural background of water vapor. The published measurements range over orders of magnitude. We now know that all high concentrations were caused by contamination. Most of the older measurements using optical techniques have been proven wrong. Only the first British measurements using the frost-point technique have survived as reliable.

In the early 1970s, mostly in relation to the CIAP program, extensive field measurements resulted in a reasonable knowledge of its vertical distribution in midlatitudes, yet the best "average" concentration can still be disputed because of the relatively small sample. In the lower stratosphere it exhibits some variation with latitude and also with season. Furthermore, we have good reason to suspect a long-term cyclic variation of perhaps $\pm 30\%$ or more.

Unlike the troposphere, the stratosphere is dry, with a relative humidity of a few percent. A typical volume mixing ratio* of 3.5 ppmv at 16 km ($P = 100$ mb and $T = -60^\circ\text{C}$) corresponds to a relative humidity of 3% (over ice). The same mixing ratio at 30 km ($P = 12$ mb and $T = -50^\circ\text{C}$) yields only 0.1%. Volume mixing ratios range from perhaps 1 to 6 ppmv at ambient temperatures from 195 to 270°K (about -80 to 0°C), where the high temperatures occur at the stratopause (around 50 km altitude). The residence time of water vapor and other constituents is longer in the stratosphere (about 1 to 2 years) than in the troposphere, where the cycle of evaporation to precipitation takes only 8 to 11 days. Such a long residence time is of importance to artificially injected water, for example, from jet aircraft exhaust.

Most atmospheric substances exist in the troposphere and stratosphere above their melting and boiling point, except water and a

*We use only volume mixing ratios. All older measurements and many present data are given as mass mixing ratios. We have converted all data to volume mixing ratios, because stratospheric trace gases are generally quoted as volume mixing ratios, especially for atmospheric chemistry and modeling. The conversion factor for water vapor is: volume m.r. = 1.607 mass m.r.

few trace gases. Because water vapor* exists in the stratosphere well below its melting and boiling points, ice will form if the water molecules hit cold surfaces on instruments, or in pipes with high flow rates, or in similar materials.

The maximum partial pressure of water vapor ($=$ saturation vapor pressure E) depends strongly on temperature, and therefore the concentration of water vapor decreases in the troposphere from the equator to the poles and with altitude. At a surface between liquid and gaseous water, equilibrium exists between evaporation and condensation. The number of molecules (per unit surface area and time) condensing (i.e., going from gaseous phase into liquid phase) depends on the vapor pressure e ; the number of molecules evaporating (i.e., leaving the liquid state) depends only on the temperature. Equilibrium depends, therefore, on the relationship $e = E(T)$. If $e < E$, more water evaporates than vapor condenses. The saturation vapor pressure (E) and number density (N_w) depend on temperature; for the equilibrium case $e = E$ (saturation), Table C1 gives some numerical values.

The maximum mixing ratios decrease by about three orders of magnitude if the frost point decreases from -58 to -98°C , or a drop of 40°C . The measured mixing ratios in the stratosphere correspond to saturation at temperatures of about -78 to -88°C at the tropopause, a point important for the discussion of stratospheric sources (C.6.2).

*The term "vapor" normally refers to a gaseous phase of a substance which - at room temperature - exists as a liquid or solid.

TABLE C1
 SATURATION VAPOR PRESSURE E(mb),
 NUMBER DENSITY N_w (molec/m³) AND VOLUME MIXING RATIOS
 FOR TEMPERATURES BETWEEN 175 AND 215°K AND THREE ALTITUDES

Frost Point		Saturation Vapor Pressure E (mb)	Number Density N_w (molec/m ³)	Saturation Volume Mixing Ratio (altitude in km)		
°K	°C			15	20	30
175	-98	2.10 (-5)	5.84 (17)	1.4(-7)	3.2(-7)	1.5(-6)*
185	-88	1.39 (-4)	5.44 (18)	1.3(-6)	2.9(-6)	1.4(-5)
195	-78	7.58 (-4)	2.82 (19)	7.0(-6)	1.5(-5)	7.3(-5)
205	-68	3.51 (-3)	1.24 (20)	3.1(-5)	6.7(-5)	3.2(-4)
215	-58	1.41 (-2)	4.75 (20)	1.2(-4)	2.6(-4)	1.2(-3)

*(-6) means 10^{-6} or 1 ppmv

C.2 MEASUREMENT TECHNIQUES

Several techniques have been used to measure water vapor concentrations, but essentially only the first two listed below have given reliable results:

- o frost-point hygrometers;
- o optical techniques, infrared absorption and emission; and
- o others, such as adsorption surfaces and cryogenic sampling.

What makes accurate measurement difficult no matter what method is used is contamination of the water vapor, and this subject is therefore addressed first in the discussion that follows.

2.1 CONTAMINATION

The most difficult obstacle is caused by contamination by water vapor around the platform and within the instrumentation package. All instruments are carried aloft by aircraft, balloons, or rockets, which, before take-off, adsorb water vapor on the ground from an environment with high water vapor concentration (several orders of magnitude larger than in the stratosphere). Often these carriers pass through clouds and adsorb more water. Reaching the stratosphere, the carriers and their instrumentation undergo extensive outgassing. Thus, measurements on ascent give much higher concentrations than on descent, and reliable researchers have used only the descent measurements.

Looking at the sun high in the sky from a balloon platform may mean to look through a "water vapor cloud" surrounding the balloon. If air is drawn into an instrument, water vapor can condense as water or ice, resulting in concentrations that are too low, or the condensate may evaporate later leading to an increase in the concentration by varying amounts. Finally, there is water vapor

trapped in instruments sealed in the laboratory at room temperature and humidity during assembly. This amount, though small, can become comparable to that in an absorption path at very high altitudes. The water vapor concentrations in aircraft cabins falsify the measurements of unsealed optical devices, and corrections are cumbersome and often unreliable. Various pitfalls have been discussed by Zander (1966,1973). They are obvious in some early measurements because they are extremely large mixing ratios above 20 km. Present investigators generally know about all of them.

2.2 FROST-POINT HYGROMETER

The frost-point hygrometer measures the ambient frost-point (or dew-point) temperature during balloon descent. It was first used successfully in England on high altitude aircraft in 1942 (Dobson et al.1946,1962). Many investigators still use it as a standard for calibrating other types of devices.

Mastenbrook's instrument, the best of the present instruments, has an optical-electronic-thermo servo loop which continuously controls the temperature of a mirror to maintain a frost deposit in equilibrium with the partial pressure of water vapor, i.e., $e = E$. Induction heating, balance against a heat sink of freely boiling Freon 13, controls the size of the condensate on the mirror and provides a capability for measuring frost points to -110°C . The temperature of the mirror, taken as the frost point of the ambient natural water vapor, is measured by a thermistor embedded in the mirror. At the same time, air pressure and temperature are measured.

In this case, there is equilibrium between e and E . Because the temperature of the mirror is measured quite accurately, the value for E can be obtained. A formula for $E(T)$ can be derived from thermodynamic principles and the results tabulated. The partial pressure of water vapor is converted to concentration N_w and

volume mixing ratio w_v by

$$N_w = \frac{e N}{P} \text{ (molec/m}^3\text{)} \quad (1)$$

$$w_v = e/P \quad (2)$$

A single measurement refers to a layer about 0.5 km thick, and the instrumental error is estimated by Mastenbrook as $\pm 0.3 \times 10^{-6}$ (g/g) or $\pm 0.5 \times 10^{-6}$ (v/v).

If we take proper precautions to avoid contamination, the frost-point hygrometer should give reliable mixing ratios because it requires the fewest assumptions. It seems strange to us that this technique has found so few users.

The British frost-point hygrometer (Mk 3) has been examined by Oliver and Cluley (1978) and a systematic error was found. A temperature gradient occurs in the hygrometer thimble leading the sensor to read too low, about 1.4°C for a thimble temperature of -40 to -49°C increasing to 2.1°C for -80 to -89°C . The recent field data of 1972-76 and the older data of 1954-55, which we use in this report, include this correction.

2.3 OPTICAL TECHNIQUES

Most investigators prefer to use optical techniques. Water vapor has a large number of spectral bands, from the near IR to the mm range; its characteristic frequencies of molecular and vibrational transitions lie in the IR range. The submillimeter atmospheric spectrum is rich, complicated, and extensive, though very weak in intensity. All these facts argue strongly for the use of Fourier spectroscopic methods. In the mm range, Waters et al. (1977) attempted measurements of a single line at 1.64 mm (183 GHz) to derive water vapor concentrations. For a long time, absorption techniques, using the sun as source, have been preferred. Recently, emission techniques have come into use. For the measurement

itself, either spectroscopic or radiometric techniques are chosen. Thus, one can classify the various measurements into:

- o spectroscopy:
 - low resolution (band) - absorption;
 - high resolution (lines) - absorption;
 - medium and high resolution - emission
- o radiometry:
 - filters - emission.

An optical measurement embodies the emission or absorption of all the (water) molecules along an optical path and of all the other molecules undergoing characteristic transitions at the same frequency. It is never a true in-situ measurement. Optical techniques are very effective in identifying the presence of a gas. If characteristic lines or bands of a certain molecule appear on a spectrum, we can be certain of its existence in the particular optical path. However, the determination of its concentration is very complicated, leading to relatively large systematic errors. It requires the transfer of the measured numbers through several analytical stages, each of which possibly involves some errors. Because these stages are often complicated, we first give a general description of some of the most important stages to help the reader understand the difficulties of obtaining reliable concentrations.

Farmer (1974) has given a good description of the theoretical basis for the relationship between the total molecular cross-section and the corresponding observed atmospheric emission and absorption.

2.3.1 Concentration and Optical Path

The molecular number density $N_w(h)$ is obtained from the optical depth by taking into account the geometric factor g relating the observer path to the radial path, and the molecular extinction

coefficient k at frequency ν . Furthermore, for emission, the temperature profile along the optical path must be known fairly well. It also requires intensity calibration because the measurements are made in terms of absolute radiance. For absorption the solar $I_o(\nu)$ requires knowledge of the solar continuum, i.e., where $k(\nu) \rightarrow 0$. The size of the sun ($30'$) and uneven intensity distribution across the disk must be (and has been) taken into account.

In practice, the intensity is measured over a finite spectral interval $\Delta\nu$, defined by the instrumental slit function in the spectroscopic case (the spectral resolution) or by the transmission characteristics of the optical filter in the radiometric case. To obtain a vertical distribution of $N_w(h)$, one has to vary zenith distance θ and the height of the observer H ; otherwise assumptions have to be introduced.

2.3.2 Extinction Coefficient

The extinction coefficient k for a particular line depends on the line intensity S at the line center and the shape factor, a complicated function involving the Doppler and Lorentzian half widths. For stratospheric conditions, Doppler and Lorentzian broadening have to be considered.

Thus, for each line, its line intensity S and its half width γ must be known; the latter depends on pressure and (less important) on local temperature; it varies within a specific band. The knowledge of S and γ enters the overall accuracy of the resulting concentration N_w .

Additionally, overlapping by lines of the same gas, or its isotopes, or other atmospheric gases, plays an important role. The region under investigation should, ideally, be free from other lines that contribute to the experimental spectrum. Thus, we should know the line position and strength of interfering gases to subtract their contribution to the experimental line spectrum.

Sometimes simplifications are introduced. The use of "equivalent width" of a line or feature provides a convenient parameter to compare observed and calculated spectra. This is useful in the analysis of isolated or very weak spectral features.

For very complex bands with closely packed or overlapping lines, "band models" have been proposed, in which the distance between line centers is treated statistically. They are used for radio-metric measurements of water vapor. Nevertheless, the application has decreased recently, because band spectra can now be handled by computers.

2.3.3 Geometrical Factor

The geometrical factor, $g(\theta, h)$, is the most powerful weighting factor available for the determination of $N_w(h)$, especially close to $\theta = 90$. The variation of g for $\theta = 90$ to 94° is large if h is below the observation altitude H (see Farmer's Figure 1 (1974) as an example). One can also vary H and keep h and v constant to obtain $N_w(h)$. In this case, θ can be $< 90^\circ$. In practice, v , H , and θ are varied. Nevertheless, careful planning, with the help of model distributions, is necessary to obtain meaningful weighting functions.

Thus, for absorption, measurements near sunrise and sunset represent the best conditions to obtain $N_w(h)$. This has been done, for example, by Murcay's group. For emission, horizon measurements can be accomplished at any time of the day or night, as Harries has done. Since water vapor does not undergo any diurnal variation, it makes no difference at what time of the day measurements are carried out. Obviously, sunrise or sunset measurements demand a high degree of planning and experience in balloon launching. Emission measurements, on the other hand, can be obtained continuously during long aircraft flights in combination with measurements of other gases.

2.3.4 Model Atmospheres

The analysis of data is performed by dividing a model atmosphere into a number of layers, assigning temperature and pressure to each of these and then solving for $N_w(h)$ by iterative methods. One first guesses $N_w(h)$ and improves the profile step by step until the difference between observed and computed values reaches a minimum of the order of the inherent error range (for example, the radiometric noise figure). By means of line-by-line computations with a computer program, the optical extinction is computed at suitable small intervals of Δv across the frequency range of interest using all values of S , γ , and ground state energies.

2.3.5 Systematic Errors

The accuracy of all these various theoretical computations, so essential to the evaluation of the optical measurements, is difficult to assess in general terms. Such uncertainties in systematic errors are caused by:

- o optical parameters S and γ in IR spectra;
- o pressure and temperature along the optical path to compute γ and Planck's function B ;
- o atmospheric composition for determining interfering and overlapping lines;
- o background level, to find where $k_v = 0$; and
- o the use of k_v as a weighting factor for $N_w(h)$; it is strongly dependent on the value of Δv .

For the line-by-line computations it depends - as stated before - on the accuracy of the theoretical line width and the line intensity S . Such data are fairly reliable for some lines and bands with uncertainties in the range of $\pm 10\%$. The accuracy, however, varies from band to band, and can easily reach $\pm 25\%$ in some cases. Investigators have used different bands, different lines within selected bands, and - over the years - different theoreti-

cal values. It is hopeless to compare the accuracy for each experiment using today's knowledge of the line parameters. Over the years, these parameters have improved because of the successful cooperation between theoreticians and experimenters. Data are now screened and collected on tape by the Air Force Geophysical Laboratories (McClatchey) and are available to everyone.

The simplified methods, such as equivalent width and band models, attain lower accuracy than the line-by-line approach. The use of high speed computers permits us now to compute line-by-line fairly good band spectra for the actual pressure and temperature conditions of a particular measurement, so that the use of band models has steadily declined.

The geometrical factor $g(H, h)$ depends on the accuracy of measuring and maintaining θ during the experiment.

The radiometric measurements require careful calibration of the radiometer and assurance of known or negligible drift of the detector. Some experimenters now incorporate regular in-flight calibration with a black body as reference standard.

The combination of errors in the various parameters and assumptions, discussed above, is hard to pin down for each experiment. Nevertheless, we believe such systematic errors lead to differences among various investigators of the order of a factor of 2. It is impossible to say who is right and who is wrong, because there is no question that everybody tried to do his best. There is also always the distinct possibility that differences among measurements may be the result of natural variations, which can be large.

The individual measurements of a particular investigator, i.e., the precision in a particular vertical profile, are high, perhaps in the range ± 10 to $\pm 30\%$. Any variation in that range should

not be automatically attributed to natural variations, although some small-scale variations are to be expected.

In summary, the analysis of the measurements using optical techniques is complicated and laborious. A comparison of such data is very difficult because each experimenter uses instruments, analysis procedures, and theoretical parameters that nobody else does. Some experimenters have changed all three in the course of years, so that measurements from different years, obtained by the same group, cannot be compared. This applies, for example, to Murcay's and Houghton's groups.

So far no simultaneous measurements using different techniques have been carried out or even planned. This is, however, a very important part of the assessment of the various measurement techniques. It should be high on a priority list of any future measurement program.

2.4 OTHER TECHNIQUES

The aluminum oxide hygrometer (Al_2O_3), developed by Panametrics, Inc., is an adsorption device. The surface, with an aluminum base and a gold layer, forms the two electrodes of a capacitor whose impedance varies with the amount of water adsorbed on the porous surface. Because the physics of the adsorption process is not well understood, a calibration can not be obtained from theoretical considerations, but only by a time-consuming laboratory investigation for each individual device, using a frost-point hygrometer as a standard.

The biggest drawback of the instrument is its long response time at very low water vapor concentrations ($e < 10 \text{ ppmv}$). For example, tests conducted by Holdeman et al. (1976) gave such large response times as to render the measurements useless. For this reason, NASA replaced this device in 1977 by a frost-point hygrometer for its GASP program.

Since most of the data look suspicious and the question of its response time is not satisfactorily resolved, we will not use such data in our discussions in Section C.3.

Cryptocapture of air samples has been done, and the samples have been analyzed in the laboratory using various techniques, such as gas chromatography. Here the greatest difficulty lies in obtaining uncontaminated samples and in determining accurately the (relatively large) sampling volume.

Stanford (1974) investigated stratospheric cloud reports, or the lack of them, and deduced an upper limit of the saturation pressure corresponding to a volume mixing ratio of < 10 to 13 ppmv for 24 km, the height of the mother-of-pearl clouds in the Northern Hemisphere. His conclusions are based on assumed stratospheric temperatures and their possible ranges (see Section C.6).

2.5 INSTRUMENTATION

All instruments to measure stratospheric water vapor have undergone a highly sophisticated development, each experimenter following his own best judgment, so that it seems useless to give detailed descriptions of the instruments. Most investigators, with the exception of Mastenbrook, whose frost-point hygrometer has been standardized, improve their instrumentation from one flight to the next.

Atmospheric application of radiometric techniques and instruments is described by Houghton and Taylor (1973), of submillimeter wave spectroscopy by Harries (1977), and of Fourier transform spectroscopy by Stone (1978). These expert reviews are recommended to those entering the field of optical stratospheric measurements of gases in the ppm and ppb range.

In general, instruments are described by the investigators, although we found some papers not very enlightening as to details.

C.3 VERTICAL PROFILES

3.1 RESULTS OF FIELD MEASUREMENTS

Field measurements have been conducted by a large number of investigators. We have collected all the published data in the form of tables according to the basic technique, following Hard's (1975) systematization, listed below.

- A. Frost-point hygrometry
- B. Absorption of IR radiation
 - B.1 Band absorption
 - B.2 Line absorption
- C. Emission of IR radiation
 - C.1 Filter radiometry
 - C.2 Spectroscopy
- D. Cryogenic samplers

We inspected each measurement carefully and eliminated all those results with mixing ratios greater than 15 ppmv above 15 km. The older measurements with high mixing ratios are contaminated or have used erroneous parameters in their analyses. We believe it serves no purpose to republish all the old data we consider unreliable. We have not set a lower limit on results, although we believe mixing ratios of less than 1 ppmv to be incorrect. Yet there is always the possibility that the stratosphere at this place and time was radically different from the "average."

Table C2 lists all the measurements that seem reasonable to us. The first column gives the author, but only the first author is listed if there are more than two. A long-term trend exists; therefore, we included time and place of the measurements, the platform, the type of instrument, the spectral range, the altitude range, and the average mixing ratio between 15 and 30 km.

TABLE C2A
STRATOSPHERIC MEASUREMENTS OF WATER VAPOR -
FROST-POINT HYGROMETER TECHNIQUE

Author; Publication Date	Location Year Platform	Altitude Range (km)	Average Mixing Ratio 15 to 30 km (ppmv)
Dobson et al. 1946	England 1942-46 13 aircraft ascents	<12	
Murgatroyd et al. 1955	South England 1954-55 35 aircraft flights ± 1.5°C	<15.7	(2.5)
Heliwell 1957	England aircraft	<15	
Mastenbrook 1968	Washington, 1964-65 Trinidad, 1964-65 Thule, 1965 balloon ± 0.5 ppmv	15 to 29	3.9 4.1 3-4.5
Mastenbrook 1974 a,b	Washington, D.C., 1964-73 about 100 balloon ascents	16 to 29	4.3
Mastenbrook 1976	Western U.S., Eastern Pacific 180 mb, = 12.5 km 6 aircraft (C141) flights Dec. 1974, March 1975	12.5	3.8 Dec. 3.1 March
Cluley 1978	England, 50-53°N 1972-76, 60 aircraft (Canberra) flights 1954-55, 77 flights	9.2 to 14.6 12.2 to 15.2	5.0 3.0

TABLE C2B

STRATOSPHERIC MEASUREMENTS OF WATER VAPOR -
OPTICAL TECHNIQUES - SUN AS SOURCEB1. Band Absorption

Author; Publication Date	Location Year Platform	Spectral Range Instrument	Altitude Range (km)	Average Mixing Ratio 15 to 30 km (ppmv)
Houghton and Seeley 1960	England, 1957-58 aircraft	2.7 μm 3790-3860 cm^{-1} Prism spectr.	10 to 15	4.6
Evans 1974	Churchill, 59°N; May 1973 rocket, sunrise	2.7 μm 3780-3860 cm^{-1} Interference filter photometer	10 to 15	3.6
de Jonckheere 1975	Woomera, Austr. April 1970 rocket, sunset	2.6 μm $^{-1}$ 3822 cm^{-1} Interference filter width 16 cm^{-1}	20 to 45	1.7

TABLE C2B
STRATOSPHERIC MEASUREMENTS OF WATER VAPOR -
OPTICAL TECHNIQUES - SUN AS SOURCE

B2. Line Absorption

Author ; Publication Date	Location Year Platform	Spectral Range Instrument	Altitude Range (km)	Average Mixing Ratio 15 to 30 km (ppmv)
Houghton, 1960	England, 1959 aircraft	6.3 μm 1617, 1633 cm^{-1} grating spectr.	14 to 20	2.2
Neporet, 1967	Russia, 52°N, August 1966 balloon	2.6 μm 3816 cm^{-1} grating spectr.	10 to 25	4.0
Murcay, 1969	New Mexico December 1967 balloon	6.5 μm 1503-1531 cm^{-1} resol.: 0.3 cm^{-1} ; grating spectr.	25 to 30 30	4.0 4.8
McKinnon & Morewood, 1970	40-70°N, April 1967-May 1968, 6 aircraft flights	2.6 μm 3854 cm^{-1} , grating spectr.	10 to 19	
Ackerman, 1974, a, b	France, 44°N	5.2 μm 1904 & 1910 cm^{-1} resol.: 0.1 cm^{-1} grid grating	20 to 37	3.4

TABLE C2B

STRATOSPHERIC MEASUREMENTS OF WATER VAPOR -
OPTICAL TECHNIQUES - SUN AS SOURCEB2. Line Absorption (Concluded)

Author; Publication Date	Location Year Platform	Spectral Range Instrument	Altitude Range (km)	Average Mixing Ratio 15 to 30 km (ppmv)
Farmer, 1974	West Europe 32-77°N; June, October, November 1973 aircraft, sunset	6.3 μm 3700, 1595 cm^{-1} resol.: 0.2 cm^{-1} Interferometer	14-20	2.4
Patel, 1974	New Mexico, October 1973, balloon	5.3 μm 1890 cm^{-1} spin-flip Raman laser, acoust. detection	28	0.6

TABLE C2C
 STRATOSPHERIC MEASUREMENTS OF WATER VAPOR -
 OPTICAL TECHNIQUES - THERMAL EMISSION
 C1. Filter Radiometer

Author; Publication Date	Location Year Platform	Spectral Range Instrument	Altitude Range (km)	Average Mixing Ratio 15 to 30 km (ppmv)
Williamsen & Houghton, 1965	England, 54°N September 1963 Balloon	5.3-8.0 μm 1250-1820 cm^{-1} radiometer	5 to 15	5.5
Pick & Houghton, 1969	England, 52°N June 1967 balloon	5.9-7.3 μm 1360-1700 cm^{-1} 4 channels, 100 cm^{-1} wide; resol.: 0.3 μm	15 to 30	4.8
Brewer & Thomson, 1972	Ontario, Canada October-November 1969, June 1970, 3 balloon fl.	20-60 μm 165-500 cm^{-1} theristor, broadband bolometer	12 to 25	2.2-4.8
Kuhn, 1973	New Mexico Thunderstorms August-September 1972, aircraft	18-23 μm 430-560 cm^{-1} filter radiometer	14 to 17	3.5-5
Chaloner, 1975	France, July 1974, balloon	30-70 μm 142-330 cm^{-1} resol.: 10^{-3} cm^{-1} gas filter and pressure modulated radiometer	15 to 39	3.8

TABLE C2C
 STRATOSPHERIC MEASUREMENTS OF WATER VAPOR -
 OPTICAL TECHNIQUES - THERMAL EMISSION
 C2. Spectroscopy

Author; Publication Date	Location Year Platform	Spectral Range Instrument	Altitude Range (km)	Average Mixing Ratio 15 to 30 km (ppmv)
Murcray, 1974	New Mexico, February-June 1971, balloon (3)	24-29 μm 340-420 cm^{-1} grating spectr.	10 to 30	2.3
	Alaska, September 1971		18 to 28	0.6
	India, April 1972		11 to 27	4.0-0.12
Harries & Burroughs, 1971	England, 1969 aircraft	300-3000 μm Michelson inter- ferometer and bolometer, resol.: 0.5 cm^{-1}	12 to 22	2.8
Harries et al. 1973 b	England, October 1971, balloon	161-416 μm 24-62 cm^{-1} Michelson inter- ferometer, bolometer	15 to 36	3.9
Harries, 1973 a	48° N-44° S Su 1972 aircraft Concorde	10-30 cm^{-1} resol.: 0.06 cm^{-1} improv. detector	11 to 15	4.8

TABLE C2C
 STRATOSPHERIC MEASUREMENTS OF WATER VAPOR -
 OPTICAL TECHNIQUES - THERMAL EMISSION

C2. Spectroscopy (Concluded)

Author; Publication Date	Location Year Platform	Spectral Range Instrument	Altitude Range (km)	Average Mixing Ratio 15 to 30 km (ppmv)
Bussoletti, 1974	50° N, May 1972, aircraft Concorde	30-250 cm^{-1} 40-300 μm step-scanning cat's eyes Michelson inter- ferometer, Ge-bolometer; resol.: 0.18 cm	11.5	3.0
Harries, 1976	France, 43°N, September 1974, balloon	Same instru. as in aircraft	16 to 35	3.9
Rogers, 1977	60°N, March 1973, rocket	6.7-7.6 μm spectrometer	49 to 70	3.5

TABLE C2D

STRATOSPHERIC MEASUREMENTS OF WATER VAPOR -
OPTICAL TECHNIQUES - THERMAL EMISSIOND-1 Miscellaneous Techniques

Author; Publication Date	Location Year Platform	Spectral Range Instrument	Altitude Range (km)	Average Mixing Ratio (ppmv)
Scholz et al. 1970	New Mexico, September 1968, rocket	Cryocapture	43 to 62	3-10
Martell & Ehhalt, 1974	New Mexico, September 1968, May 1973, rockets	Cryocapture	43 to 62 41 to 51	4 4

Other lists of water vapor measurements are given by Gutnick (1961) for the mostly unreliable earlier measurements, in the CIAP monograph 1 (p. 3-58, 1975), by Mastenbrook (1974a,b) and by Harries (1976).

Table C3 lists the volume mixing ratio in ppmv for each series from 10 to 30 km in steps of 1 km and in 5 km steps thereafter. The list does not contain interpolated values, because, if necessary, they can be computed very easily. In some cases, the values are given for every kilometer, because the original paper gives only a straight line and we do not know at what altitude measurements have been made. The data are given in the same order as in Table C2 with a double line between columns indicating a new group (for example, end of group B1). If possible, we estimate the systematic error and report it at the bottom in parentheses. If the systematic errors and the precision are estimated by the author, they are given at the bottom, but without parentheses. Unfortunately, such vital information is not estimated by all authors. In general, we believe the authors underestimate their systematic errors.

The data are also plotted in Figures C1 through C5 as number density vs. altitude, for each group separately, to show the results in more detail with volume mixing ratios of 10^{-6} and 10^{-5} as guidelines. Such representations may be useful to modelers. One should also remember that some data are averages of many measurements, as in the case of Mastenbrook's results; most of the other data are based on just one balloon flight. Therefore, a single profile may show some variability, but the average of many profiles will not.

Frost-point hygrometer measurements. The British conducted airplane measurements with top altitudes of 14 to 15 km. The data are generally taken in the lower stratosphere, but some within the tropopause region. Most of their data are published by Murgatroyd et al.(1955). The results are given in altitude

TABLE C3
RESULTS OF STRATOSPHERIC WATER-VAPOR MEASUREMENTS*

Group A

Altitude (km)	Dobson 1946	Murgatroyd 1955	Helliwell 1957	Mastenbrook 1968	Mastenbrook 1974	Mastenbrook		Cluley 1978		
						Dec.	Mar.	1976	54- 55	72- 76
10	4.2			12.0				3.8	3.1	
11	3.0			5.7	8.0					
12	1.2	8.0		3.0	5.9					
13				2.4	5.0					
14				2.3	4.3					
15										
16										
17										
18										
19										
20										
21										
22										
23										
24										
25										
26										
27										
28										
29										
30										
35										
40										
45										
50										

Systematic
Error
Precision

±1.5°C
±10%

±10%
±10%

±6%

*Mixing ratios are given in ppmv

TABLE C3
RESULTS OF STRATOSPHERIC WATER-VAPOR MEASUREMENTS^a

Group B1				Group B2			
Altitude (km)	Houghton 1960	Evans 1974	De Jonckheere 1975	Houghton 1960	Neporet 1967	Murcay 1969	McKinnon 1970
10	4.6	4.0				1.9	
11	4.6	3.1				4.8	
12	4.6	2.6				1.6	
13	4.6	3.0				2.4	
14	4.6	3.4				2.4	
15	4.6	3.8				1.3	
16	4.6	3.8				3.2	
17		3.7				2.4	
18		3.7				2.4	
19		3.9				2.6	
20		4.0	2.0			2.6	
21		3.9				2.4	
22		3.8				3.4	
23		3.7				3.4	
24		3.5				3.4	
25		3.4	1.4			3.4	
26		3.3				3.4	
27		3.3				3.4	
28		3.4				3.4	
29		3.5				3.4	
30		2.9	1.5			3.4	
35		3.5	0.5			3.4	
40		5.0	0.7			3.4	
45		5.7	0.7			3.4	
50		3.9				3.4	

Syste-
matic
Error

Precision

$\pm 20\%$ $\pm 30\%$ $\pm 20\%$ $\pm 15\%$?

^aMixing ratios are given in ppmv

TABLE C3
RESULTS OF STRATOSPHERIC WATER-VAPOR MEASUREMENTS*

Group C 1

Altitude (km)	Williamsen 1966	Pick 1969	Brewer 1972	Kuhn 1973	Chaloner 1975
10					
11					
12	5.5		3.2		
13	5.5		3.2		
14	5.5		3.2	5.0	
15	5.5	4.8	3.2	4.3	
16	5.5	4.8	3.2	3.8	5.0
17	5.5	4.8	3.2	3.5	
18	5.5	4.8	3.2		5.0
19	5.5	4.8	3.2		
20	5.5	4.8	3.2		
21	5.5	4.8	3.2		
22	5.5	4.8	3.2		
23	5.5	4.8	3.2		
24	5.5	4.8	3.2		
25	5.5	4.8	3.2		2.5
26		4.8			
27		4.8			3.0
28		4.8			
29		4.8			4.0
30		4.8			4.2
35					5.8
40					
45					
50					

Syste-
matic
Error

±50% ±30%

Precision

*Mixing ratios are given in ppmv

TABLE C3
RESULTS OF STRATOSPHERIC WATER-VAPOR MEASUREMENTS*

Syste- matic

metric Error $\pm 30\%$

Precision

*Mixing ratios are given in ppm

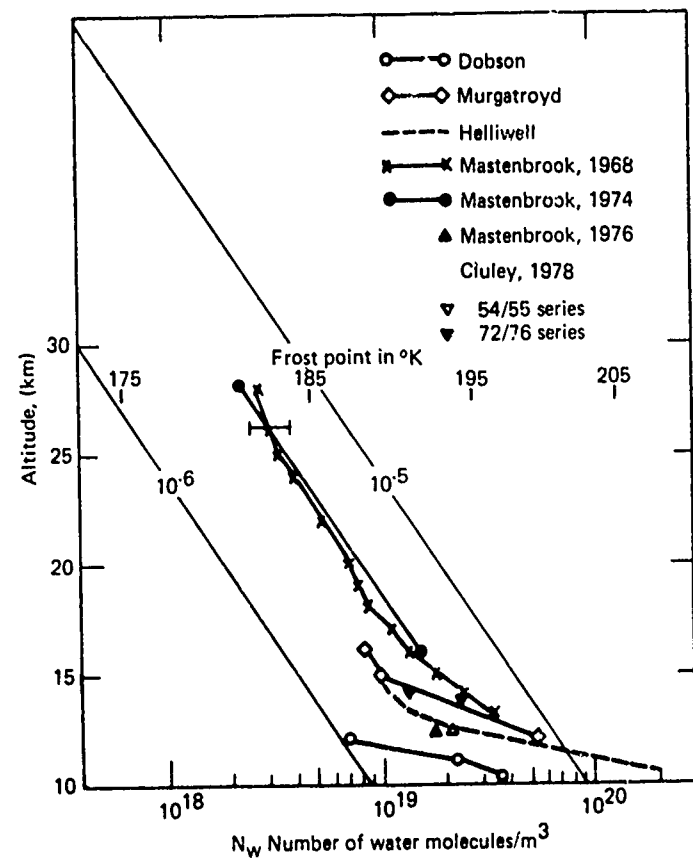


Figure C1 Results of Field Measurements of Water Vapor Using Frost-point Hygrometer Technique. Slanted solid lines represent 1 and 10 ppmv.

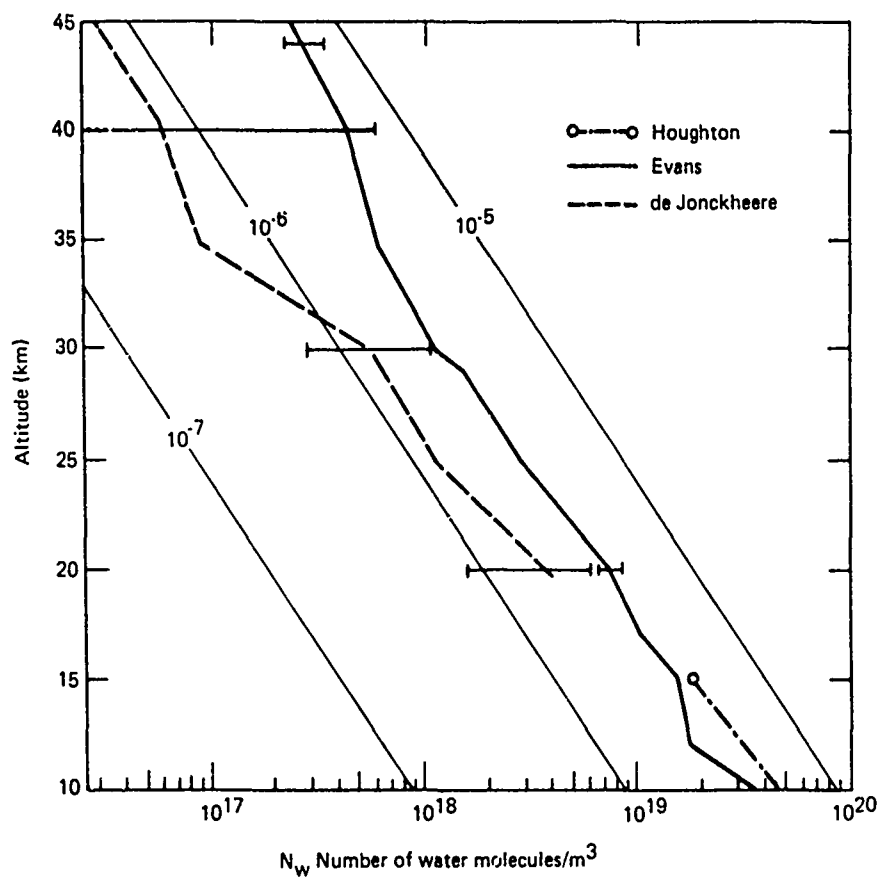


Figure C2 Results of Field Measurements of Water Vapor Using Band Absorption Technique. Slanted solid lines represent 1 and 10 ppmv.

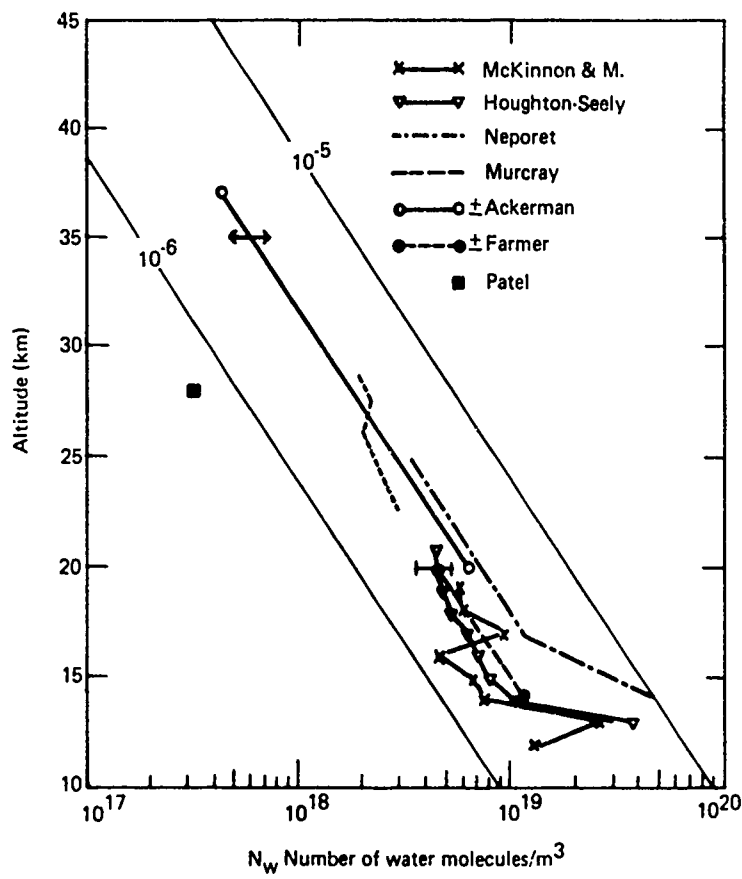


Figure C3 Results of Field Measurements of Water Vapor Using Line Absorption Technique. Slanted solid lines represent 1 and 10 ppmv.

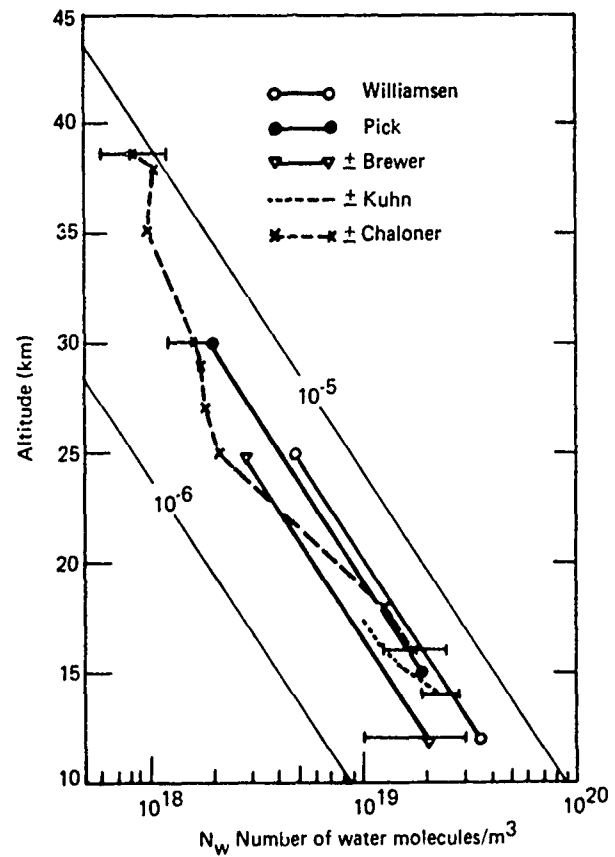


Figure C4 Results of Field Measurements of Water Vapor Using Thermal Emission and Filter Technique. Slanted solid lines represent 1 and 10 ppmv.

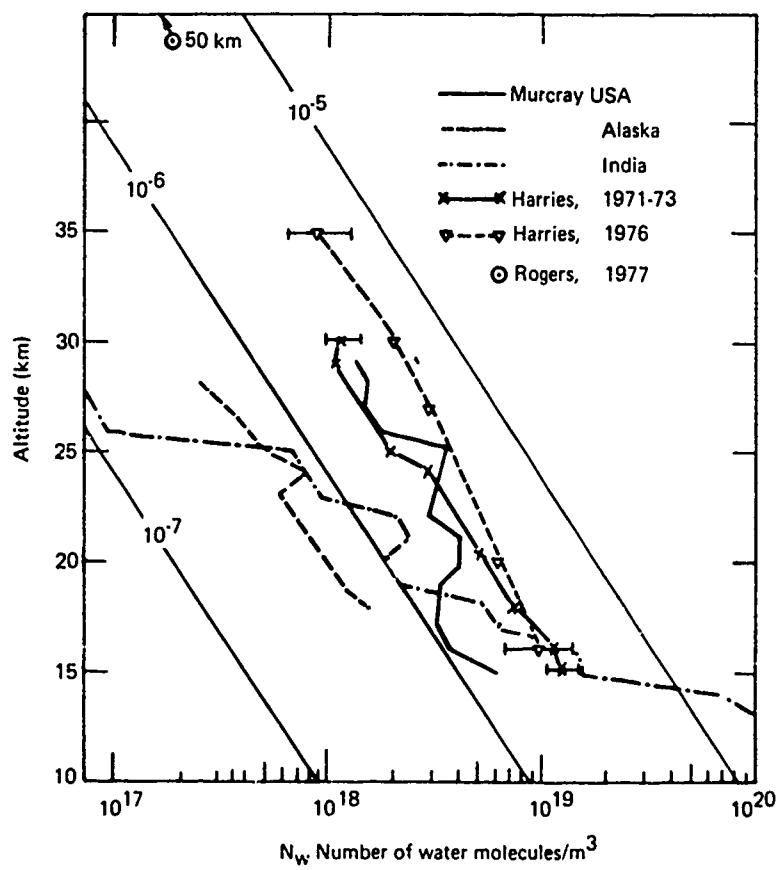


Figure C5 Results of Field Measurements of Water Vapor Using Thermal Emission and Spectroscopy.
 Slanted solid lines represent 0.1, 1, and 10 ppmv.

above or below the tropopause, not in altitude above mean sea level (MSL). This is the correct way for the tropopause region, yet hard to translate into our tables. Other British data, from Nairobi to Norway, are summarized by Gutnick (1961). The British measurements were the first indication of a "dry" stratosphere with averages of 3.2 ppmv or frost points of -80 to -85°C; they started such measurements in 1942, and 13 ascents were reported by Dobson et al. in 1946. These early results still seem to be correct and in agreement with current measurements, especially with regard to a possible long-term trend. In contrast, all the U.S. measurements cited by Gutnick (1961) are obviously wrong, with the exception of Murcray's spectroscopic measurements.

Such flights by the Meteorological Research Flight (MRF) have been resumed over southern England in 1972, and a total of 60 flights, using a Canberra aircraft, have been made between 1972 and 1976. They cover an altitude range from 9.2 to 14.6 km and latitudes 50 to 53°N. From their data, Cluley and Oliver (1978) select 52 obtained at the highest altitude and at least 100 mb above the tropopause as "representative stratospheric mixing ratios" leading to an average of 5.0 ± 0.5 ppmv. They also reevaluated the earlier MRF series of 77 flights from 1954-55, partly reported by Murgatroyd et al. (1955), and obtained an average of 3.0 ± 0.3 ppmv. Their reevaluation takes into account the corrections discussed in Section C.2.1. Extreme values are 3.5 and 6.8 ppmv for the 1972-76 series and 1.6 and 6.1 for the 1954-55 series.

There exists only one continuous series for Washington, D.C., starting in 1964 (Mastenbrook 1968, 1974 a,b). He made about 100 balloon flights between 1964 and 1973 with the same instrumentation and obtained - on the average - a practically constant median value of 4.3 ppmv between 16 and 28 km and extrema of about 1.6 and 9.6 ppmv. His data are given for selected pressure levels which we have converted to approximate altitudes. The earlier series yielded slightly lower values. Figure C1 also

contains the frost point at the appropriate number density. The frost points decrease from about 200°K to 180°K over the range in which measurements have been made (see also Table C1).

Recently, Mastenbrook (1976) employed his frost-point hygrometer on aircraft. While his June 1974 measurements were taken mostly in the upper troposphere, the winter 1974-75 flights occurred in the lower stratosphere. The measurements were averaged over 2.5 minutes of flighttime and from those I computed averages given in Table C3 and shown in Figure C1. They clearly indicate a decrease in mixing ratios from December to March, i.e., a drying out of the midlatitude stratosphere in winter. Further details are discussed in Section C.4.

Optical Measurements. Optical measurements are - without exception - based on very few flights, mostly only one and, in some rare cases, up to four flights. For example, Williamson and Houghton (1965) state that they made 12 balloon flights but published only "the best." Does this mean the other flights gave unusable or unbelievable data? The continuous change of instrumentation is very unfortunate. How can one compare the accuracy of data obtained in different years by groups like Houghton's or Murcray's if they change their technique from one measurement to the next? It is impossible. Such changes by the best experimenters indicate to me that it is inherently very difficult to obtain reliable absolute concentrations and also make me aware of possible large uncertainties in their previous technique. In general, the optical techniques yield less accurate concentrations as outsiders normally assume.

For band absorption, the method used most in earlier experiments, we kept only the data by Houghton and Seely (1960) which cover the range 10 to 15 km and gave a mixing ratio of 4.6 ppmv, an acceptable value. The other two curves in Figure C2 are rocket flights. Evans (1970) data are for Churchill, Canada, and de Jonckheere's data are for Australia. The Canadian data seem

reasonable, 3.6 ppmv up to 30 km and 2.6 to 5.7 ppmv above. The Australian measurements yield very low mixing ratios, 1.7 ppmv up to 30 km and well below 1 ppmv above 32 km. These results appear to us as too low and not correct above 32 km, perhaps also below 30 km. However, in the absence of other data from the Southern Hemisphere, it is difficult to judge if his results represent the true conditions over Australia or not. All other measurements using band absorption have been rejected.

For line absorption, we have a large number of measurements up to 20 km, but very few above that altitude, as shown in Figure C3. The data by Neporet et al.(1967), Ackerman (1974 a, b), and Murcray et al.(1969) agree within the expected variability. The one point by Patel et al.(1975), using a spin-flip laser as light source and not the sun, for 28 km is probably wrong. Their brief publication makes it impossible to analyze the errors. Systematic errors given by Ackerman and Farmer are probably overoptimistic and we believe should lie in the $\pm 20\%$ range, and for most other line absorption measurements they are about $\pm 30\%$.

Thermal emission measurements were started by Houghton in the mid 1960s. They have the advantage of complete independence of the position of the sun: they can be made day or night and permit one to obtain a profile below balloon altitudes. The first group uses the emission in bands and limits the spectral range by selective filters. Kuhn's data are discussed in Section C.3.4; here we cite only his thunderstorm flights over New Mexico and use the data for the upwind conditions. The profile by Chaloner et al.(1975) was obtained by a novel and promising technique. Emission in the rotational band from 30 to 70 μm was measured with a pressure modulator radiometer. It employs a particular form of gas filter correlation spectroscopy. The gas pressure in a cell filled with water vapor of about 14 mb is modulated while the light passes through the cell to the detector. In this way the water vapor acts as a band filter, because only the intensity of the water vapor bands changes during the modulation.

Their flight reached 39 km with an increase in mixing ratio from 2.5 ppmv at 25 km to about 9 ± 3 ppmv at 38 km. Only future flights can prove or disprove so large an increase in the 30 to 40 km region, not shown by other techniques.

16 balloon flights with a radiometer (40-200 μm) were carried out at Mildura and Longreach, Australia, by Hyson (1978) from 1973 to 1976. Some observations look reasonable, others not at all. Averages of 5 ppmv and more have been obtained in the 16 to 20 km range, yet individual observations vary from about 2 to 16 ppmv and the systematic error is estimated by the author as $\pm 100\%$. Since he used the Goody band-model and other questionable assumptions, we do not believe his measurements to be reliable, although some single flights give acceptable results. Because these are the only Southern Hemisphere data using balloons, we mention them, although we do not enter these data into our tables.

Systematic errors are estimated by Kuhn as ± 1 ppmv or about ± 20 to 40% and should be of similar magnitude for the other investigators, with perhaps larger errors for the earliest applications of this technique.

Spectroscopy of thermal emission is used by Murcray (see Goldman et al. 1973) with a grating spectrometer in the IR, while the British and French investigators preferred the submillimeter region and a Michelson interferometer and Fourier transform to obtain a spectrum. Murcray (1974) obtained fairly low concentrations on three flights; we give the average. We also show his single flights for Alaska and India, both with extremely low mixing ratios. They are suspect as being much too low and not in agreement with other data. The numerous data obtained by Harries fall within the range of most midlatitude measurements. These results are listed in Table C3 and shown on Figure C5. Systematic errors should also be of the order of $\pm 30\%$ and probably vary from one instrument to the next. The precision is of the order of $\pm 10\%$.

The zenith radiance was measured between 6.7 and 7.6 μm , using a cryogenic rocket-borne spectrometer by Rogers et al.(1977) to determine the IR emission of water vapor. Comparing the experimental data with a high-altitude radiance model computation leads to a mixing ratio of 3.5 ± 2.2 ppmv between 49 and 70 km, a reasonable value for a latitude of 60°N .

Cryocapture and subsequent analysis in the laboratory using rockets as carriers have been done by Scholz, and the same data subsequently reanalyzed with additional new data by Martell and Ehhalt. The results for the stratopause are similar to those in the lower stratosphere with a value of about 4 ppmv.

The results of this group are listed in Table C3. As expected, the systematic errors are large, but they lead to reasonable mixing ratios at the top of the stratosphere.

3.2 AVERAGE PROFILE

For theoretical studies and for models, one needs a good average profile for perhaps three latitude regions. The question is how to derive such a profile? Harries (1976) has taken 15 data sets and assigned each with equal weight and derived a curve given in Figure C6. The average lies between 3 and 4.5 ppmv. There is a slight increase with height, which he attributes to the production of water from the oxidation of methane. Yet we cannot agree with his method. It is certainly unfair to give equal weight to data based on a single balloon flight and the same weight to the nearly 100 flights by Mastenbrook. Furthermore, for 15 km he has 9 data points, for 19 km 12, and for 30 km only 5. This is an incorrect method by which to arrive at an average; it leads to the fluctuations in his average and also to the increase with height.

For the altitude range of 15 to 30 km, we have derived an average for each investigator and show the result in Figure C7. The

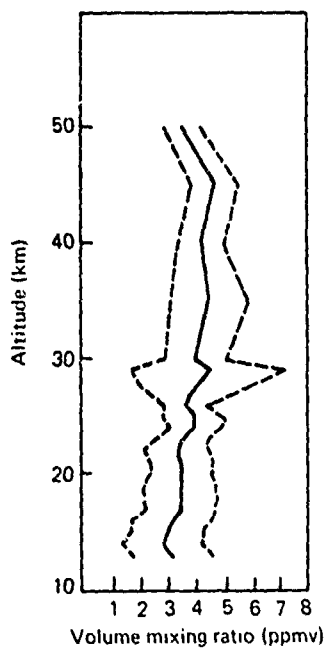


Figure C6 The Mean Mid-latitude Northern Hemisphere Vertical Profile in ppmv Derived by Harries 1976. The broken lines represent the rms variance among individual measurements at each level.

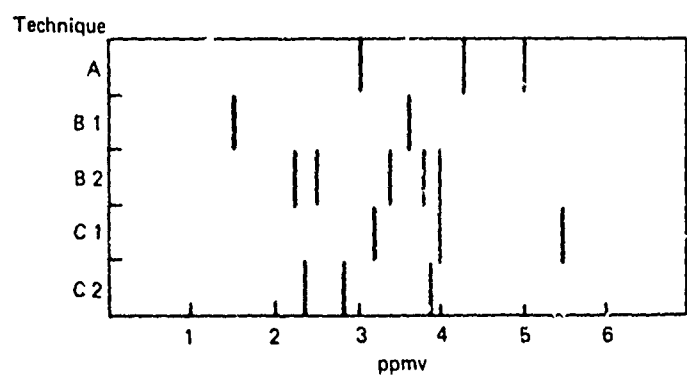


Figure C7 Average Volume Mixing Ratio for the Altitude Range 15-30 km. Techniques labeled acc. to Table C2.

optical measurements (excluding the Australian data) are bunched between 2 and 4 ppmv; only Williamson obtained 5.5 ppmv. The optical measurements give a mean value of 3.5 ± 0.9 ppmv. The frost-point measurements by Mastenbrook give 4.3 ppmv. Weighting the two averages by the number of flights leads to an average of 4.15 ppmv, valid for the period 1969-70 and for the Continental U.S.

Figure C8 shows the band within which the data for midlatitudes are situated. The band is wider at low than at high altitudes, a result caused by the larger number of data points below 20 km. The band's lower limit of the mixing ratio lies between 1.8 and 3.3 ppmv; its upper limit between 4.7 and 5.5 ppmv. Also indicated is our average of 4.15 ppmv. We strongly believe that the average mixing ratio is constant with altitude and a value around 4 ppmv applies to the period 1970. There are seasonal and long-term trends discussed in Section 3.4, and latitudinal variations studied in Section C.4.

3.3 NATURAL FLUCTUATIONS

All parameters exhibit systematic and unsystematic variations in the stratosphere. Those for pressure and temperature are well known and explored. Of course, these variations also exist for all trace gases, and the systematic variations are discussed in Section 3.4. Here we will deal only with the unsystematic or "natural" variability, a parameter quite important for understanding how unrepresentative a single measurement can be.

The optical measurements do not permit us to study this phenomenon because the proper data base is lacking. Thus, we are left with the frost-point hygrometer data, and histograms are shown in Figures C9 and C10. Mastenbrook (1974 a) measured no values below 1.5 ppmv at any altitude over Washington. The values above 10 ppmv, except for two, have been obtained in the earliest flights and may be attributed to problems with the aspirating blower. His data lead to a standard deviation of about ± 1.1 ppmv for all altitudes above 15 km. If the long-term trend is sub-

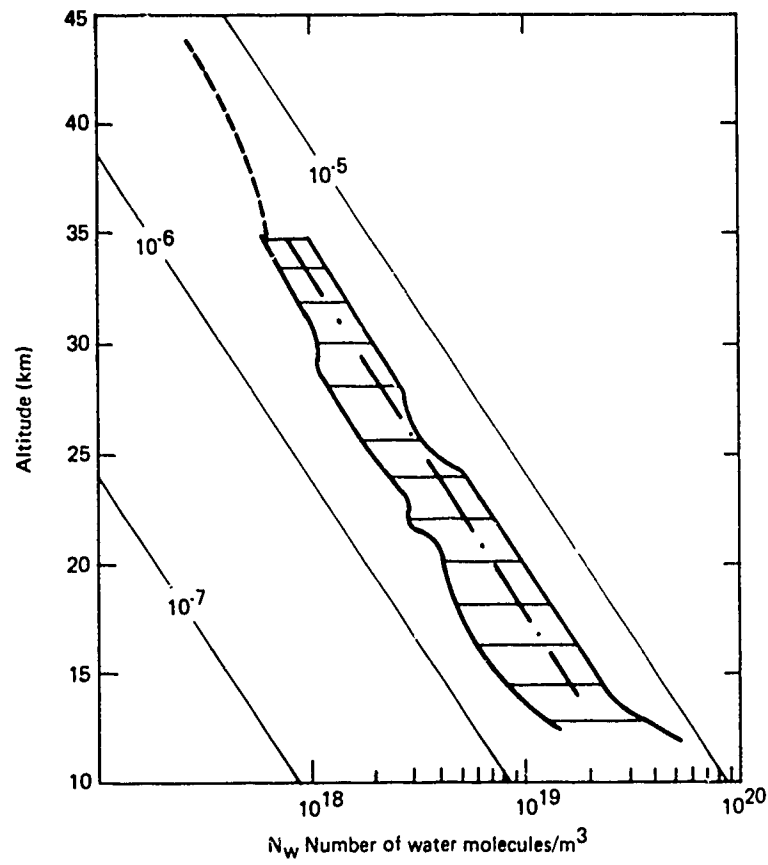


Figure C8 Range and Average of Mid-latitude Northern Hemisphere Water Vapor Profile. Average indicated by - - - is 4.15 ppmv. Band encloses all reliable data. Above 35 km small number of data indicated by an average (- - - -).

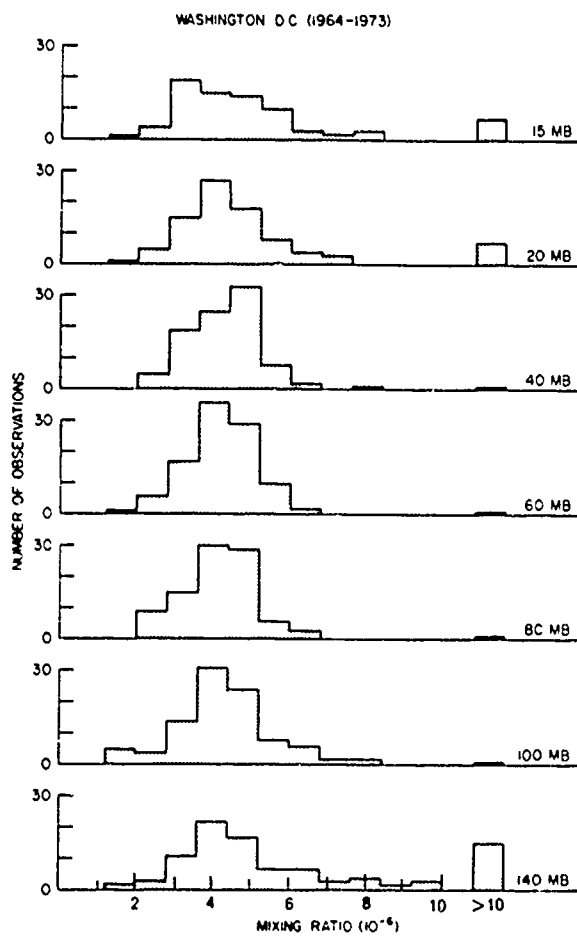


Figure C9 Histogram of Volume Mixing Ratio. Selected pressure levels, 15 to 140 mb (about 14 to 28 km) for the period 1964-73 at Washington, D.C. (Source: Mastenbrook 1974 a).

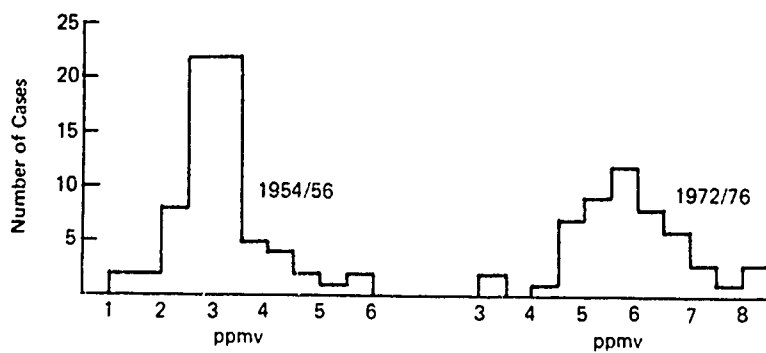


Figure C10 Histogram of Volume Mixing Ratio Over England. Observations have been normalized to January 1955 and July 1974 by taking out seasonal variation and long-term trend.

tracted from the individual data, the variability should be smaller, for one standard deviation perhaps only ± 0.6 ppmv, or $\pm 15\%$. Unfortunately, we can not reanalyze his data because the results for individual flights are not available.

Histograms for the two English series have been prepared from the published "representative stratospheric mixing ratios" (Cluley and Oliver 1978). Some of the highest values are probably incursions of tropospheric air into the stratosphere, related to jet streams or tropospheric fronts, as explained in detail by the authors. We concur with such an explanation. For the 1954-55 series, we subtracted the seasonal variation (see numerical values in Section 3.4.1 and Table C4), and for the 1972-76 series, we subtracted both the seasonal and the long-term variations and normalized to July 1974. In 1954-55, 67% of all observations fall between 2.5 and 3.5 ppmv, and, for the 1972-76 series, 69% fall between 4.5 and 6.5 ppmv. Using the raw data for the last series, we see that the observations fall to somewhat lower mixing ratios, because of the uneven distribution of the measurements during the selected time span. The British observations yield a standard deviation of ± 10 to 20%, or about the same value as obtained for Washington, D.C. The reader will obtain a good insight into these natural fluctuations by studying Figures C11 and C12.

3.4 TEMPORAL VARIATIONS

3.4.1 Seasonal Variations

To investigate temporal variations, the best series is again that obtained by Mastenbrook from 1964-73. The amplitude of the seasonal variation is largest in the lowest stratosphere and decreases with altitude; its phase progresses in time with altitude. His analysis for three pressure levels is shown in Figure C11, and numerical values are listed in Table C4. He also published, in 1968, the results of a 6-year data base; they are reprinted in

TABLE C4
AMPLITUDE AND PHASE OF SEASONAL VARIATION, LONG-TERM TREND AND AVERAGE

A. Balloon Observations, Washington, D.C., after Mastenbrook (1974a)

Pressure Level (mb)	Corresp. Altitude (km)	Annual Cycle		Long-term Trend (ppmv/decade)	Significance		Average (ppmv)
		Ampl. (ppmv)	Phase Max.		Annual Cycle	Long-term Trend	
50	20.5	0.24	Apr	+1.56	-	0.01	4.3
70	18.5	0.30	Feb	+1.54	0.05	0.01	4.2
96	17	0.40	Nov	+1.38	0.05	0.01	4.25

B. Aircraft Observations

Author Place	Corresp. Altitude (km)	Annual Cycle		Long-term Trend (ppmv/decade)	Significance		Average (ppmv)
		Ampl. (ppmv)	Phase Max.		Annual Cycle	Long-term Trend	
Cluley, England, 1954-55	13 to 15	0.50	Nov.	+2.16	-	0.05	3.01 (Jan 55)
	13 to 14	0.50	Dec.	-2.57		0.05	5.14 (Jul 74)
Harries, England, 1969-72	17	0.96	Mar.	+3.2		?	3.2 (Jan 69)
McKinnon, U.S. 1967-68	17.7	0.16	Dec.	<+1.6		?	2.4 (Jan 67)

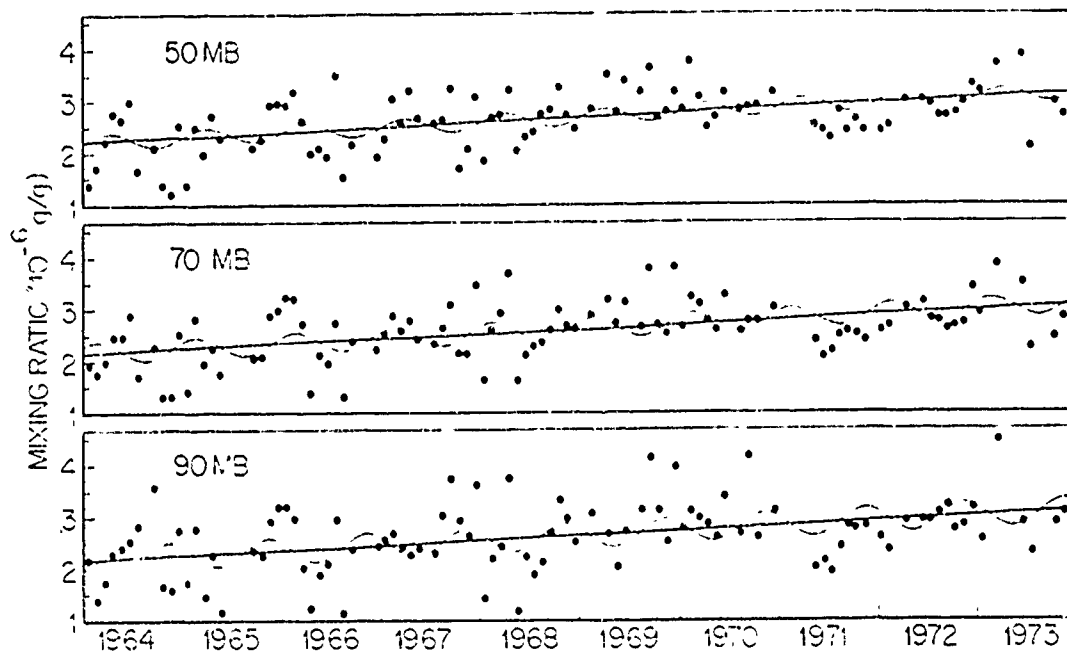
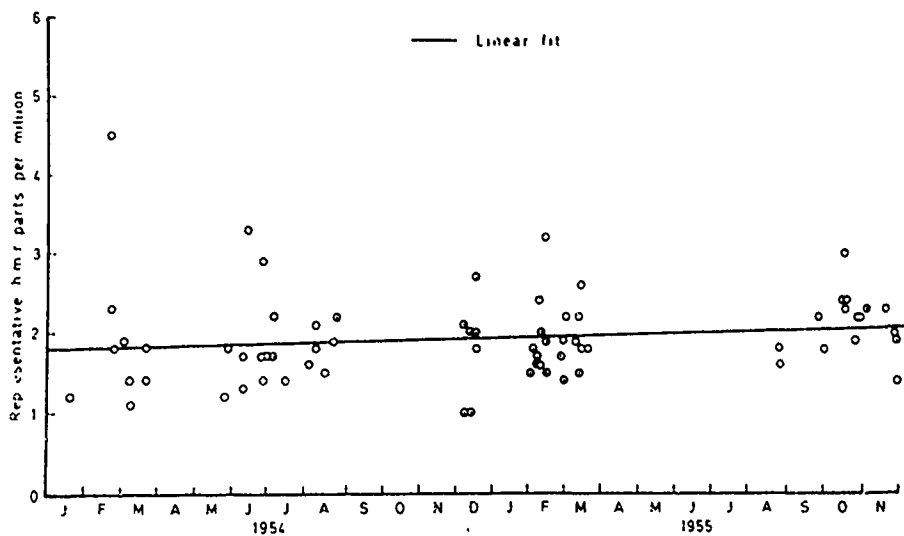
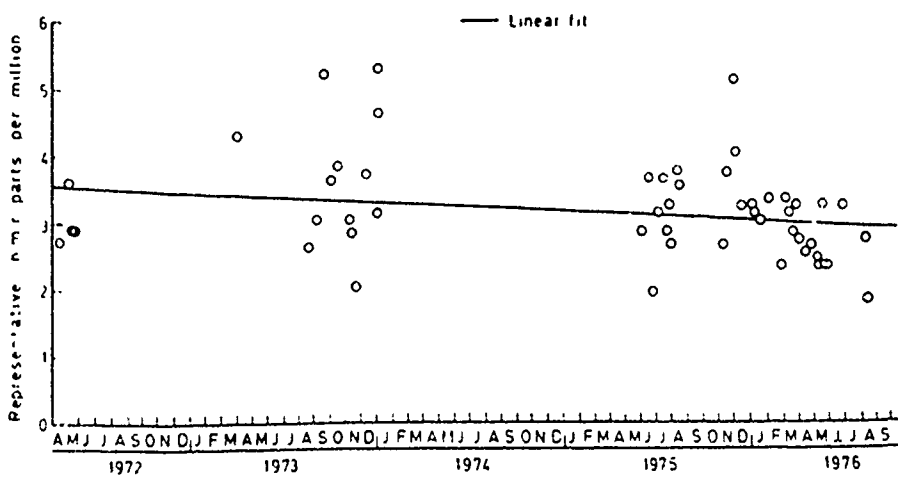


Figure C11 Time Series Analysis of Water Vapor Mass Mixing Ratios for Three Selected Pressure Levels at Washington, D.C., for the Period 1964-1973. The curves represent the best fit of a linear trend and annual cycle (Source: Mastenbrook 1974 b). Multiply by 1.6 to obtain ppmv.



(a)



(b)

Figure C12 Time Sequence of Mixing Ratios Over Southern England Data Collected by the Meteorological Research Flight (a) 1954/55. (b) 1972-1976 (Source: Cluley and Oliver 1978). The long-term trend computed by the authors is also indicated. Results in ppm(m); multiply by 1.6 to obtain ppmv.

CIAP Monograph 1 (p. 3.62), where 6 levels from 100 to 50 mb had been analyzed.

Over Washington, D.C., the amplitude is small, of the order of ± 5 to 10% of the mean mixing ratio. The annual cycle is significant for altitudes below 20 km only. Other periods, such as the biennial variation, cannot be extracted from the sample.

From the aircraft measurements listed in part B above, only the MRF observations are numerous enough to enable one to deduce amplitude and phase. The amplitudes are somewhat larger than those by Mastenbrook for the 90 mb level (17 km) but agree with his analysis of the first six years for the 100 to 130 mb level (about 15 km), where he obtained an amplitude of ± 0.85 ppmv. Harries did not have enough data to derive a reliable amplitude, and he assumed a phase term of 0, i.e., maximum in March, which does not agree with the other data in Table C4. McKinnon and Morewood (1970) found an annual cycle of ± 0.16 ppmv in the overburden for the flight level of 17.7 km. Since their measurement of the vertical column is weighted in favor of the lowest levels, the phase (Dec) is consistent with that given in Table C4 for 90 mb.

All published data for Washington and England are shown in Figures C11 and C12, indicating convincingly the difficulty in deriving an exact magnitude and phase of the seasonal variation because of the large unsystematic fluctuations of the mixing ratio.

Aircraft flights at the 12-km level were reported by Mastenbrook (1976). These flights, at about $40 \pm 5^\circ\text{N}$, were mainly east to west flights over the western U.S., and are discussed in Section C.4. Of interest here are Mastenbrook's results in relation to the seasonal variation. Using only the strictly stratospheric parts of the flights, the measurements in December 1974 gave 3.8 ± 0.3 ppmv, while in March 1975 they resulted in a lower mixing ratio of 3.1 ± 0.3 ppmv. This seasonal decrease from December to

March is interpreted as a drying out during the winter and leads to an amplitude of greater than ± 0.35 ppmv of the annual variation in agreement with Figure C11. These averages fit well into the mean value for 1976, as can be seen by comparing them with the other data given in Figure C13.

It would be very useful if a series of such flights spaced about 3 or 4 months apart could be carried out in the 15 to 20 km altitude region, to be safely in the stratosphere in all seasons. From such data, a seasonal variation can be established much more accurately than from a few balloon flights spaced irregularly throughout the year. The aircraft flights at a fixed level can lead to a much more reliable average for that height regime than a single balloon flight with just one data point for the same height.

We conclude that an annual cycle has been found in three independent series of field measurements with an amplitude of about ± 10 to 20% at 15 km, decreasing to $\pm 5\%$ above 20 km. Its phase changes with altitude, from November (maximum) at 15 km to April at 20 km.

3.4.2 Long-Term Variations

Ever since Mastenbrook published his first six years of data in 1971, the question of a long-term trend in stratospheric water vapor concentration has been discussed. There exist the relatively low mixing ratios, around 3 ppmv, obtained in England in 1954-55 and the higher values of Mastenbrook for Washington, D.C., slightly increasing from around 3.7 ppmv in 1964 to about 4.5 ppmv in 1969. These field measurements, accepted as fairly reliable, seemed to establish a clear trend of steadily increasing water vapor concentration in the stratosphere and fired all kinds of speculations as to the future.

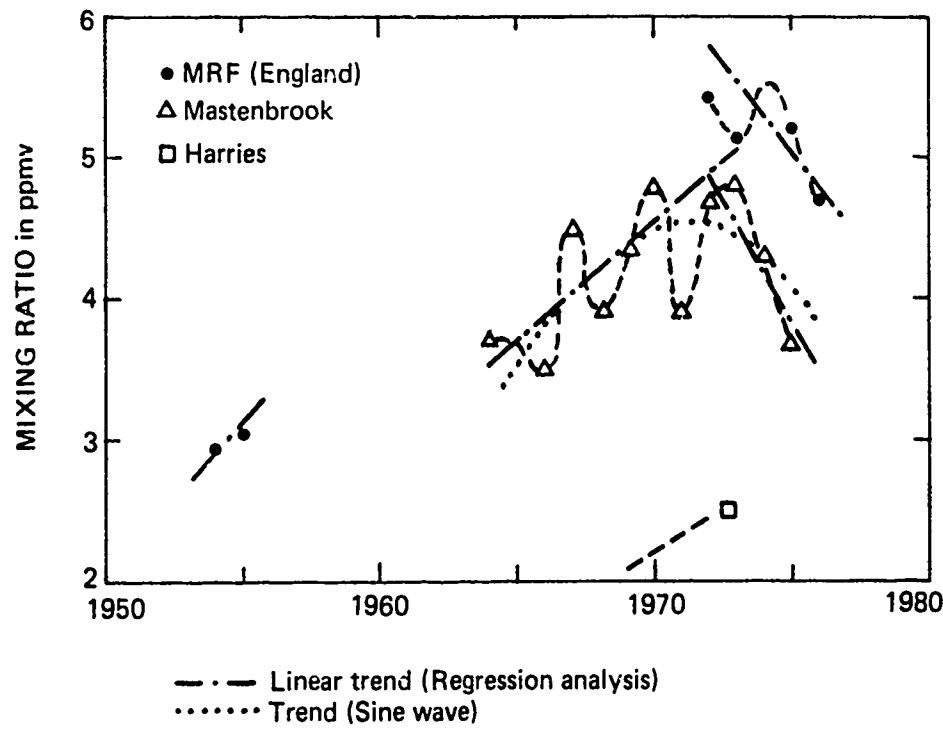


Figure C13 Long-term Trends of Annual Mean Water-vapor Mixing-ratios in the Lower Stratosphere in ppmv from 1954 to 1976. Notice difference between Washington, D.C. and England. The data for Harries are incorrect; they should read 3.2 ppmv for November 1969 and 4.1 ppmv for January 1972.

To us it seems unlikely that stratospheric water vapor concentrations could steadily increase, because its concentration depends on its influx through the cold trap, which is determined by the tropical tropopause temperature (see Section C.6.2). Therefore, a cyclic variation with variable periods, similar to total ozone and other meteorological parameters, seems more realistic than a linear trend.

Annual mean values (data taken from Cluley and Oliver 1978) are listed in Table C5 and are shown in Figure C13. What the data clearly show is an overall increase from 1954 to about 1973, followed by a steep decrease thereafter. The short-term variation from one year to the next is also obvious, probably partly due to the limited and uneven distribution of the observations and partly real. In Table C5, the first line under England lists the mean values obtained from the raw data. For line "N 1" the seasonal variation was taken out before computing the mean. These values are entered on Figure C13. Finally, "N 2" is computed by taking out the seasonal variation and the long-term trend and normalizing the average to July 1972, the middle of the measurement period. Parentheses indicate that a small sample exists, and the average may not be representative.

Another point worth mentioning is that the British data are somewhat larger, 0.5 to 1 ppmv, than the Washington data. The difference is at times larger than the systematic errors and may be real, indicating latitudinal or meridional differences, which could only be resolved by making simultaneous measurements. The optical measurements by Harries are 1 to 2 ppmv lower than the MRF data and indicate the fairly large discrepancies among completely different techniques.

From the raw data various authors determined long-term trends by a regression analysis; they are listed in Table C4. The increase amounts to about 1.4 ppmv per decade and the decrease to 2.5 ppmv

TABLE C5
ANNUAL MEAN VALUES OF WATER VAPOR MIXING RATIO FOR ABOUT
15-KM ALTITUDE (PPMV)

LOCATION	YEAR														
	54	55	64	65	66	67	68	69	70	71	72	73	74	75	76
Washington															
England	2.9	3.1	3.7	3.7	3.5	4.5	3.9	4.3	4.8	3.9	4.7	4.8	4.3	3.7	-
England N 1															
England N 2															
Harries															

per decade. The deductions from the short series of 1954-55 and from Harries are, of course, uncertain.

We have also computed some trends and list our results in Table C6. First, we used the annual means from Table C4, leaving out the data for 1974 in the MRF series, because only two measurements were made in that year. The decrease for the Mastenbrook series is large, about 3.5 ppmv per decade, but smaller for the MRF series with about 1.1 ppmv per decade. We expect some humps in the generally decreasing period, so that the trend over a longer time period may come out to somewhere between 1 and 2 ppmv per decade, or comparable to the trend during the increasing part of the cycle. Secondly, we took out the seasonal trend, and, using all observations, we obtain a numerically equal but opposite trend for 1954-55 and 1972-76 of 1.9 ppmv per decade. Trends are shown on Figure C13 as dash-dot lines.

Since the measurements so far indicate a cyclic variation, linear trend computations may be somewhat misleading. It seems more objective to fit a sine curve (dotted line) through the data, yet neither the amplitude nor the length of the period can be established at this time. Consequently, it is necessary to continue Mastenbrook's measurements for many more years if one wants to solve this riddle.

The best explanation of the source of stratospheric water vapor is still the tropical tropopause temperature which controls the admission of water vapor (Dobson et al. 1946; Brewer et al. 1949). The increase in water mixing ratios has been related to changes in the tropical tropopause temperature, yet the evidence presented by Mastenbrook (1974a) is rather limited. He selected data for Singapore and the measured saturation water vapor pressure, and the mixing ratios measured over Washington show some agreement if the curves are shifted by 5 years. Such a 5-year shift is unacceptable on meteorological grounds. Juggling two curves until they look alike is no proof of cause and effect. The

TABLE C 6
LONG-TERM TRENDS

Source of Data	Period	Trend (ppmv/decade)
Mastenbrook	1964-73	+ 1.2
Mastenbrook	1972-75	- 3.5
MRF	1972-76	~ 1.1
MRF	1954-55	+ 1.9
MRF	1972-76	- 1.9

injection of water vapor occurs in many places of the tropical part of the Hadley cell, and the meteorological conditions of all places determine the amount of water vapor fed into the stratosphere. This is discussed in detail in Section C 6.2.1.

C4. LATITUDINAL VARIATIONS

Several data sets exist. They are difficult to compare, because the aircraft measurements in the tropics have been made too close to the tropopause and may not represent true stratospheric conditions. The results are collected in Tables C7 and C8 and are presented in Figure C14.

Balloon flights are rare. Mastenbrook (1968) concluded from his measurements at Trinidad, Washington, and Thule, Greenland, that no systematic latitudinal gradient was evident and that the gradient, if it exists, must be of small magnitude (<0.016 ppmv/deg lat). This conclusion, however, is based on only three flights in Thule. Murcray et al.(1973) report one measurement at Hyderabad, India, and one at Fairbanks, Alaska, shown in Table C3. We believe their results are unacceptable, because there is no particular reason to expect such an extremely dry tropical or polar stratosphere. These are all the balloon data we have found outside the midlatitudes.

Aircraft measurements, restricted to the lowest stratosphere, are more numerous. Unfortunately, there are some drawbacks. Most flights have been carried out over a long time span, so that portions of the flights from one month are fitted to those from another month. Ultimately, this may lead to artificial maxima or minima in a cross section. Because these secondary midlatitude maxima are unreal, they are unrepresentative of average seasonal or annual conditions. For large parts of the track, the height of the tropopause is unknown, so that some data may have been taken too close to the tropopause and thus may falsify the general picture by showing too high a concentration. Furthermore, the tropopause bulge in the tropics demands flights above 18 km to ensure that the aircraft samples contain uncontaminated air. Yet only a few aircraft can reach that altitude. Consequently, some of the published mixing ratios may be too high. A reliable concept of an average latitudinal variation can only be based on

TABLE C7
WATER-VAPOR MIXING RATIOS AT 14 TO 16 KM ALTITUDE
AT LATITUDES FROM 75°N TO 50°S (ppmv)*

Latitude	Murgatroyd	McKinnon	Farmer	Murcray	Kuhn 1975	Harries	Hilsenrath	Kuhn* 1977
75 N			2.3		3.3		3.5	
70	2.6	2.9	2.2	0.6	3.0	2.3	3.8	
60		2.8	2.3		5.1	2.5	2.9	
50	2.7	2.7	2.3		4.3	3.2	3.0	
40	2.9-3.9	2.6	2.3		4.7	3.8	9.6	6.2
30	(2.4)	2.4	(3.3)		5.7	4.3	5.1	7.5
20		2.4		4.0	5.5	4.6	3.5	8.0
10		2.6			9.3	4.7	7.7	12.3
0		2.5			5.8	4.6	6.5	8.0
10 S		2.4			3.9	4.3	5.9	5.4
20		2.2			4.3	3.7	5.1	4.3
30		2.0			6.9	2.6	4.8	3.7
40		2.2			4.5	2.5	5.0	3.7
50					4.2			

± 0.25

± 0.35

*Kuhn's 1977 data for 12 km

TABLE C8
INDIVIDUAL MEASUREMENTS OF MIXING RATIOS AT ABOUT 15 km (ppmv)

FARMER	
Latitude	Mixing Ratio
76	2.2 \pm 0.25
75	2.3
74	2.6
72	2.3
69	2.1
67	2.4
63	2.3
56	2.3
37	2.3
36	2.3
34	2.4
32	3.3

HARRIES AND STONE (1972)			
Latitude	Alt. (km)	Δh^* (km)	Mixing ratio
48 N	14.6	3.3	3.93 \pm 0.35
10 N	15.6	0.5	6.22
35 S	13.7	2.5	5.90
35 S	14.9	3.8	3.60
37 S	14.4	3.5	2.85
40 S	12.1	1.0	3.60
40 S	14.9	3.2	3.15
30 S	15.8	5.0	2.49

* Δh is the difference between
flight level and tropopause in km.

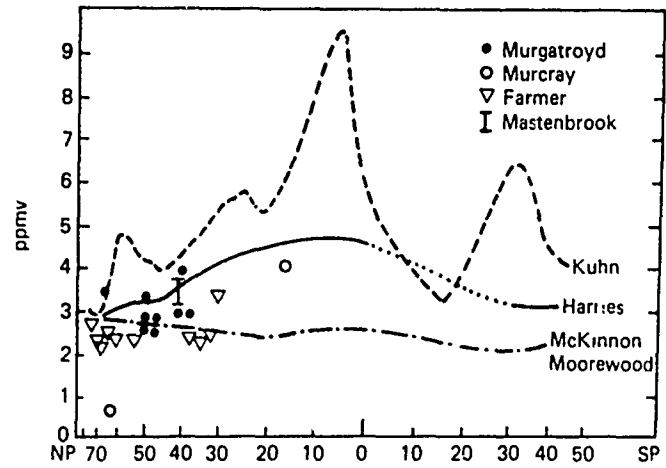


Figure C14 Latitudinal Distribution of Water-vapor Mixing Ratios in ppmv for an Altitude of 16 km.

measurements obtained during several flights, a situation seldom realized. All these drawbacks should be kept in mind when comparing and sorting the following measurements. Naturally, I would prefer to discuss meridional cross sections obtained around 20 km and not at 14 to 17 km.

The early British data from 1954-57, collected by Gutnick (1961), range from Tripoli, 33°N, to the Norwegian Sea at 67°N; they are taken at 10 to 15 km. Almost all show mixing ratios around 3 ppmv for 14 to 15 km (Average 2.9 ± 0.4 ppmv with extremes of 2.4 and 3.8 ppmv). The data were remarkably constant regardless of time of year or geographic location. No discernible latitude gradient was obtained over 44 degrees of latitude.

An extensive program was conducted by McKinnon and Morewood (1970) making 56 flights between April 1967 and May 1968 at 17.7 km altitude. Since they measured the overburden from solar IR absorption, they obtained concentrations by assuming a constant mixing ratio above flight level. This assumption may hold for the average, but it may not be exact for instantaneous profiles. They obtained a gradient during the northern hemisphere winter with largest mixing ratios of 2.8 ppmv at 65°N and a maximum of 2.0 ppmv at 35°S with an intermediate minimum at 25°N and a maximum of 10°N. Their absolute values are on the low side, i.e., 37% below Mastenbrook's data for that time period, although they did not measure values below 1.8 ppmv. This systematic deviation is impossible to trace to any particular calibration or assumption.

Harries (1976) measured water vapor emission using a Michelson interferometer and the Concorde as platform. He found for the 14 to 17 km altitudes a clear latitude variation with about 3 ppmv for 60 to 70°N, 4.5 to 4.7 ppmv between 0 and 20°N, and 3.1 ppmv at 30 to 40°S. His results apply to northern summer, and his precision of a single measurement was ± 0.35 ppmv. Over the equatorial region, the aircraft was often less than 1 km above the tropopause, which he found at times hard to define.

Kuhn et al. (1975) measured water vapor emission between 270 and 520 cm^{-1} and 15.2 and 19.7 km on a WB-57F from September 1973 to January 1974 and latitudes 52°S and 75°N. The overburden was determined from twelve flights. A large maximum was found over the intertropical convergence zone (ITCZ) of about 4 μm water/ cm^2 column above flight level and about 2 μm water/ cm^2 column from 20 to 80°N. They converted the overburden to concentrations in 16 km altitude. Their results are on the high side for all latitudes even if we assume a constant mixing ratio above flight level. In their paper, Kuhn et al. assume a fixed decrease of water vapor with altitude, proportional to p_i ($0.3 (p_i)$ = flight level).

The reason for this unusual assumption is unclear and dubious, leading to concentrations even 30% larger than those given in Figure C14 and Table C7. This assumption and the resulting high values seem incorrect to us. The near doubling of the concentration over the ITCZ spanning some 15 degrees of latitude is notable. The result demands an average tropopause that is "warm," (see Table C11) a very unlikely climatological situation (see Section C 6.1). While a singular high concentration can occur in a tower of an upwelling tropical thunderstorm, the average concentration should be smaller than 7 ppmv, we estimate somewhere between 5 and 7 ppmv. The peaks from 26 to 33°S are attributed to thunderstorm over the flight path, again not an "average" condition. We believe they could also result from fitting observations from different flights or some irregularities above the aircraft making the assumptions for data reduction questionable. As stated before, the overburden measurements hinge on the temperature and water vapor concentration profiles above the flight path. Thus, we express strong reservations about these results.

On NASA's interhemispheric survey, Kuhn (1977) measured the overburden between 40°N and 40°S and gives a result for 12.1 km, listed in Table C7 after correction and conversion to mixing ratio at 12 km. Naturally, the tropical data are within the

troposphere, yet the measurements below 20°S could have been made in the lower stratosphere and may be useful.

Six aircraft flights in the 180 to 200 mb level (approximately 12 km) have been carried out by Mastenbrook (1976) over the western U.S. at about $40 \pm 5^\circ\text{N}$. Only one flight extended over 10° latitude within the stratosphere and no latitudinal gradient was observed, only the expected normal fluctuations. This result is not surprising, because one needs a much larger latitudinal range to measure the small gradient. Because the weather situations were obviously carefully selected, Mastenbrook's east-west flights occurred in the stratosphere north of the polar jet stream. Most of the December flights found values of less than 4.2 ppmv, with mixing ratios of 3.0 to 3.7 ppmv over 1600 km of flight. During March 1975, the mixing ratio stayed mostly below 3.4 ppmv, with values between 2.6 and 3.2 ppmv over 3500 km flight. Low values of 2.6 to 3.0 ppmv occurred in a 10° latitude range north of the polar jet and 3.3 km above the tropopause. He concluded from such measurements that the stratosphere dries out during the winter months.

Farmer (1974) measured absorption using the sun as source and a fast scanning stepped interferometer in the 1 to 8 μm range. For water vapor, he used the $6.27 \mu\text{m}$ band centered at 1594.73 cm^{-1} with a resolution of 0.2 cm^{-1} and a precision of a single measurement of $\pm 0.25 \text{ ppmv}$. Measurements were made from the Concorde at an altitude of about 14 km. For the height range 14 to 20 km, he determined the average mixing ratio to be $2.4 \pm 0.3 \text{ ppmv}$. No significant latitudinal variation nor height variation was found. The increase in mixing ratio near 30°N was caused by the closeness of the tropopause.

At about 70°N , the mixing ratios obtained by Harries, Kuhn, Farmer, and McKinnon and Morewood agree; they are between 2.2 and 3.0 ppmv; only Murcray obtained 0.6 ppmv at 16 km. Earlier British data between 10 and 14 km near 70°N gave 4.8 ppmv at 13

and 2.6 ppmv at 14 km in agreement with all the recent data. Murcray's result is a factor of 5 lower than all the other measurements. That is why we believe his data are unrealistic.

In his review article Harries investigated all latitude measurements according to height regime, although practically all data are from the tropopause to 17 km, an altitude regime in which the tropical tropopause appears. As we have stated in the beginning, from a few balloon data no worthwhile conclusion as to the latitudinal variation can be drawn. To undo the systematic differences, in Figure C15, Harries (1976) arbitrarily adjusted data up to a factor of 2 to get the absolute value into a closer agreement. Because we don't know the true value, such arbitrary manipulation does not mean much.

Our conclusions are summarized below.

- o Any deduction of a latitudinal gradient of mixing ratio from the existing field measurements between the tropopause and 18 km is still controversial, as Table C7 and Figures C14 and C15 clearly demonstrate. For practical reasons, we divide our discussion into two regimes, one from the equator to 30°N/S and one from 30 to 75°N.

For the latitudes 30 to 75°N, the data sets published by Murgatroyd, McKinnon and Moorecraft, and Farmer (Tables C7 and C8) show either no discernible latitude variation at all or of a magnitude comparable to its natural variation or systematic uncertainty. Only Harries shows a systematic decrease by about 45% between 40 and 70°N, a value which seems large to us. Kuhn's mixing ratios are much higher than any of the other investigators found, and the decrease northward includes an unlikely hump at 60°; therefore, we reject his results. Hilsenrath's data, although more or less constant from 50 to 75°N, show such erratic behavior (see his original cross-section) that we cannot believe them

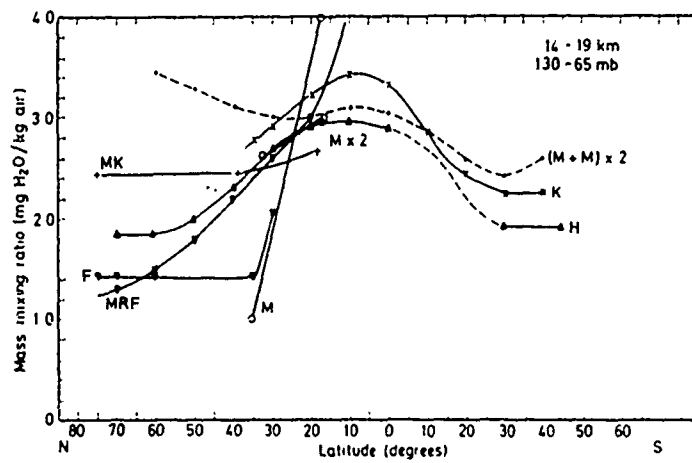


Figure C15 The Measured Latitude Variation of the Mass Mixing Ratio Averaged over the Layer 130-65 mb, or about 14-19 km (Source: Harries 1976). Mx2 and $(M+M) \times 2$ represent the curves by Murcray and McKinnon and Moorewood arbitrarily multiplied by a factor 2. F = Farmer; MRF = Murgatroyd; K = Kuhn; H = Harries.

to represent true conditions. In addition, he used a questionable technique. We are of the opinion that the data support a very small gradient between 30 and 75°N, smaller than its seasonal and long-term variation, both masking its exact magnitude. Furthermore, it may also change with season, i.e., with the changes in the stratospheric circulation.

A tropical maximum above the upwelling part of the Hadley cell should exist, giving rise to a gradient between the equator and 30°N and S. McKinnon and Harries both show an increase of about 10% towards the maximum; a small, yet acceptable gradient, while Kuhn and Hilsenrath obtain unreasonably large mixing ratios at 10°N. Their observations are rejected for reasons discussed above. Table C8 shows for 10°N (Harries and Stone) an example of a very high mixing ratio when the aircraft was only 0.5 km above the tropopause. This example points to the importance of measuring well above the tropopause, especially in the upwelling part of the Hadley cell.

- o Systematic differences exist among techniques, as we discuss in Section C3. Therefore, the absolute value of such a latitudinal gradient is uncertain.
- o Above 20 km, no conclusions about a latitudinal gradient can be drawn at this time, because the necessary field measurements are non-existent. There is a need to conduct reliable field measurements at and above 20 km between the tropics and polar regions.

C5. EXPERIMENTS FOR SOURCE DETERMINATION

The overburden can be measured by optical techniques and can give some indications about variation of water vapor distribution, at least in shallow layers near the flight level. One expects such variations over the tropical convergence zone, over thunderstorms and over jet streams. Kuhn and his associates have made such measurements, and we report some of their results. They measured the emission from water vapor in the 270 to 520 cm^{-1} band and determined the radiant power received by the radiometer from the zenith sky emission.

5.1 THE INTERTROPICAL CONVERGENCE ZONE (ITCZ)

Measurements in the ITCZ had been made on several occasions. One result is discussed here (Barrett et al. 1974). An extensive flight pattern was executed at 16.8 and 18.3 km above a large and intensive convective storm system. These data (about 0.7 km above the tropopause) were used in conjunction with the wind, temperature, and position data from the aircraft to calculate the lateral fluxes of water vapor (and ozone). Figure C16 shows the distribution of the overburden at 16.8 km, where the presence of four bubbles of high water vapor content with 4, 5, and 9 g/m^2 column is clearly evident. The driest air lies near the southwest boundary with 3 g/m^2 column. The observed correlation of the wind and water-vapor fields is consistent with the idea that the excess water vapor is indeed brought up from below.

At 18.3, only two traverses were made, but gave negligible variations between 3.1 and 3.4 g/m^2 column, from which we computed a mixing ratio of approximately 7 and 7.5 ppmv, except at two points, where it increased to 4.5 g/m^2 column. Thus, the water vapor was put into a shallow layer just above the tropopause. From these data a transport of 1,254 kg/sec into the layer was computed. For the investigated area this corresponds to 12 $\text{g}/(\text{km}^2 \text{ sec})$, where km^2 refers to the storm area only, a value

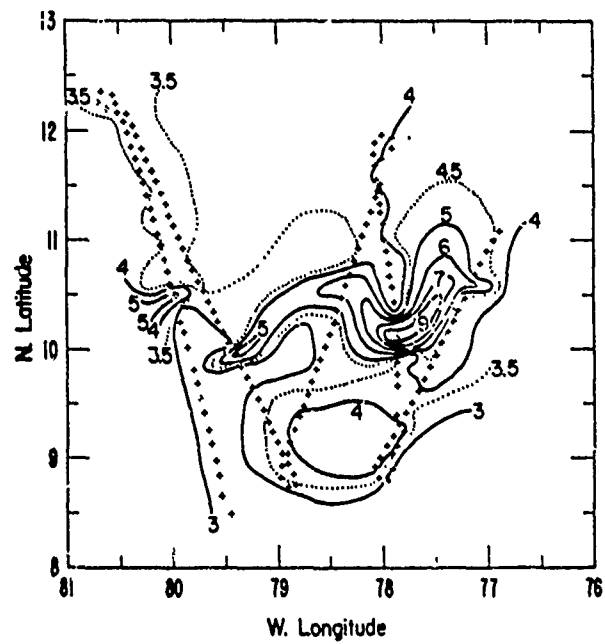


Figure C16 Isopleths of Water-vapor Overburden Above 16.8 km in Units of g/m^2 Column Over a Thunderstorm Area Near the ITCZ. Measurements from airplane flights by Kuhn (Source: Barrett et al. 1974).

estimated to be about 450% accurate. This example shows that a tropical storm system can bring water vapor into the stratosphere. Nevertheless, it is not possible from this one case to compute the total flux on a yearly basis, a number needed for computations of source and sink strength.

5.2 THUNDERSTORM INJECTION

The same group tried to determine the role midlatitude thunderstorms play in injecting water vapor into the stratosphere by circumnavigating cells of several thunderstorms in Texas and New Mexico in 1972 and 1973. The results were measurements of overburden at several altitudes from 13 to 17 km. Clearly, the downwind values exceeded those upwind by about 40%. Above the top of the cell, the overburden was larger by about 100% compared to upwind or downwind from the cell. The residence time for stratospheric water-vapor injection was difficult to ascertain because of the on-storm time limitations of the aircraft. However, about 1.5 hours after storm maturity and as far as 60 km downstream, the excess of water vapor burden was still evident. Again, there is proof that thunderstorm cells of very active storms can inject water vapor into the lowest stratosphere, yet absolute values are difficult to ascertain because some of it may return into the troposphere with the downward motion of the individual cells. Some of it, however, may be retained in the stratosphere.

5.3 POLAR JET STREAM

Kuhn et al.(1976) report 8 flights, using a C-141-A aircraft during the winter 1975-76 over the western U.S. and eastern Pacific. The objective was to measure the overburden in winter-time polar jet streams from altitudes of 12.1 to 14.8 km. A composite of all data is shown in Figure C17 for 13.4 km. Many observations were made in a mixing region between the upper troposphere and lower stratosphere. A singular feature is the

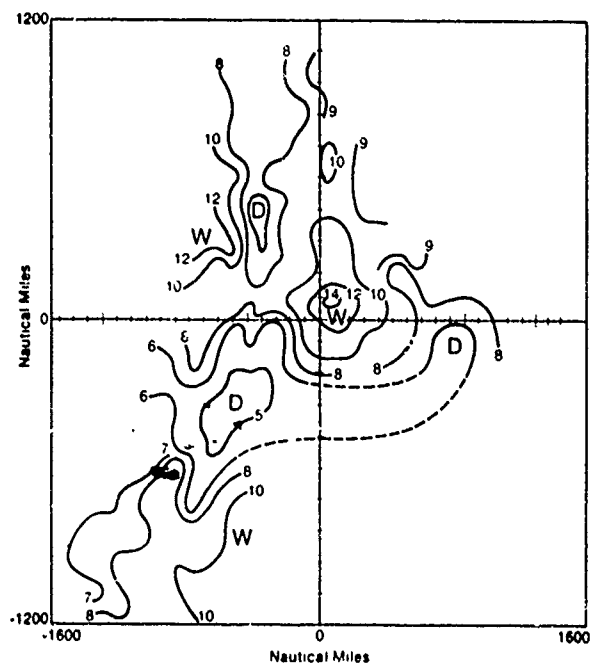


Figure C17 Isopleths of Mean Water Vapor Overburden in g/m^2 Column based on Idealized Midlatitude Polar Jet Stream. Maximum of jet is at intersection, ordinate perpendicular to jet axis (Source: Kuhn et al 1976).

region of highest water vapor burden, 14 g/m^2 column in the upper right quadrant near the jet maximum intersection. Kuhn et al. interpret this maximum as due to the divergence aloft in advance of the trough, forcing moist tropospheric air upward into the lower stratosphere. The convergence aloft, typically occurring to the rear of the trough, results in subsidence, i.e., bringing dry stratospheric air downward into the troposphere and could produce the dry area of 5 g/m^2 column south of the jet stream.

The trouble with this investigation is that it is unclear which part is in the stratosphere and which is not. Without the dynamic picture of these particular jets, one cannot determine how much water is put into the stratosphere and how much stratospheric air is brought down into the troposphere. The water vapor measurements do not prove it either. The choice of an optical technique measuring overburden for such an investigation is unfortunate, because one cannot convert the overburden, measured at 13 km, into local mixing ratios and derive a vertical mixing ratio profile. As can be guessed from Figure C17, the mixing ratio changes not only horizontally but also vertically.

It seems to us that studies of tropospheric-stratospheric transport of water vapor should use in-situ techniques, such as the frostpoint hygrometer, and not optical techniques giving only overburden. A simultaneous use of these techniques, however, would prove beneficial. All these studies show that thunderstorm cells which break through the tropopause can transport water vapor into the stratosphere. But such cells have updrafts, downdrafts and a limited lifetime, so that numerical data of the effective mass transport are still elusive. In a jet-stream system, there occurs a clear break in the tropopause and consequently an exchange of air upward and downward. At this time, water vapor could be injected into the stratosphere, but also dry air could be moved into the tropopause. We believe more air is moved downward than upward. The above reported field measurements have proven that

such processes can be considered as sources of stratospheric water vapor. Unfortunately, they have not delivered the data necessary for budgetary considerations.

C.6 SOURCES AND SINKS

6.1 GLOBAL MASS

The mass of stratospheric water vapor can be estimated from the field measurements presented in Sections C3 and C4. There we concluded the mixing ratio to be constant with altitude and a small latitudinal gradient to exist with a maximum in the tropics and a minimum in the polar caps. Although no data are available south of 50°S, this uncertainty contributes little to the global mass. Table C9 lists our own estimates and those of others. The earlier estimates, based mainly on estimates of source strength and residence time, had been derived before the present field measurements became available.

The estimates by various authors vary between 1 and $2.3 \cdot 10^{12}$ kg. From our data presentation, one notes that the outside limits are 1.2 and $3.0 \cdot 10^{12}$ kg. Averaging the latitude variation of mixing ratio gives 3.84 ppmv, based on Harries data, and leads to a mass of $2.3 \cdot 10^{12}$ kg. There are probably also some seasonal variations, so that we propose a global mass of 2 to $2.5 \cdot 10^{12}$ kg for the period around 1970. If the early British measurements are considered as an indication of the worldwide distribution at that time, the global mass should have increased by about 40% in about 20 years. However, such a change in global mass must be regarded as highly speculative.

6.2 SOURCES AND THEIR STRENGTH

Source and sink strength must be roughly in balance, at least over a time span of a year or so. By assuming a residence time of 1 to 2 years, the source strength is about 1 to $2 \cdot 10^{12}$ kg/year, based on the global mass given in Table C9. Other estimates are: Ellsaesser (1974) 1.1 and Weickmann (1975) $1.5 \cdot 10^{12}$ kg/year. We believe the order of magnitude has been correctly assessed.

TABLE C9A

ESTIMATES OF GLOBAL MASS OF STRATOSPHERIC WATER VAPOR

Literature	Mass (10^{12} kg)	Residence Time (Years)
Newell 1970	1.0	6.3
SCEP 1970	2.31	-
Sissenwine 1972	1.2	2.1
Ellsaesser 1974	1.67	1.6
Weickmann 1975	1.8	1.2
Penndorf 1977	2-2.5	1-2

TABLE C9B

AVERAGE GLOBAL MIXING RATIO AND GLOBAL MASS

Mixing ratio (ppmv)	2.0	3.84	4.0	4.15	5.0
Mass (10^{12} kg)	1.2	2.3	2.4	2.5	3.0

The most thorough investigation of the sources was carried out by Ellsaesser (1974), while that by Weickmann (1975) brings in additional viewpoints but lacks in the critical evaluation of the background literature. Numerical estimates are given in Table C10.

So far, no more plausible explanation of the dry stratosphere has been advanced than the original one by Dobson et al. (1946), who proposed that all the air entering the stratosphere is forced through the cold trap of the tropical tropopause. Although we now have a better data base for water vapor and better models for the stratospheric circulation than 30 years ago, gaps in knowledge are still large enough to make some of the numerical estimates uncertain.

6.2.1 The Hadley Cell

The Hadley cell flux was carefully investigated by Ellsaesser using 16 studies. These estimates range from 0.76 to $9.7 \cdot 10^{17}$ kg air/year transported into the stratospheric Hadley cell. The large range indicates our limited knowledge; for example, the estimates of the vertical velocity range from 0.01 to 0.06 cm/sec and of its latitudinal extent from 15°N to 15°S to 27°N to 27°S . Obviously, the meteorologists have not yet agreed on a consistent model for the "average" Hadley cell. Ellsaesser chose a transport of $3.3 \cdot 10^{17}$ kg air/year, which we will adopt as reasonable.

Other crucial parameters are the tropical tropopause temperature and pressure, because the saturation pressure of water vapor E depends in a very sensitive manner on this temperature (see Table C1). Ellsaesser found several climatological studies of the tropical tropopause conditions yielding average temperatures between -76 and -84°C for the monthly mean values; of course, on individual days it can be warmer or colder. Although the average pressure is about 100 mb, monthly mean values range between 95 and 115 mb. Such pressure variations alone introduce a variation in E by about $\pm 10\%$. Table C11 lists mixing ratios as a function

TABLE C10

ESTIMATES OF SOURCES AND SINKS FOR STRATOSPHERIC WATER VAPOR*

Sources	Weickmann	Ellsaesser	Penndorf
Hadley Cell	5.5 \pm 0.5	11.3	11.3
Tropical Thunderstorms	6 \pm ?		
Extratropical Thunderstorms	2 \pm ?	-	<0.5
Methane Oxidation	1.4 \pm 0.9	-	<<1
Total	14.9	11.3	13
Sinks			
Return Hadley Cell	**	8.3	**
Tropopause Breaks	-	+	**
Winter Greenland	**	+	+
Winter Siberia	**	+	+
Winter Antarctica	**	3	**
Total		11.3	

*Units are 10^{11} kg/year

**Means this is an important sink; + means it is an unimportant sink.

TABLE C11

SATURATION MIXING RATIOS FOR SELECTED TROPOPAUSE PRESSURES
AND TEMPERATURES (ppmv)

Temperatures (°C)	Pressure (mb)		
	95	100	115
-77	9.36	8.89	7.73
-80	5.76	5.47	4.76
-83	3.49	3.32	2.89
-86	2.08	1.98	1.72

of tropopause pressure and temperature so that the reader can get a feeling of the expected range of values. Figure C18 is a sample of monthly mean values of tropopause pressure, temperature and saturation mixing ratio (after Mastenbrook 1974) for Singapore from 1960 to 1968. They are smoothed. The tropopause pressure varies between 87 and 115 mb, its temperature between -78 and -88°C, and its saturation mixing ratio between 1.6 and 6.7 ppmv. It would be very useful to have similar statistical data for other equatorial stations to derive an acceptable worldwide average. Over Singapore, the saturation mixing-ratio was low in 1960 and high in 1965. I do not know if this was a local effect or not.

Mixing ratios at the cold trap are therefore between about 2 and 7 ppmv, because high temperatures are connected with high pressure and low temperatures with low pressure. All previous statistical studies are insufficient for our investigation. They do not give us monthly mixing ratios at the cold trap. In addition, the updraft in the Hadley cell is probably also cyclic. It can not be measured directly, only derived from radiative transfer calculations. Since the meteorological conditions are so complicated and the field data so sparse, all investigators constructed their own model of the Hadley cell by selecting specific "average" values for temperature, pressure, and updraft to obtain a value for the mixing ratio.

Harries (1976) unjustifiably criticizes Ellsaesser's choice of parameters, because "there is considerable uncertainty in both temperature and pressure." The point, however, is that the cold trap conditions are not "uncertain," they are "variable" as all meteorological parameters are. Ellsaesser's selection is just a reasonable annual average. It is hoped that some day one can build a model based on extensive statistical investigations, such as deriving monthly averages of all important parameters for each 10° field for a year or even five years. Summation over the latitudinal extent of the Hadley cell would give an average

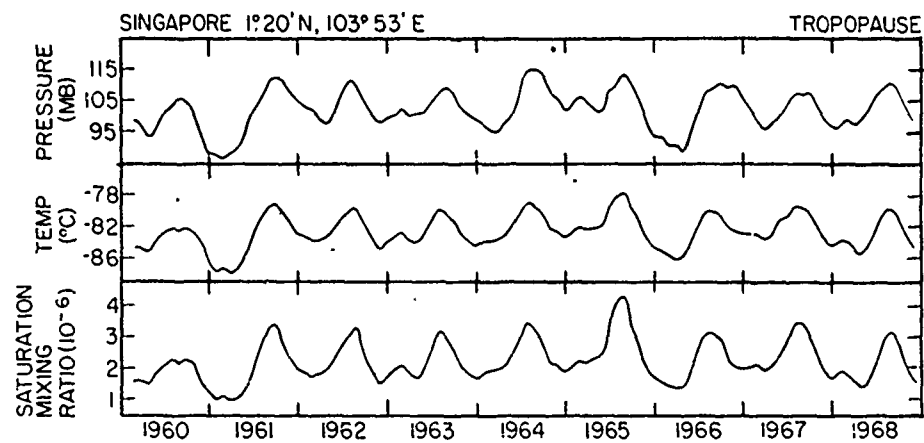


Figure C18 Tropopause Conditions for Singapore. Three-month running averages are computed for pressure, temperature and saturation mixing ratio. The saturation mixing ratio is computed from the tropopause pressure and temperature. Saturation of the up-welling air must not always occur. This depends on the humidity of the air (Source: Mastenbrook 1974 a). Saturation mass mixing ratio is given; multiply by 1.6 to obtain saturation volume mixing ratio.

source strength and its annual variation. Should the need for such a time-consuming and expensive study arise, we are certain that it will be carried out.

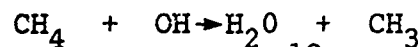
The injection into the Hadley cell has been estimated between 1.6 and $11.5 \cdot 10^{11}$ kg/year, with Ellsaesser giving $11.3 \cdot 10^{11}$ kg/year and Weickmann giving 5.5 for the steady upwelling and $6 \cdot 10^{11}$ kg/year due to thunderstorm injection; both totals are thus about equal. We consider these investigations to represent the best effort so far and to specify the expected order of magnitude.

Some tropical thunderstorms can penetrate the tropopause. Weickmann concludes from a flight program in summer 1974 over the eastern Atlantic that only thunderstorms over tropical land masses reach into the stratosphere, while those originating over oceans do not. Observations of such a cell, reported in Section 5.1, yield a vapor flux of 1,254 kg/sec or $12 \text{ g } /(\text{km}^2 \text{ sec})$. It is of course dangerous to extrapolate one single measurement to all tropical thunderstorms. Furthermore, how many of such thunderstorms occur per year and how long does each one last? There is no easy answer to these questions. One can make a simple calculation: One storm produces $1.2 \cdot 10^3$ kg/sec, it lasts for 30 minutes, there are 100 of such storms per day in the tropics during a rainy season lasting 100 days. The result is about $2 \cdot 10^{10}$ kg/year, or 2% of the global source strength. This rough estimate may give an order of magnitude. We believe Weickmann's estimate is too high. If the tropical thunderstorm contribution is small, the main source of stratospheric water vapor is the steady updraft through the tropopause of the Hadley cell, as Ellsaesser proposed.

Other sources have been proposed, but they are of minor or no importance. We cite here only those which may contribute small amounts.

6.2.2 Methane

Stratospheric oxidation of methane (CH_4) has been estimated by several authors, but most conclude its contribution to be minor, of the order of 0.15 to 0.35 ppmv/year, corresponding to 0.9 to $2.1 \cdot 10^{11}$ kg/year. All estimates depend first of all on the CH_4 flux through the tropopause. This, we believe, is larger than most authors estimate. With a tropospheric mixing ratio of 0.7 ppmv, the Hadley cell injects CH_4 at a rate of $2.4 \cdot 10^{11}$ kg/year, based on the fact that as water goes, so go the other constituents. Ehhalt's estimate is similar. The production of water is caused by the reaction



with a rate constant $k = 2.36 \times 10^{-12} \exp(-1710/T)$. This reaction alone could add water vapor at a rate of less than $3 \cdot 10^{11}$ kg/year. This is not the only reaction involving CH_4 , however; others, for example, involve oxygen, ozone, chlorine, and for OH there is a long list of reactants, with OH concentration, ranging from about 1 pptv in the lower stratosphere to 1 ppbv in the upper stratosphere, being the limiting factor in producing water vapor by the reaction cited above. Only a careful model calculation of all reactions involving CH_4 and OH can therefore lead to a reasonable estimate. Analyzing Weickmann's numerical data, we find that he assumes that 60% of all the injected CH_4 goes into water vapor production. Such an efficiency, in the presence of other competing reactions, seems very high indeed. Keeping in mind the number of competing reactions leads us to conclude that some water vapor will be produced from methane but that the amount will be small, with an upper limit of perhaps 1×10^{11} kg/year or about 0.15 ppmv/year. The constant mixing ratio to perhaps 30 km speaks of a very minor contribution.

6.2.3 Extratropical Thunderstorms

The contribution by continental thunderstorms (southern U.S., southern Russia) has been proposed, especially by Sissenwine. Kuhn's measurements indicate that they can inject water vapor into the stratosphere, and radar data have shown that anvils of such thunderstorms can reach the lower stratosphere. Weickmann attributes 13% of the global source strength to this source. Listed below are Kuhn's (1973) field measurements for one thunderstorm over Texas.

Layer (km)	Mixing ratio (ppmv)	
	upwind	downwind
15.5-16.1	3.8	29.8
14.6-15.5	4.3	11.6
13.7-14.6	5.0	4.6

Locally, the background mixing ratio could go up by a factor of 10 to 50. But the injected mass for each thunderstorm, which can not be derived from Kuhn's measurements, is important. Another parameter is the number of such storms per thunderstorm season. The argument for its contribution to be small goes as follows. Only a limited number of very severe thunderstorms can penetrate the tropopause. This fact, I think, is agreed on by all investigators. Around any strong updraft must be an area of downdraft of equal mass, and thunderstorm measurements have shown this to be true. A large portion of the injected water vapor is carried back into the tropopause and not deposited in the lower stratosphere. Since the stratospheric circulation in these latitudes is downward (downward side of the Hadley cell), water vapor can not be transported upward above, for example, 15 km (The above table shows it above 5 km, but the general downward motion will bring it down). If it is an important source, it should show up in the field measurements with peaks in the latitudinal distribu-

tion, and the seasonal variation over Washington, D.C., should be much larger than observed. We believe its contribution to be less than $5 \cdot 10^{10}$ kg/year, or less than 5% and restricted to the layers close to the tropopause. It may never reach the middle stratosphere. Field measurements at or above 20 km during the thunderstorm season should be undertaken to verify one or the other viewpoint.

6.2.4 Tropopause Gaps

It has been well established that there is a considerable exchange of mass between troposphere and stratosphere caused by the meridional vertical circulation around the jetstream core. In this region, the tropopause becomes diffuse, multiple, or otherwise ill-defined, and air moving isentropically can pass to and from the polar stratosphere to the midlatitude troposphere. A study by Reiter about air mass movement gave a net movement into the troposphere. The aerosol measurements by the Wyoming group under Hofmann also showed losses in the troposphere, and the recent ozone studies also prove the intrusion of stratospheric air rich in ozone into the troposphere. Kuhn's field measurements, reported in Section C5.3, were inconclusive, because they showed regions with high over-burden when the airplane was still in the troposphere. We believe such gaps act as a sink and not as a source.

6.3 SINKS

The stratospheric sinks of water vapor have been elusive. Weickmann gives only a listing of possible sinks, but is unable to estimate their strength. Ellsaesser estimates the strength of the return Hadley cell and proposes another sink over the Antarctic during the polar night (see Table C11). The return Hadley cell should transport water vapor downward and the magnitude is probably correctly estimated by Ellsaesser. The problem is where and how to get rid of the rest, perhaps $2.4 \cdot 10^{11}$ kg/year.

It is an established fact that in local winter the Antarctic stratosphere is much colder than over the Arctic, with temperatures around -80 to -100°C . Water vapor arriving there would freeze out and the ice crystals would fall through the atmosphere. Evenly distributed over Antarctica they would produce only a $21\text{ }\mu\text{m}$ layer (water equivalent). Weickmann believes some sinks could also occur over Greenland and Siberia during winter, but the temperatures do not go much below -75°C even during the coldest month, and from Table C10 it follows that that is not enough to freeze out the water vapor. Even for a tropopause pressure of 300 mb and -75°C , saturation vapor pressure gives a mixing ratio of 6.5 ppmv . Since the Arctic is too warm to freeze out water vapor (there are no clouds observed either), I do not believe that the Arctic can act as a sink in the same way as the Antarctic does. Harries' (1976) arguments against Ellsaesser's proposal are incorrect, because the low temperatures in Antarctica can freeze out any reasonable amount of water vapor down to mixing ratios of 0.5 ppmv .

Stanford (1977) investigated another interesting aspect of the Antarctic sink, stratospheric clouds. During the Norwegian Antarctic expedition to Maudheim (71°S) in 1950-51, the observers noted a class of long lasting, thin, very high clouds, which they termed stratospheric cirrostratus (Cist). Using the balloonsonde data (the balloons reached only 20 km) from Maudheim, the saturation mixing ratio of water vapor was computed and compared with the appearance of these clouds. The clouds appeared only during the austral winter from the end of June to the middle of August in 1950 and from the middle of July to the end of August in 1951. During those periods, the saturation mixing ratio between 100 and 50 mb was in general less than 8 ppmv , during the core of the winter less than 4.5 ppmv . Daily radiosonde data and daily reports of Cist reveal extremely low saturation mixing ratios of at times 1.5 ppmv , but at other times as high as 8 ppmv .

The relatively high mixing ratios of 8 ppmv could be explained if the temperature above 20 km is colder than below and the freeze-out started above 20 km. Another point is that we do not know the actual mixing ratio during those years, which might have been higher than in later years. Further observations of such clouds from recent years should be very helpful, because the present radiosonde network is extensive and reaches higher altitudes.

Aerosols contain about 25% water, and therefore they had been proposed to act as an additional sink. But Ellsaesser already discounted this sink as too small. Using recent data on the global aerosol mass (Penndorf 1975) of 0.44 to $0.53 \cdot 10^9$ kg, a 25% water content and a residence time of 6 months yields about $2.6 \cdot 10^8$ kg/year as sink strength. Thus the effect is small, only about 0.02%.

We believe tropopause breaks could act as a sink, as we discussed in Section C6.2.4. Yet its strength is hard to estimate.

C.7 REFERENCES

Ackerman,M., Stratospheric water vapor from high resolution infrared spectra, *Aeronom. Acta*, A-129, 1974a.

Ackerman,M., Stratospheric water vapor from high resolution infrared spectra, *Plan.Space Sci.*, 22, 1265, 1974b.

Brewer,A.W., Evidence for a world wide circulation provided by the measurements of helium and water vapor distribution in the stratosphere, *Quart.J.Roy.Met. Soc.*, 25, 351, 1949.

Brewer,A.W., and K.P.B.Thomson, A radiometer-sonde for observing stratospheric emission due to water vapor in its rotational band, *Quart.J. Roy.Meteor.Soc.*, 98, 187, 1972.

Busoletti,E., and J.P. Baluteau, Determination of H_2O/O_2 stratospheric mixing ratio from high resolution spectra in the far infrared, *Infrared Phys.*, 14, 293, 1974.

Chaloner,C.P., et al.,(5 authors), Stratospheric measurements of H_2O and the diurnal change of NO and NO_2 , *Nature*, 258, 696, 1975.

CIAP,Monograph 1, The natural stratosphere, DOT-TST-75-51, 1975.

Cluley,A.P., and M.J.Oliver, Aircraft measurements of humidity in the lower stratosphere over southern England, 1972-76, *Quart.J.Roy.Meteor. Soc.*, 104, 511, 1978.

De Jonckheere,C.G., A measurement of the mixing ratio of water vapor from 15 to 45 km, *Quart.J.Roy.Meteor. Soc.*, 101, 217, 1975.

Dobson,G.M.B., A.W.Brewer, and B.M.Cwilong, Meteorology of the lower stratosphere, *Proc.Roy.Soc.,London*, A 185, 144, 1946.

Dobson,G.M.B., A.W.Brewer, and J.T.Houghton, The humidity of the stratosphere, *J.Geophys. Res.*, 67, 902, 1962.

Ellsaesser,H.W., Water budget of the stratosphere, *Proc. 3rd CIAP Conf.*, DOT-TSC-OST-74-15, 273, 1974.

Ellsaesser,H.W., Comments on "the distribution of water vapor in the stratosphere by J.E.Harries", *Rev.Geophys.Space Phys.*, 15, 501, 1977.

Evans,W.F.J., Rocket measurements of water vapor in the stratosphere, *Proc. Intern.Conf. on struct.*,..., Melbourne, IAMSP 1.249, 1974.

Farmer, C.B., Infrared measurements of stratospheric composition, Can.J.Chem., 52, 1544, 1974.

Farmer, C.B., J.F.Raper, R.A.Toth, and R.A.Schindler, Recent results of aircraft infrared observations of the stratosphere, Proc. 3rd Conf.CIAP, DOT-TSC-OST-74-15, 234, 1974.

Goldman, A., et al. (5 authors), Distribution of water vapor in the stratosphere as determined from balloon measurements of atm. emission spectra in the 24-29 μ m region, Appl. Optics 10, 45, 1973.

Gutnick, M., How dry is the sky?, J.Geophys. Res., 66, 2867, 1961.

Hard, T., Water vapor measurement data, Unpubl manusc., TSC, DOT, 1975.

Harries, J.E., Measurements of stratospheric water vapor using infrared techniques, J.Atmos. Sci., 30, 1691, 1973.

Harries, J.E., The distribution of water vapor in the stratosphere, Rev. Geophys. Space Phys., 14, 565, 1976.

Harries, J.E., Submillimeter wave spectroscopy of the atmosphere, J. Opt. Soc. Am., 67, 880, 1977.

Harries, J.E., and W.J.Burroughs, Measurements of submillimeter wavelength radiation emitted by the stratosphere, Quart. J. Roy. Meteor. Soc., 97, 519, 1971.

Harries, J.E., and N.W.B.Stone, Measurements of some hydrogen-oxygen-nitrogen components in the stratosphere from Concorde 002, Proc. 2nd Conf. CIAP, DOT-TST-OST-73-4, 78, 1973.

Helliwell, N.C., J.K.MacKenzie, and M.J.Kepley, Some further observations from aircraft of frost point and temperatures up to 50,000 feet, Quart.J. Roy. Meteor. Soc., 83, 257, 1957.

Hilsenrath, E., B.Guenther, and P.Dunn, Water vapor in the lower stratosphere measured from aircraft flight, J.Geophys. Res., 82, 5453, 1977.

Holdeman, J.D., F.M.Humanik, and E.A.Lezberg, GASP, data report for tape VL 4, NASA-TM-X-73574, 1976.

Houghton, J.T., and J.S.Seely, Spectroscopic observations of the water vapor content of the stratosphere, Quart.J. Roy. Meteor. Soc., 86, 358, 1960.

Houghton, J.T., and T.W.Taylor, Remote soundings from artificial satellites and space probes of the atmospheres of the earth

and the planets, Rep. Progr. Phys., 36, 827, 1973.

Hyson, P., Stratospheric water vapor measurements over Australia, 1973-1976, Quart. J. Roy. Meteor. Soc., 104, 225, 1978.

Kuhn, P.M., Stratospheric and upper tropospheric water vapor experiment, in : NASA-TMX-73630, 45, 1977.

Kuhn, P.M., and L.P.Stearns, Radiometric observations of atmospheric water vapor injected by thunderstorms, J. Atmos. Sci., 30, 507, 1973.

Kuhn, P.M., E.Magazine, and L.P.Stearns, Stratospheric areal distribution of water vapor burden and the jet stream, Geophys. Res. Lett., 3, 529, 1976.

Kuhn, P.M., L.P.Stearns, and M.S.Lojko, Latitudinal profiles of stratospheric water vapor, Geophys. Res. Lett., 2, 227, 1975.

Martell, E.A., and D.E.Ehhalt, Hydrogen and carbon compounds in the upper stratosphere and lower mesosphere, Proc. Intern. Conf. on struct.,..., Melbourne, IAMAP 1, 223, 1974.

Mastenbrook, H.J., Water vapor distribution in the stratosphere and high troposphere, J. Atmos. Sci., 25, 299, 1968.

Mastenbrook, H.J., The variability of water vapor in the stratosphere, J. Atmos. Sci., 28, 1495, 1971.

Mastenbrook, H.J., Water-vapor measurements in the lower stratosphere, Can. J. Chem., 52, 1527, 1974a.

Mastenbrook, H.J., Stratospheric water vapor distribution and variability, Proc. Intern. Conf. on struct.,..., Melbourne, IAMAP 1, 233, 1974b.

Mastenbrook, H.J., Measurements of stratospheric water vapor from NASA C-141 aircraft, NRL report No 7960, 1976.

McKinnon, D., and H.W. Morewood, Water vapor distribution in the lower stratosphere over North and South America, J. Atmos. Sci., 27, 483, 1970.

Murcray, D.G., T.G.Kyle, and W.J.Williams, Distribution of water vapor in the stratosphere as derived from setting sun absorption data, J. Geophys. Res., 74, 5369, 1969.

Murcray, D.G. et al. (6 authors), Vertical distribution from airborne measurements of atmospheric emission and absorption

infrared spectra, Proc. 2nd CIAP Conf., DOT-TSC-OST-73-4, 86, 1973.

Murcray, D.G., et al. (10 authors), Recent results of stratospheric trace gas measurements from balloon-borne spectrometers, Proc. 3rd CIAP Conf., DOT-TSC-OST-74-15, 184, 1974.

Murgatroyd, R.J., P. Goldsmith, and W.E.H. Hollings, Some recent measurements of humidity from aircraft up to the heights of about 50,000 feet over southern England, Quart. J. Roy. Meteor. Soc., 81, 533, 1955.

Neporet, B.S. et al. (4 authors), Determination of moisture in the atmosphere from absorption of solar radiation, Appl. Optics, 6, 1845, 1967.

Newell, R.E., Water vapor pollution in the stratosphere by supersonic transporter ?, Nature, 226, 70, 1970.

Oliver, M.J., and A.P. Cluley, A systematic error in the measurements of frost point using a Meteorological Office Mk 3 hygrometer, Quart. J. Roy. Meteor. Soc., 104, 503, 1978.

Patel, C.K.N., E.Y. Burkhardt, and C.A. Lambert, Spectroscopic measurements of stratospheric nitric oxide and water vapor, Science, 184, 1173, 1974.

Penndorf, R., The results of CIAP's stratospheric measurements program, DOT-TST-75-106, 1975.

Pick, D.R., and J.T. Houghton, Measurements of atmospheric infrared emission with a balloon-borne multifilter radiometer, Quart. J. Roy. Meteor. Soc., 95, 535, 1969.

Rogers, J.W., et al. (5 authors), Rocket borne measurements of mesosphere H_2O in the auroral zone, Geophys. Res. Lett., 4, 366, 1977.

SCEP, Man's impact on the global environment, MIT Press, 1970.

Scholz, T.G. et al. (4 authors), Water vapor, molecular hydrogen, methane, and tritium concentrations near the stratopause, J. Geophys. Res., 75, 3049, 1970.

Sissenwine, N., A.J. Kantor, and D.D. Grantham, How dry is the sky ? A decade later and the SST, AFCRL-72-0294, 1974.

Stanford, J.L., Stratospheric water-vapor upper limits inferred from upper air observations, Part I : Northern Hemisphere, Bull. Am. Meteor. Soc., 55, 194, 1974.

Stanford, J.L., On the nature of possible stratospheric clouds in the Antarctic, Tellus, 29, 530, 1977.

Stone, N.W.B., Expanding field of far infrared Fourier transform spectroscopy in the laboratory, industry, and the environment, Appl. Optics, 17, 1332, 1978.

Waters, J.W., et al. (6 authors), The microwave limb sounder experiment. Observations of stratospheric and mesospheric water vapor, NASA-TM-X-73630, 1977.

Weickmann, H.K., Water vapor and cloud formation from engine effluents, CIAP Monograph III, DOT-TST-75-53, Chapter 7, 7, 1975.

Williamson, E.T., and J.T. Houghton, Radiometric measurements of emission from stratospheric water vapor, Quart. J. Roy. Meteor. Soc., 91, 330, 1965.

Zander, R., Moisture contamination at altitude by balloon and associated equipment, J. Geophys. Res., 71, 3775, 1966.

Zander, R., Water vapor above 25 km altitude, Pure Appl. Geophys., 106-108, 1346, 1973.